Investigating the role of climate warming on vegetation productivity and shrub distributions in the Beaufort Delta region of Canada

by

Jordan Hillel Seider
Bachelor of Science (Honours), University of Waterloo, 2018

A Thesis Submitted in Partial Fulfillment
of the Requirements for the Degree of

MASTER OF SCIENCE

in the School of Environmental Studies

We acknowledge and respect the lək^{w}əŋən peoples on whose traditional territory the university stands and the Songhees, Esquimalt and W̱SÁNEĆ peoples whose historical relationships with the land continue to this day.

Investigating the role of climate warming on vegetation productivity and shrub distributions in the Beaufort Delta region of Canada

by

Jordan Hillel Seider
Bachelor of Science (Honours), University of Waterloo, 2018

Supervisory Committee

Dr. Trevor C. Lantz, School of Environmental Studies
Supervisor

Dr. Christopher Bone, Department of Geography
Outside Member

Abstract

Climate warming across the circumpolar north has driven rapid shifts in vegetation productivity and structure, altering the community composition and function of tundra ecosystems. In my MSc thesis, I examined the biophysical factors mediating the effects of climate on vegetation dynamics, and assessed the impact of data type on models of vegetation change. In my first data chapter, I combined field sampling of soils and vegetation and random forests modelling to identify the determinants of spatial heterogeneity in Enhanced Vegetation Index trends derived from the Landsat archive (1984-2016). This analysis showed that over 70% of the Beaufort Delta region has exhibited significant increases in vegetation productivity (greening) from 1984 to 2016. Greening was more common and rapid in lower elevation areas with existing shrub-dominated land cover on till blanket and glaciofluvial deposits. The influence of surficial geology and topography on productivity trends suggests that soil moisture and nutrient availability are mediating the impact of climate warming in the low Arctic tundra. In my second data chapter, I investigated the response of three tundra shrub species (green alder, dwarf birch, and lingonberry) to climate warming using species distribution modelling. In this study, I also explored how data type affects model performance and output. This analysis shows that the use of pseudo-absence data (a common practice in species distribution modelling) results in differences in projected habitat suitability when compared to models parameterized using true absence data. Projections of habitat suitability under a climate warming scenario suggest that shrubs will respond individualistically, likely in response to physiological and ecological differences among species. Overall, my thesis emphasizes the importance of vegetation change at a landscape scale and how larger climate modelling efforts must account for landscape-scale variation in biophysical variables, individualistic responses at the species-level, and data quality.

My findings are relevant to land management in the region and suggest that further research continue to explore how vegetation change and rapid shrub expansion will affect tundra landscapes, wildlife, and broader carbon and energy exchange in the future.

Table of Contents

List of Tables

List of Figures

Acknowledgements

Thank you to all the funding agencies that supported this research and to the Inuvialuit communities of the North for allowing me to work on their lands. I would also like to thank everyone who provided their input and comments that helped improve each manuscript, notably, Mike Wulder, Txomin Hermosilla, and Jon Wang.

I appreciate the support of my supervisor, Trevor Lantz, for guiding me through this research, and to committee member, Chris Bone, for his valuable comments and commitment to producing a strong thesis.

I owe a huge thank you to everyone in Environmental Studies: staff, students, and faculty, for creating such a welcoming and supportive atmosphere. Many thanks to Team Pear for all their encouragement and a pear cider like nobody has ever had, and to Team Rhubarb, Team Cocoa, and the rest of Group ENVI for making ES the friendly place that it is. I would not have made it this far without all the incredible members of the Arctic Landscape Ecology Lab (Kiyo Campbell, Tracey Proverbs, Angel Chen, Nicola Shipman, Zander Chila, Hana Travers-Smith, Tait Overeem, Mike Newton, Grant Francis, and Emma Street) and the many discussions that ended in either confusion, tears, or laughter - sometimes all at once.

I choose not to single out anyone else for fear of forgetting someone, but know there were many others who provided invaluable support to me academically and personally throughout this journey. You know who are you are and I sincerely thank you.

I would like to acknowledge the COVID-19 pandemic, which in no way made this any easier.

Finally, a sincere thank you to my parents and siblings for always asking when I would finish. Not at all a stressful question. This one is for you.

1 Introduction

1.1 OVERVIEW AND OBJECTIVES

Air temperatures in the Arctic are increasing at a rate almost three times that of the rest of the northern hemisphere (Johannessen and others 2016; Davy and others 2018). This climate warming has resulted in changes to permafrost dynamics, soil nutrient levels, fire regimes, precipitation patterns, and a wide range of ecological processes within Arctic ecosystems (Post and others 2009; Callaghan and others 2011). Increases in vegetation productivity, the proliferation of upright shrubs, and species range shifts are all examples of climate change impacts with consequences reaching far beyond the Arctic (Pearson and others 2013; Myers-Smith and others 2015). Climate change is also accelerating the release of carbon stored in permafrost soils and increasing surface temperatures through positive feedback loops driven, in part, by increasing shrub cover and decreasing snow cover reducing surface albedo (McGuire and others 2006; Euskirchen and others 2009; Schaefer and others 2014). It is crucial that we develop a detailed understanding of how Arctic ecosystems are responding to climate change because the impacts of rapid warming provide an indication of the changes that should be anticipated as temperatures increase across the rest of the globe. Climate change is rapidly transforming Arctic ecosystems and we must understand what is happening now so we can better manage and protect these vital ecosystems for the future.

Changes to tundra vegetation dynamics (notably, increases in tundra productivity) also bring up more immediate concerns for wildlife as well as cultural land use. Shrub proliferation over once lichen-dominated tundra causes concern for many species that rely on this resource like the prominent Porcupine Caribou herd (Wildlife Management Advisory Council and Aklavik Hunters and Trappers Committee 2018). In addition to changes in vegetation communities

altering food availability, taller vegetation makes it difficult to move across the land, putting some species at risk as it is more difficult to avoid predators (Joly and others 2007). Inuvialuit and Gwich'in communities carry out subsistence hunting and trapping on the land, which may also be impacted with increased difficulty navigating tall shrubs on foot or motorized all-terrain vehicles or snow machines. As a large portion of land-use in this region is associated with cultural activities (Tyson and others 2016; Wildlife Management Advisory Council and Aklavik Hunters and Trappers Committee 2018; Proverbs and Lantz 2020), landscape changes associated with climate warming are of great importance.

My MSc research looks into the past and forecasts into the future to examine the impacts of climate warming on the productivity of tundra vegetation and the distributions of common tundra shrubs across the Beaufort Delta region in the western Canadian Arctic. With this research, I seek to answer the following questions:

1) What biophysical drivers are responsible for heterogeneous patterns in observed tundra vegetation change in the Beaufort Delta region?
2) What is the influence of data type (true absences vs. pseudo-absences) on species distribution modelling the projections of habitat suitability of three common tundra shrub species?

In Chapter 2, I use trends in a vegetation index derived from satellite imagery to investigate the effect of biophysical drivers on spatial patterns in tundra vegetation productivity. Combining data from field surveys with random forests models to rank variable importance provides insight on how warming is affecting vegetation community composition. In Chapter 3, I explore the effect of data type on the performance and habitat suitability projected by species distribution models (SDMs) of three tundra shrub species. Specifically, I assess the impact of parameterizing

models with true absences or pseudo-absences on the performance of SDMs and evaluate model outputs to understand species' responses to projected climate warming. The remainder of this chapter provides background and context to topics that guide my research, but that I do not discuss in detail in Chapters 2 or 3.

1.2 STUDY AREA

1.2.1 Beaufort Delta Region

My MSc research focuses on the Beaufort Delta region of the western Canadian Arctic. This region stretches across the Yukon North Slope and the Tuktoyaktuk Coastlands of the Northwest Territories and includes Banks Island, NWT. Differences between the climate normals of 1981-2010 and 1951-1980 show that annual mean temperature has increased by 1.6°C and 1.3°C at Inuvik, NWT (mainland) and Sachs Harbour, NWT (Banks Island), respectively (Environment and Climate Change Canada [ECCC] 2021). Regional temperatures are projected to continue rising (Serreze and Barry 2011), with likely impacts to local communities, wildlife, and vegetation (Arctic Monitoring and Assessment Programme [AMAP] 2004; Post and others 2009).

The Beaufort Delta region is home to Inuvialuit and Gwich'in communities who have stewarded the land for many generations (Alunik and Morrison 2003; Vuntut Gwitch'in First Nation and Smith 2010). Cultural practices such as fishing, hunting/trapping, and gathering from the land are heavily entwined with the regional environment where changes or disturbances to these ecosystems directly affect community wellbeing and public health (Parlee and Furgal 2012). In addition to climate warming driven by global greenhouse gas emissions, recent studies indicate that the cumulative impacts of oil and natural gas exploration, resource extraction, infrastructure development, and natural processes (fire, permafrost thaw, etc.) also pose a serious threat to

management and conservation initiatives on Inuvialuit (Tyson and others 2016) and Gwich'in (Proverbs and Lantz 2020) lands.

1.2.2 Inuvialuit Settlement Region Land Claim

Inuvialuit are the Inuit of the western Canadian Arctic in what is now known as the Inuvialuit Settlement Region (ISR; Alunik and Morrison 2003). In 1984, the Inuvialuit Final Agreement (IFA) was signed establishing the land claim of the Inuvialuit and formalizing the ISR (Indian and Northern Affairs Canada [INAC] 1984). The ISR covers approximately 91,000 km^2 of land in traditional Inuvialuit territory across much of western Northwest Territories and the Yukon North Slope (Figure 1.1). The IFA recognized Inuvialuit title to this land area, which surrounds six Inuvialuit communities in Northwest Territories: Aklavik, Inuvik, Paulatuk, Sachs Harbour, Tuktoyaktuk, and Ulukhaktok (INAC 1984). The IFA also sets out provisions honouring the Inuvialuit right to preserve and protect the environment and their cultural lands (INAC 1984). In the ISR, Inuvialuit people have the right to hunt and trap while maintaining the rights of other indigenous groups to harvest wildlife in the area as well (INAC 1984). The ISR is the home of Inuvialuit people and permission is required to conduct research on their land. As such, proper documentation and community engagement to pursue this project across the Yukon North Slope and Tuktoyaktuk Coastlands was obtained prior to initiating fieldwork (Yukon Scientists and Explorers Act Licence [19-45S&E]; Northwest Territories Scientific Research Licence [16520]; Inuvialuit Land Access Permit [ILA18TN012]).

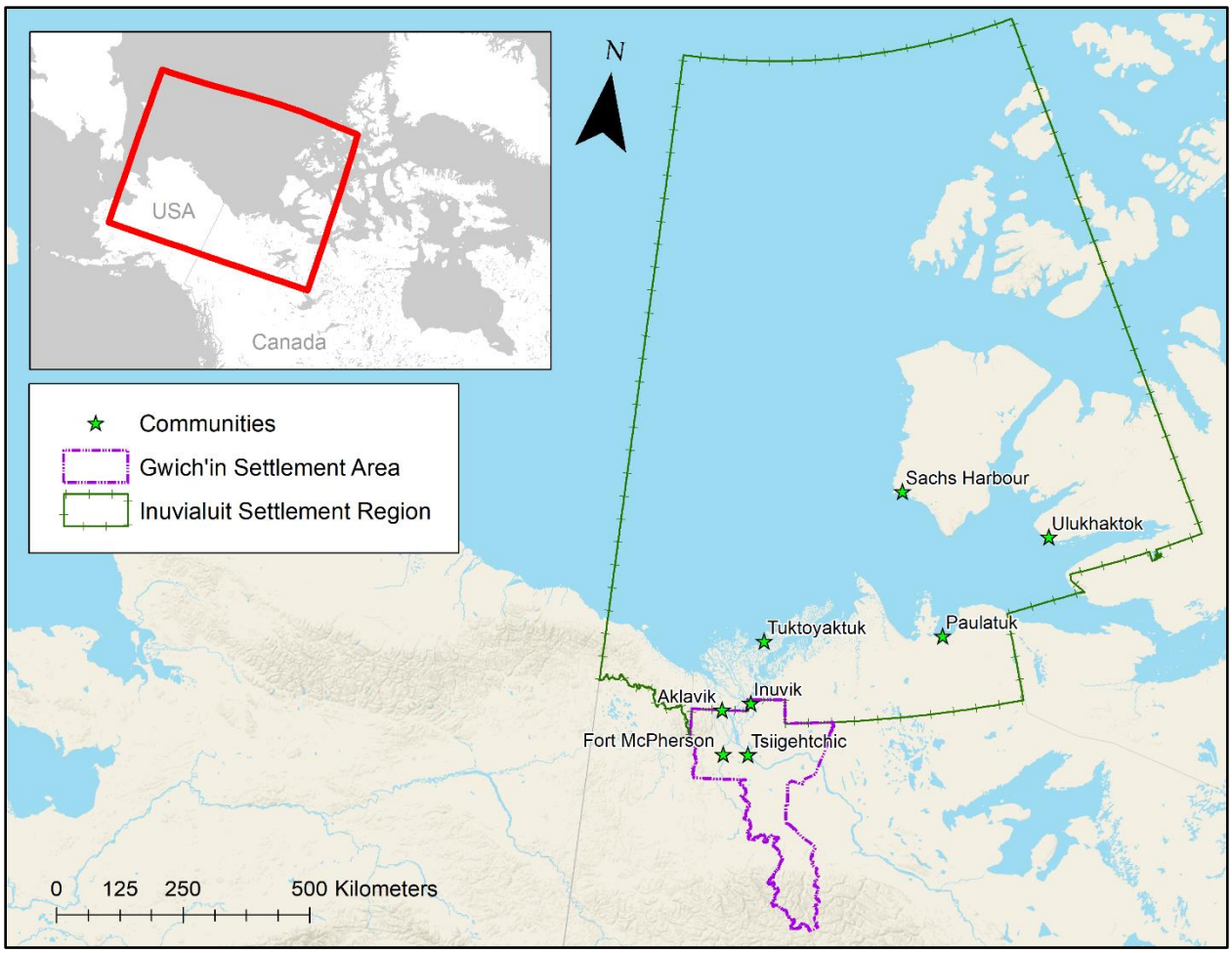

Figure 1.1. Gwich'in Settlement Area (purple dashed border) and Inuvialuit Settlement Region (green ticked border) in northern Yukon and Northwest Territories. Inset map shows the extent of the main map as it relates to Canada and Alaska, USA.

1.2.3 Gwich'in Settlement Region Land Claim

The Gwich'in are an indigenous people whose traditional territory ranges from northeastern Alaska through the northern Yukon and into the Northwest Territories in the Mackenzie Delta region (Vuntut Gwitch'in First Nation and Smith 2010). Signed in 1992, the Gwich'in Comprehensive Land Claim Agreement (GCLCA) acknowledges Gwich'in rights and title, setting out approximately 24,000 km^2 in the Yukon and Northwest Territories as the Gwich'in Settlement Region (GSR; INAC 1992). The Gwich'in Settlement Area in the Northwest Territories (Figure 1.1) encompasses the communities of Aklavik, Fort McPherson, Inuvik, and

Tsiigehtchic (INAC 1992). Like the IFA, the GCLCA recognizes Gwich'in land rights and sets out the mechanisms guiding land use and harvesting, which are regulated by the Gwich'in Tribal Council and Gwich'in Renewable Resources Board (INAC 1992).

1.3 REMOTE SENSING

Conducting research in the Arctic can be both expensive and logistically challenging. As such, remote sensing is a valuable tool to collect high quality, spatially extensive, and long-term data without the need for multiple field excursions. For the purposes of my thesis, this section focusses on data from satellite imagery, but there are many other forms of remote sensing used to monitor Arctic ecosystems including remotely piloted aircraft systems (RPAS; or drones; see Assmann and others 2020), light detection and ranging (LiDAR; Greaves and others 2015), and air photos (see Moffat and others 2016).

1.3.1 Landsat Mission and Best-Available-Pixel Workflow

Since 2008, scenes from Landsat satellite missions have been available, open access, for use by scientists, researchers, and the public (Wulder and others 2012). Data from Landsat satellites captured the globe as early as 1972 with the launch of Landsat-1 (Wulder and others 2012). Current satellites in orbit (Landsat-7 and Landat-8 missions) are working beyond their design life (Wulder and others 2012) with a new mission (Landsat-9) launched in 2021 and expected to be functional shortly after (Masek and others 2020). Throughout its history, the Landsat program has delivered high resolution (30-metre), analysis-ready imagery with a 16-day repeat cycle (Wulder and others 2019) making it valuable to time series analysis across large areas. My thesis research uses Landsat data and takes advantage of advances in image processing and the use of large-scale composite images to study changes in tundra ecosystems.

Access to such data has made it possible to study large areas of Earth in high resolution at landscape, regional, and global scales. The Landsat dataset, however, is not perfect. Image quality and availability for specific analyses are subject to cloud cover, time of year, viewing angle, and other potentially interfering factors such as sensor calibration or the failure of the scan line corrector mechanism in Landsat-7 (Gutman and others 2013; White and others 2014). One solution developed for creating broad-scale mosaics for time-series is the best-available-pixel (BAP) composite imagery method developed by White et al. (2014). This method takes advantage of the Landsat mission's vast image catalogue with many repeats to create gap-free composite images using the "best available pixel" based on a number of defined criteria (White and others 2014). The annual BAP composite creates a mosaic considering all available pixels from a given time period (such as a specific growing season). Each pixel in the composite is selected from this group to minimize cloud cover, atmospheric opacity, and cloud shadows, or optimize a defined target day-of-year (White and others 2014).

Subsequently, Hermosilla et al. (2016) developed the Composite2Change method (using annual BAP) to create a time series of Landsat imagery covering all of Canada. This analysis used all available Landsat Thematic Mapper (TM) and Enhanced Thematic Mapper Plus (ETM+) images from between 1984 and 2012 using August 1 as the target day of year (Hermosilla and others 2016). An update to this imagery by Hermosilla et al. (2017) extended the time series to 2016 and ranked images from TM and the Landsat-8 Operational Land Imager (OLI) higher than the ETM+ of Landsat-7 due to the scan line correction failure. This new release also provided gap-free imagery by filling in missing pixels using a proxy value for surface-reflectance (Hermosilla and others 2017). This gap-free, composite mosaic time-series of multispectral Landsat imagery is particularly valuable as data to study Canadian landscapes. I use these data in Chapter 2 to

map trends in the Enhanced Vegetation Index between 1984 and 2016 in an effort to understand drivers of tundra vegetation productivity.

1.3.2 Vegetation Indices

Developments in remote sensing have increased the availability and accessibility of broad-scale data in remote Arctic ecosystems, revealing landscape and regional patterns in a suite of ecological parameters (Laidler and Treitz 2003). The use of high-resolution satellite imagery and aerial photography have allowed researchers to study changes in tundra vegetation (Bhatt and others 2010), lakes (Kuhn and Butman 2021), permafrost terrain (Pastick and others 2015), snow cover (Macander and others 2015), and other sensitive Arctic systems (Laidler and Treitz 2003). To study vegetation dynamics, indices such as the Normalized Difference Vegetation Index (NDVI) estimate the photosynthetic activity of plants by measuring reflectance in the red and near-infrared bands of a satellite image (Tucker 1978). Since chlorophyll absorbs red light while reflecting near-infrared light, vegetation indices are able to estimate amounts of plant cover and productivity (Pettorelli and others 2005). High reflectance of near-infrared relative to red from the ground indicates greater plant cover than a lower ratio (Tucker 1978). NDVI is calculated using Equation 1 where NIR is the near-infrared band and RED is the red band of the visible spectrum (Tucker 1978). The Enhanced Vegetation Index (EVI) is a variation on NDVI intended to account for atmospheric noise and soil reflectance (Gao and others 2000). As a newer index of vegetation cover, EVI has some advantages over NDVI in its application to vegetation monitoring. Equation 2 for EVI shows the use of the BLUE band of the visible spectrum with satellite-specific correction terms (C1, C2, and L) to account for soil (L) and atmospheric/aerosol (C1 and C2) influences (Gao and others 2000). It has been shown that EVI is more sensitive to

differences in vascular phytomass and net primary productivity (Kushida and others 2015) and to variability of soil moisture (Raynolds and Walker 2016).

$$NDVI = \frac{NIR - RED}{NIR + RED} \quad [1]$$

$$EVI = 2.5 \times \frac{NIR - RED}{NIR + (C_1 \times RED) - (C_2 \times BLUE) + L} \quad [2]$$

Increases in computing power have facilitated the use of larger data sets and an increase in ecological model complexity (De'ath 2007; Kruse and others 2018). My MSc research benefit from these advances and utilized the national high-performance computing grid maintained by Compute Canada (Baldwin 2012).

1.4 RANDOM FORESTS MACHINE LEARNING ALGORITHM

Random forests (RF) modelling is an ensemble learning method involving the assembly of many classification or regression trees used for predictive modeling (Breiman 2001). The use of classification and regression trees (CART) allow researchers to model a single response variable using multiple predictors (De'ath and Fabricius 2000). CART splits data using a single predictor variable to increase homogeneity of the response groups in the decision tree (De'ath and Fabricius 2000). The output of CART is a single decision tree that can be used to predict the response given a set of predictor values and is useful in modeling complex, non-linear relationships (De'ath and Fabricius 2000; James and others 2013). RF builds off CART analyses by using bootstrap aggregation (or bagging) to subset available data (Cutler and others 2007). Bagging is a method of random subsampling of the data to create a decision tree where each successive decision tree uses a different random subset (with replacement). In RF modelling, a random subset of predictor variables are also selected to generate individual trees (Prasad and

others 2006). Using this bagging technique, RF is relatively well-suited to reducing the likelihood of model overfitting and is capable of working with very large datasets with many predictor variables (Cutler and others 2007). Additionally, the use of bagging and model averaging in RF reduces prediction error when compared to CART models by reducing variance in the data (De'ath 2007).

Error in RF models can be determined in a number of ways. The bagging method is unique because it makes use of the "out-of-bag" data (data not used to build a given tree) to determine prediction error (De'ath 2007). Another method is by cross validation in which data are split into training and validation sets prior to model construction and the validation data are used to determine the predictive error of the model. Some argue that with a large number of trees grown, the out-of-bag error provides a better estimate of error (Prasad and others 2006); however, others still use cross validation techniques (James and others 2013).

As a non-parametric method, RF does not require any assumptions regarding the distribution of data, does not assume linearity (Cutler and others 2007), and provides many benefits over other modelling approaches. The RF method is useful for more than just its predictive capabilities. The mean decrease in model accuracy upon removal of a given variable calculated using out-of-bag data also provides a measure of variable importance (Cutler and others 2007). RF models are not without limitation, and one critical drawback is that RF, as a machine learning technique, is essentially a "black box" that we cannot open. Users cannot be sure exactly what the trees look like and there are no formula outputs or diagrams to draw mechanistic conclusions (Cutler and others 2007). Furthermore, the prediction capability of this method is weak beyond the extent of the data you use to train the model. While not always a concern, as discussed by Evans et al. (2009), imbalance in sample data poses a problem that must be accounted for through techniques

to minimize oversampling any particular response. Finally, RF is not a tool for statistical inference or hypothesis testing as there are no p-values or confidence intervals involved (Cutler and others 2007).

In Chapter 2 of this thesis, I implement both classification and regression RF algorithms to understand drivers of change in tundra vegetation between 1984 and 2016. Using classified (classification RF) or raw (regression RF) EVI trends over this period as the response, I am able to rank biophysical drivers as they relate to areas of significant increases in tundra productivity (significant tundra greening). In Chapter 3, I used RF as one of five algorithms implemented as part of the ensemble species distribution modelling of three tundra shrub species. The classification RF used in this context has a binary presence/absence response used to predict habitat suitability across the Beaufort Delta region.

1.5 ECOLOGICAL THEORY IN SPECIES DISTRIBUTION MODELING

1.5.1 Scale

The concept of spatial scale and the impact of spatial scale on ecological research has long been an area of study (Wiens 1989; Levin 1992). Ecological variability varies across both spatial and temporal scales making conclusions regarding patterns and drivers of variation particularly difficult (Levin 1992). In species distribution modeling (or habitat suitability modeling), grain size and extent both have an important influence on model construction and interpretation. Grain size refers to the spatial resolution of the data. Larger grain sizes represent coarser interpretations of the earth's surface whereas smaller grain sizes provide greater detail but require higher quality sensors and more physical data storage. Spatial extent refers to the total area of study. Larger study areas have greater extents and encompass greater variability in environmental and climate predictors but may miss nuances experienced by specialist species or local adaptations by

ecotypes (Trivedi and others 2008; Vale and others 2014). The combination of grain size and extent are what define the scale of study. The relative influence of biotic and abiotic drivers of ecological responses also differ across scales (Pearson and Dawson 2003). Climate is generally the dominant driver when considered across large areas, but at finer scales, soil conditions and microclimate can drive heterogeneity in ecological responses (Austin and Van Niel 2011). Even with the advancement of remote sensing technologies, some products may be limited in their spatial resolution, which influences how appropriate they are for use in species distribution modeling at finer scales (Elith and Leathwick 2009).

1.5.2 Niche Theory

Species distribution modelling attempts to quantify a species' niche (Hirzel and Le Lay 2008). A species' niche can be broadly defined as the specific biotic and abiotic requirements for needed for a species to survive that are influenced by climate, resource availability, biological competition, or any number of other environmental or biological factors. This familiar framework is defined by Hutchinson's niche concept (Hutchinson 1957), itself building off of previous descriptions by other ecologists (see Chase and Leibold 2003; Pironon and others 2018). Additional factors such as competition, herbivory, allelopathy, and disease can also limit the actual distribution of a given species, often referred to as the realized niche of a species. The fundamental niche covers the entire spectrum of suitable conditions whereas the realized niche describes the conditions a species actually occupies. Since species distribution models are built from observations in the field, these models are only capable of quantifying the spatial extent of the realized niche (Austin and others 1990; Pearson and Dawson 2003). However, considering the resolution of modeled predictors, Araújo & Guisan (2006) propose that coarser resolution data may not be able to model negative interactions such as competitive exclusion, thus giving a

better picture of the fundamental niche. Complications like this, and others such as dispersal limitations, make applying niche concepts to species distribution modeling a complex task with no clear solution. Understanding and accounting for limitations in correlative ecological niche modeling in the form of species distribution models is still an active area of research. As such, it is important to understand what information models are capable of providing and to be mindful in the interpretation of results. The SDMs created in Chapter 3 of this thesis do not account for dispersal mechanisms or biological interactions. Instead, I focus on the role of environmental and climate variables that describe the realized niche of tundra shrubs in the Beaufort Delta region and how projected changes in climate patterns will affect habitat suitability across the landscape.

2 Biophysical determinants of shifting tundra vegetation productivity in the Beaufort Delta region of Canada

Jordan H. Seider[1], Trevor C. Lantz[1], Txomin Hermosilla[2], Michael A. Wulder[2], Jonathan A. Wang[3]

1. School of Environmental Studies, University of Victoria
2. Canadian Forest Service (Pacific Forestry Centre), Natural Resources Canada
3. Department of Earth System Science, University of California, Irvine

2.1 INTRODUCTION

Increasing temperatures in the Arctic (AMAP 2004; Serreze and others 2009; Johannessen and others 2016; Davy and others 2018) are driving rapid changes to the structure and composition of tundra vegetation. Plot-based and fine-scale remote sensing studies have documented shifts in the dominant vegetation, with deciduous shrubs now proliferating in what was once lichen- and graminoid-dominated tundra (Elmendorf and others 2012; Ropars and Boudreau 2012; Lantz and others 2013; Moffat and others 2016; Travers-Smith and Lantz 2020). Vegetation productivity can also be measured at broad scales using multispectral satellite vegetation indices (Gao and others 2000) such as the Enhanced Vegetation Index (EVI) and the Normalized Difference Vegetation Index (NDVI). Changes in these indices have been observed across the Arctic with increasing productivity referred to as 'tundra greening' (Jia and others 2003; Bhatt and others 2010; Epstein and others 2012). Continental and pan-Arctic scale changes in vegetation productivity have generally been attributed to rapid temperature increases at high latitudes (Jia and others 2003; Bhatt and others 2010; Miller and Smith 2012; Fraser and others 2014a; Berner and others 2020). Plot-scale warming experiments and repeated observation also provide evidence that vegetation change has been caused by increasing temperature (Chapin and others 1995; Walker and others 2006; Hudson and Henry 2009; Elmendorf and others 2012).

Although widespread, observed increases in Arctic vegetation productivity have not been uniform, with some regions exhibiting stable or decreasing productivity (Jia and others 2006; Bhatt and others 2010; Epstein and others 2012; Ju and Masek 2016). Recent evidence suggests that variation in the response of tundra vegetation is related to both broad-scale (Wang and Friedl 2019; Berner and others 2020; Campbell and others 2021; Chen and others 2021) and fine-scale (Moffat and others 2016; Myers-Smith and others 2019; Bjorkman and others 2020) variation in

biophysical factors, but few studies have explored linkages between these scales. In their conceptual model, Pearson and Dawson (2003) suggest that climate variables (long-term temperature and precipitation trends) have greater influence at a global and continental scales, whereas biophysical variables (such as soil moisture, surface topography and soil conditions, land cover, and land use) are likely to influence processes at landscape or local scales.

At the landscape-scale, research suggests that variability in soil moisture, land cover type, and landscape position are responsible for the heterogeneous response of Arctic vegetation productivity (Ropars and Boudreau 2012; Tape and others 2012; Martin and others 2017; Bonney and others 2018; Campbell and others 2021). In this study, we explore the environmental factors driving heterogeneity in vegetation productivity trends across the Beaufort Delta region by combining plot-based fieldwork with an analysis of the Landsat satellite archive (Wulder and others 2019). We use a random forests (RF) ensemble decision tree algorithm to determine the environmental factors influencing spatial heterogeneity in tundra productivity trends in the Beaufort Delta region. Ultimately, we seek to understand how variation in environmental conditions influences the spatial patterns of vegetation productivity at a landscape-scale. An improved understanding of factors mediating tundra vegetation change will contribute to local and regional planning and inform earth system models that include feedbacks between vegetation growth and ecological processes such as permafrost, albedo, and evapotranspiration (Verseghy 1991; Verseghy and others 1993; Verseghy 2000; Bonan and others 2003; Quillet and others 2010).

2.2 STUDY AREA

This study focuses on the tundra ecosystems across the Yukon North Slope (0.54 MHa) and Tuktoyaktuk Coastlands (2.92 MHa). These Low Arctic ecosystems are located in the Beaufort

Delta region of the western Canadian Arctic (Figure 2.1a). This coastal region borders the Beaufort Sea to the north and is bounded by the northern edge of the subarctic forest to the south (Timoney and others 1992). Both regions are located within the Inuvialuit Settlement Region and are significant to the communities of Tuktoyaktuk (population of 900), Inuvik (population of 3200), and Aklavik (population of 600), who use these lands for hunting, fishing, trapping, traditional harvesting of plants, and other cultural practices (Alunik and Morrison 2003; Murray and others 2005; Tyson and others 2016).

The Yukon North Slope extends from the foothills of the Richardson Mountains to the coast of the Beaufort Sea. Areas at high elevation drain to the Beaufort via the deeply incised canyons of the Babbage, Blow, and Big Fish Rivers among others (Rampton 1982; Yukon Ecoregions Working Group [YEWG] 2004). Rolling hills and hummocky terrain dominate the eastern portion of the Yukon North Slope that ends in a steep escarpment at the Mackenzie Delta (Rampton 1982). Average annual temperature between 1984 and 2016 at Shingle Point was -9.2 ℃ with an average summer temperature (June through August) of 9.0 ℃ (ECCC 2018b). On average, Shingle Point received 254 mm of precipitation annually (ECCC 2018b), about half of which fell as rain (Burn and Zhang 2009). The Tuktoyaktuk Coastlands extends from the eastern limit of the Mackenzie Delta to Cape Bathurst to the east. This gently rolling landscape is scattered with lakes and ponds and is characterized by hummocky terrain in upland areas and polygonal terrain and wetlands at lower elevations (Rampton 1988; Ecosystem Classification Group [ECG] 2012). The climate at Tuktoyaktuk is similar to Shingle Point, with average annual and summer temperatures between 1984 and 2016 of -9.4 ℃ and 8.9 ℃, respectively (ECCC 2018a). Average total precipitation during this period was 146 mm, about 40% of which fell as rain (ECCC 2018a). The Yukon North Slope and Tuktoyaktuk Coastlands are separated by the

low-lying alluvial terrain in the Mackenzie Delta ecoregion. This dynamic ecosystem was excluded from our study area because much of it is forested and the tundra communities present are strongly influenced by hydrological dynamics (Gill 1972, 1973; Pearce 1986; Burn and Kokelj 2009).

The Yukon North Slope hosts a diversity of terrain types including coastal beaches and estuaries, low-lying wetlands, upland tussock tundra, and shrub tundra (YEWG 2004; Wang and others 2019). The upland tundra in the foothills of the Richardson Mountains occurs on well-drained soils that support characteristic communities of tall and dwarf shrubs, lichens, graminoids and forbs (YEWG 2004). The Tuktoyaktuk Coastlands is largely covered by shrub and tussock tundra with wetter areas dominated by sedge and moss tundra (ECG 2012; Moffat and others 2016). In the southern portion of this region, scattered spruce woodlands are located along sheltered creeks and other low-lying areas (Lantz and others 2019).

Both the Yukon North Slope and Tuktoyaktuk Coastlands are underlain by continuous permafrost and are characterized by thermokarst features including polygonal terrain, earth hummocks, thaw slumps and pingos (Rampton 1982, 1988; YEWG 2004; ECG 2012). The Laurentide Ice Sheet covered most of this region during the Wisconsinan glaciation with the exception of land south and west of the Richardson Mountains and the northern tip of the Tuktoyaktuk Peninsula and Cape Bathurst (Jessop 1971; Hughes and others 1981; Duk-Rodkin and Hughes 1995; YEWG 2004; ECG 2012).

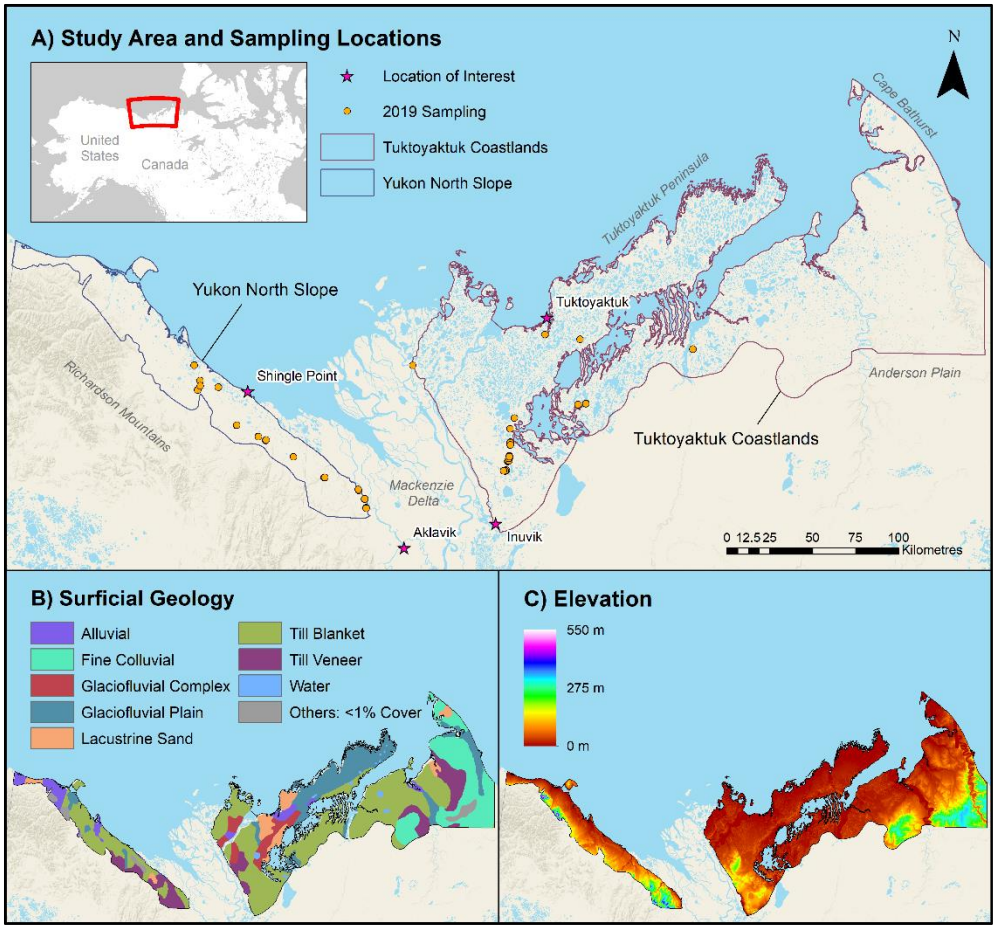

Figure 2.1. A) Study area and site locations from the 2019 field season with inset showing the extent the map in the context of northwestern Canada and Alaska, USA. B) Surficial geology classes comprising greater than 1% of the study area (Fulton 1989) and C) elevation in metres (Porter and others 2018) used in random forests analyses across the study area.

2.3 METHODS

To investigate the drivers of vegetation change in the Beaufort Delta region we combined RF modelling of regional EVI trends with multivariate analyses of plot-scale field data. We classified pixel-based trends in EVI (1984-2016) as: 1) exhibiting significant increases in EVI or 2) un-trended. We used these binary classes (increasing EVI/un-trended EVI) as response variables in a classification RF model to determine the factors facilitating and constraining increased productivity. To identify the factors influencing the magnitude of greening, we also performed a regression RF model that predicted the slope of significant positive EVI trends. To

facilitate site selection for field sampling and multivariate analyses, pixels exhibiting significant increases in EVI were further classified as moderate or high magnitude greening.

2.3.1 EVI Trend Analysis

To document changes in the productivity of tundra vegetation across the study area, we tracked changes in EVI using the Landsat satellite archive (1984-2016). EVI is a modified form of NDVI in which the blue band of the visible spectrum and satellite-specific correction terms (C_1, C_2, and L) account for soil (L) and atmospheric/aerosol (C_1 and C_2) influences (as calculated in Equation 3; Gao and others 2000).

$$EVI = 2.5 \times \frac{NIR - RED}{NIR + (C_1 \times RED) - (C_2 \times BLUE) + L} \qquad (3)$$

We used EVI in this analysis because it is sensitive to differences in vascular plant phytomass and vascular net primary productivity (Kushida and others 2015) and it performs well across a range of soil moisture conditions (Raynolds and Walker 2016). We obtained the EVI trend surface from Chen and others (2021) who generated the trend surface using annual composite Landsat images from 1984 to 2016. These images were obtained using the Composite2Change method for selecting best-available-pixels from the Landsat archive to produce a gap-free surface reflectance raster for each year (Hermosilla and others 2016). The imagery used to produce best-available-pixel composites were cross-calibrated among Landsat sensors (see: Markham and Helder 2012; Hermosilla and others 2016). Composite imagery was used to calculate EVI on a pixel basis (30-metre spatial resolution) for each year and a pixel-based, non-parametric Theil-Sen regression was performed on the resulting time series (Theil 1950; Sen 1968) using the *EcoGenetics* package (Roser and others 2017) in R (R Core Team 2019). The significance of pixel-based slopes was assessed using a Mann-Kendall test for monotonic trends (Mann 1945;

Kendall 1948) performed using the *Kendall* package in R (McLeod 2011). In our analysis, we used the resulting p-values to determine whether significant change ($p < 0.05$) had occurred in each pixel from 1984 to 2016.

We also used the raster surface derived from Theil-Sen regression of EVI trends to classify the study area into site types exhibiting: 1) high greening, 2) moderate greening, 3) no significant change (stable sites), and 4) browning (see histogram: Supplementary Figure 1) for the purpose of our field investigation. Areas showing non-significant EVI trends ($p > 0.05$) were classified as stable. Pixels with significant increases in EVI were further classified based on the slope of the EVI trend. Pixels with slopes that were within one standard deviation (SD; 1.45×10^{-3} per year) of the mean EVI trend ($< 2.24 \times 10^{-3}$ + SD per year) were classified as moderate greening and pixels with an increase greater than one standard deviation above the mean EVI trend ($> 2.24 \times 10^{-3}$ + SD per year) were classified as high greening. Pixels with a significant negative slope (decline in EVI over time) were classified as browning. Since browning pixels only accounted for 0.63% of pixels in the study area, we did not consider this class as a category in this analysis.

2.3.2 Random Forests Analysis and Variable Importance

To identify the biophysical variables that best explain spatial variation in EVI trends, we used two RF models (Breiman 2001). RF models are decision-tree based, ensemble machine-learning methods involving the assembly of many regression or classification trees using a subset of available data to increase predictive capability (Breiman 2001; De'ath 2007). The RF method can also be used to determine variable importance by measuring the mean decrease in model accuracy upon removal of a given variable (Cutler and others 2007). In our first analysis, we used a classification RF to discriminate pixels showing a significant increase in EVI ($p < 0.05$, positive slope) from un-trended pixels ($p > 0.05$). In a second analysis, we used a regression RF

to model the magnitude of the change in EVI (Theil-Sen regression slope) of pixels exhibiting significant increases in EVI ($p < 0.05$, positive slope) using the same suite of biophysical variables. We created both models using the *randomForests* package (Liaw and Wiener 2002) in R. Explanatory variables used in each model are presented in Table 2.1. We ran the classification RF model using a random selection of 40,000 pixels of each class to ensure balanced sampling. For the regression RF, we used a random sample of 1% (66,442 pixels) of all pixels in the study area. We ran each model using 1000 trees and calculated the variable importance using the *importance* function (Liaw and Wiener 2002). We assessed the influence of the four variables that had the largest impact on model accuracy using partial dependence plots showing the marginal effect of a given variable on the modelled parameter while keeping all other variables constant (Friedman 2001; Hastie and others 2009). For a classification RF, partial dependence plots show the probability of significant greening. The partial dependence plots for a regression RF show the predicted magnitude of the slope in the EVI trend.

2.3.3 Explanatory Variables

Broad-scale biophysical data used in this study were obtained from a variety of sources (Table 2.1) and data processing and aggregation were completed using the R statistical software (R Core Team 2019). We selected explanatory variables known to effect growth and productivity but were not able to directly assess the influence of microclimate because suitable data are not available to adequately capture climate variability at such fine scales. A digital elevation model (DEM), with 2-metre spatial resolution (Figure 2.1c), was sourced from the Polar Geospatial Center's (PGC) ArcticDEM dataset (Porter and others 2018). We calculated slope, aspect, and terrain ruggedness index (TRI) from this DEM using the *terrain* function from the *raster* package (Hijmans 2020). TRI is the absolute difference between the elevation of a given cell and

its surrounding neighbours (Riley and others 1999). The topographic wetness index (TWI) is a DEM-driven index of soil moisture in which potential soil moisture availability is calculated based on the slope and flow directions of the surrounding landscape (Kopecký and Čížková 2010). Flat areas surrounded by upslope terrain will have higher TWI values (as moisture will tend to accumulate in these areas) compared to steep sloping cells that will have lower values (as moisture will tend to run off). TWI was calculated using the *upslope.area* function from the *dynatopmodel* package (Metcalfe and others 2018). Topographic position index (TPI) is another DEM-driven index that defines the relative elevation of a cell based on the mean elevation of surrounding cells (De Reu and others 2013). Where TPI is positive, the cell has a higher elevation than the mean of the surrounding cells. A negative TPI indicates that the cell has a lower elevation than the mean of the surrounding cells. TPI was calculated using the *tpi* function in the *spatialEco* package (Evans 2020). We calculated solar insolation using the Equation 4 provided by Roberts and Cooper (1989):

$$solar\ insolation = \frac{1 - \cos(aspect - 30)}{2} \qquad (4)$$

This index of solar insolation ranges from 0 to 1, with north-northeast facing aspects taking on values close to zero, and south-southwest aspects having values closer to 1. Data on land cover were obtained from the classification created by Wang and others (2019). This land cover classification includes 15 terrain types derived from a RF classification model for Landsat surface-reflectance at 30-metre resolution using high-resolution field photos and imagery from the NASA ABoVE project to assign land cover classes for each year between 1984 and 2014 (Wang and others 2019). We used land cover data from 1984 as a predictor in the RF models to test the sensitivity of different vegetation classes to shifts in productivity. The average overall

accuracy for these land cover data is 84.1 ± 4.1% (mean and 95% confidence interval across all years of the time series; Wang and others 2019). Surficial geology data were obtained from Fulton (1989), cropped to the extent of the study area and rasterized for further analysis (Figure 2.1b). We masked out any cells of the land cover and geology layers that were occupied by classes representing less than 1% of the study area (class descriptions can be found in Supplementary Tables 1 and 2). Spatial resolution of the data sources described above were matched to the EVI trend data (30 metres). Where resolution of a dataset was finer than 30 metres, cells were aggregated by taking the mean of sub-pixels. We resampled continuous data using a bilinear interpolation method while categorical data used the nearest neighbour method. These operations were performed with the *resample* function from the *raster* package (Hijmans 2020). Surficial geology and elevation data are shown in Figure 2.1b and Figure 2.1c; all other explanatory variables can be found in Supplementary Figure 2.

Table 2.1. Explanatory variables used in random forests modelling. *20 metre resolution corresponds to the smallest size polygon (approximately 20 m^2) in the original source data.

Explanatory Variables	Units	Resolution	Source
Elevation	metres	2 metres	PGC ArcticDEM (Porter and others 2018)
Slope	degrees	2 metres	PGC ArcticDEM derivative
Topographic Wetness	index	2 metres	PGC ArcticDEM derivative
Topographic Position	index	2 metres	PGC ArcticDEM derivative
Terrain Ruggedness	index	2 metres	PGC ArcticDEM derivative
Solar Insolation	index	2 metres	PGC ArcticDEM derivative
Land Cover (1984)	category	30 metres	NASA ABoVE (Wang and others 2019)
Surficial Geology	category	20 metres*	Fulton 1989

2.3.4 Field Surveys

To assess the influence of biophysical variables on recent changes in tundra productivity we measured biotic and abiotic variables at sites across the study area. Field sites were selected by randomly choosing 40 points in each of the productivity classes defined using the EVI trend

(moderate greening, high greening, and stability). Randomization was constrained such that the pixel (30 m^2) containing the selected point was surrounded by the same greening class. We visited 21 stable sites, 32 moderate greening sites, and 26 high greening sites in July and August of 2019 (Figure 1.1a). At each site, we measured a suite of biotic and abiotic variables, as described below.

Vegetation surveys and soil sampling were conducted along two intersecting 30-metre transects. Transects were orientated in north-south and east-west directions such that the 15-metre mark on both transects was centered on the predetermined site coordinate. These dimensions were selected to create a plot corresponding to the 30-metre resolution of one Landsat pixel. Thaw depth and soil moisture were measured at 5-metre intervals along each transect as well as inside all vegetation quadrats at a site. We measured soil moisture at 3-5 cm below the surface using a handheld moisture probe (Delta-T Devices HH2 Moisture Meter with ML3 ThetaProbe Soil Moisture Sensor). Thaw depth was measured using a graduated metal probe inserted into the ground until the depth of refusal. We visually estimated the percent cover of plant species or species groups inside nested 5 m^2 and 1 m^2 quadrats at four locations at every site. We positioned quadrats using a random point located inside each of the four quadrants of the cross transect (northwest, northeast, southwest, and southeast). We estimated the cover of upright shrubs and trees using the larger quadrat and the cover of dwarf shrubs, graminoids, herbaceous species, lichens, and bryophytes using the smaller quadrat.

When vegetation cover estimates were completed, we collected a composite active layer soil sample from within each quadrat using a small shovel. The profile exposed during sample collection was also used to estimate the thickness of the moss layer and organic soil horizon. Soil samples were stored at -20°C before they were submitted for analysis of gravimetric soil

moisture, macronutrients including nitrogen and phosphorus, and micronutrients including magnesium, sulphur and calcium. Chemical analyses were carried out using an inductively coupled plasma mass spectrometer (ICP-MS) at the Chemical Services Laboratory at the Pacific Forestry Centre of the Canadian Forest Service in Victoria, British Columbia.

2.3.5 Vegetation Community and Environmental Data Analysis

To explore differences in community composition among sites exhibiting different levels of landscape scale greening we used non-metric multidimensional scaling (NMDS) ordination. We applied a log(x + 1) transformation to the raw vegetation percent cover data and ran the NMDS using a Bray-Curtis dissimilarity matrix of the transformed percent cover data. This analysis was set to repeat 100 times and select the best two-dimensional representation of the original data. The NMDS was performed using the *metaMDS* function from the *vegan* package (Oksanen and others 2019) in R. We used the analysis of similarities (ANOSIM; Clarke 1993) function (*anosim*) from *vegan* (Oksanen and others 2019) to test for statistically significant differences in vegetation community composition among the three sites types (stable, moderate greening, and high greening). To identify the species making the greatest contribution to differences among site types, a similarity percentage (SIMPER) analysis was conducted using the *simper* function in the *vegan* package (Oksanen and others 2019). We also compared the cover of vegetation classes in 1984 and 2014 using the multiyear land cover classification presented in Wang and others (2019). Specifically, we calculated the percent cover of land cover classes in 1984 and 2014 and compared the differences across the entire study area and between the Yukon North Slope and Tuktoyaktuk Coastlands.

2.4 RESULTS

2.4.1 Study Area Response Overview

Approximately 70% of the study area showed significant increases in EVI between 1984 and 2016 (Figure 2.2, Table 2.1). Split across the study area, 71% of the Tuktoyaktuk Coastlands showed significant greening compared to 66% of the Yukon North Slope (Table 2.2). The Tuktoyaktuk Coastlands also had a higher average EVI trend than the Yukon North Slope but was similar to the average across the entire study area (Table 2.2).

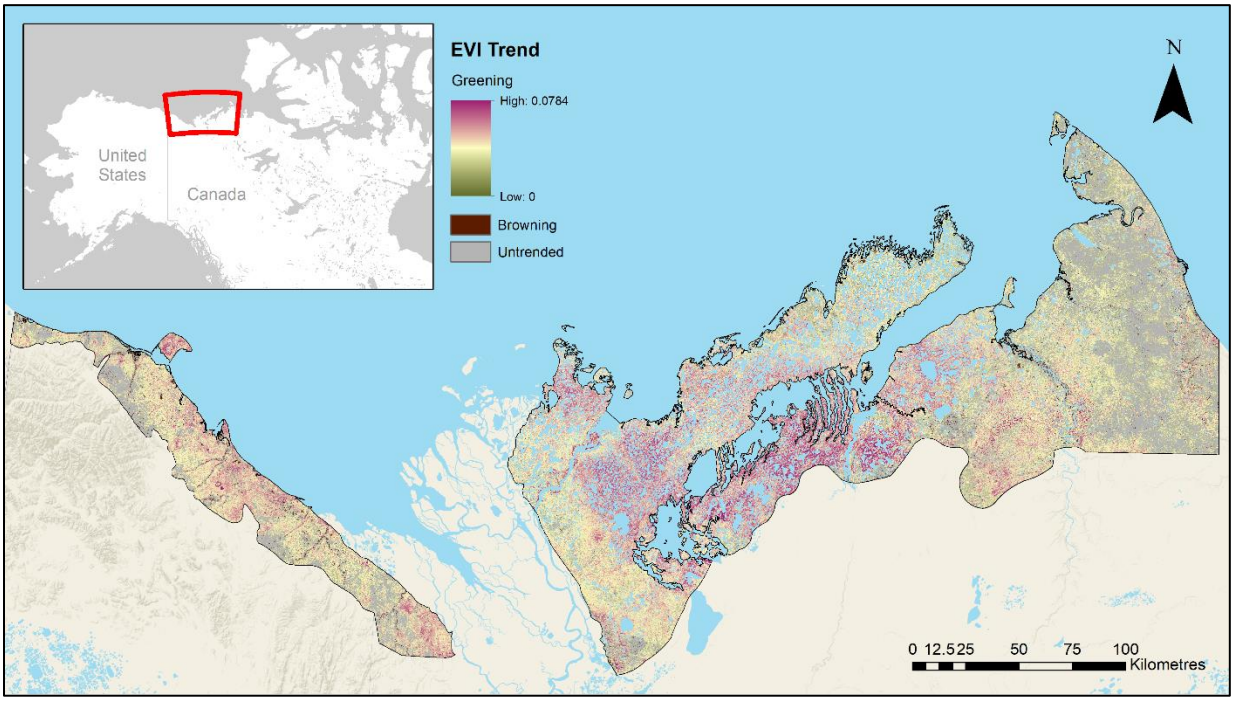

Figure 2.2. Raw EVI trends (from Chen and others 2021) where un-trended and browning pixels are grey and brown, respectively. The inset at the top left shows the extent of the main map in the context of northwestern Canada and Alaska, USA.

Table 2.2. Greening responses across the study area.

Region	Area	Percent of Region Greening	Mean EVI Trend in Region (Per Year)
Entire Study Area	34,627 km^2	70.2%	2.239 x 10^{-3}
Tuktoyaktuk Coastlands	29,184 km^2	71.1%	2.274 x 10^{-3}
Yukon North Slope	5,443 km^2	66.2%	2.97 10^{-3}

2.4.2 Classification Random Forests Analysis

The top four predictors in the classification RF were surficial geology, elevation, land cover in 1984, and TWI (Figure 2.3). This model had user's accuracy of 72.05% and was capable of classifying pixels as stable and greening with user's accuracy of 73.5% and 70.6%, respectively. The area under the curve (AUC) of the receiver operating characteristic (ROC) is 0.796 (see Supplementary Figure 3).

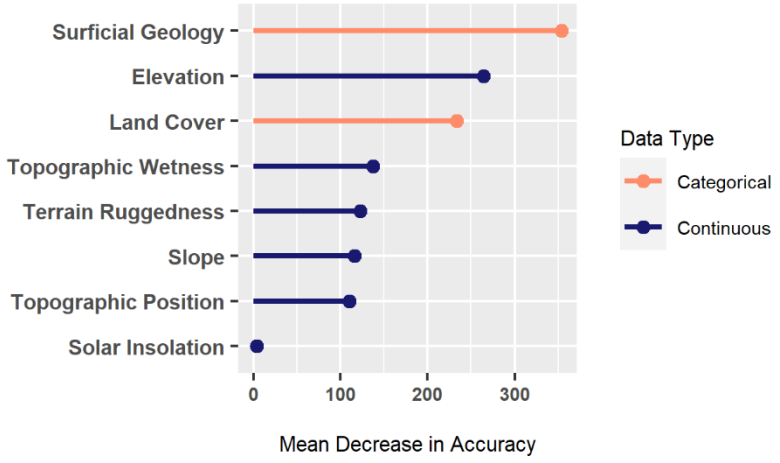

Figure 2.3. Variable importance in the classification random forest (predicting probability of significant greening) measured as the mean decrease in model accuracy scaled by the standard error of the change in model accuracy.

Partial dependence plots for surficial geology show that till blanket, glaciofluvial complex, glaciofluvial plain, and lacustrine sand were more likely to exhibit greening than colluvial and alluvial materials, which had a greater probability of being stable (Figure 2.4a). The partial dependence plot for elevation shows that the greatest probability of greening occurred at elevations between 0 to 60 metres (Figure 2.4b). Elevations above approximately 60 metres had a higher probability of being stable. This analysis also showed that significant greening was most likely in low shrub, tussock tundra, and sparsely vegetated land cover classes, while tall shrub, fen, and barren cover classes were more likely to be stable (Figure 2.4c). With respect to

topographic variables, the partial dependence plot for topographic wetness (TWI) indicates an increased probability of greening at moderate landscape wetness (Figure 2.4d). Values of TWI greater than 7.5, at which significant greening was less likely, were largely associated with the margins of ponds and lakes as well as coastal tundra areas on the Tuktoyaktuk Peninsula.

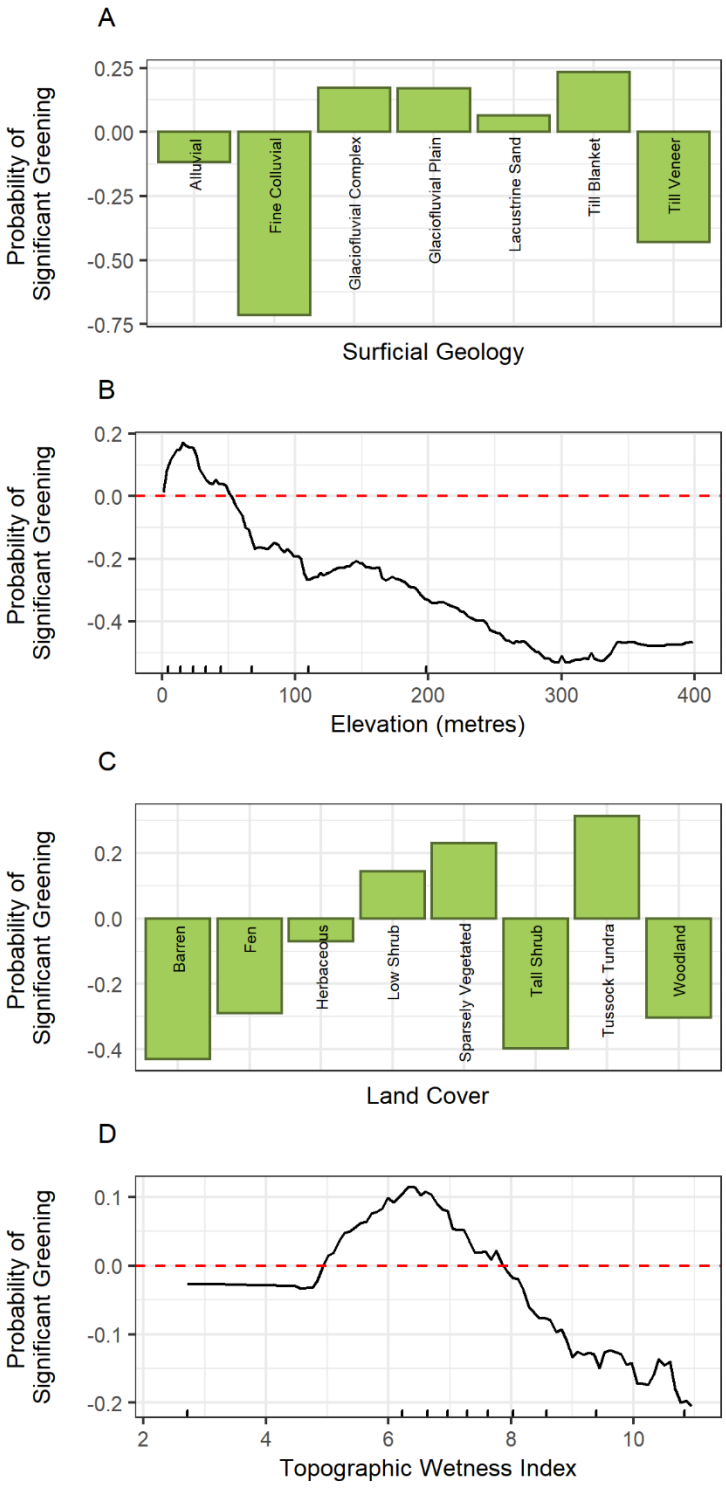

Figure 2.4. Partial dependence plots for top four variables in order of importance from classification random forest: (A) Quaternary surficial geology (Fulton 1989), (B) elevation in metres (Porter and others 2018), (C) land cover in 1984 (Wang and others 2019), and (D) topographic wetness index. The dashed line on the y-axis in plots B and D indicate the point at which elevation (beyond ~50 metres) and wetness (lower than ~5 and greater than ~8) do not impact greening probabilities and are presented with decile rug marks of training data.

2.4.3 Regression Random Forests Analysis

The four most important variables in the regression RF, which predicted the magnitude of greening, were surficial geology, elevation, and land cover, and TWI followed by a suite of variables related to topography (Figure 2.5). This model explained 20.41% of the variance in EVI trend based on the out-of-bag data.

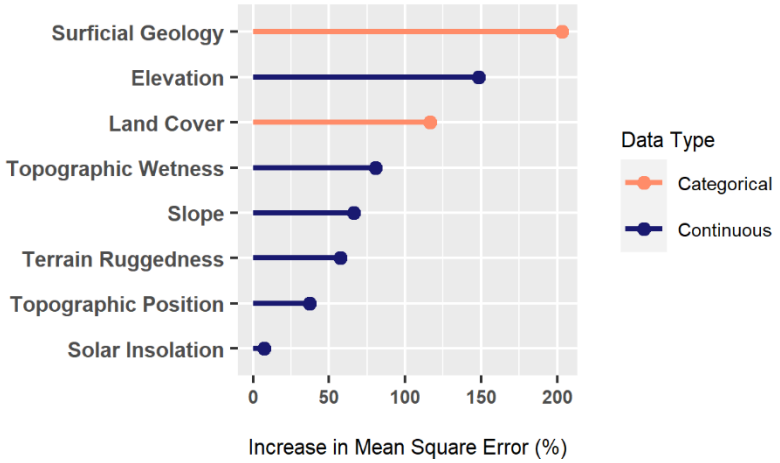

Figure 2.5. Variable importance in the regression random forest (predicting trends in enhanced vegetation index) measured as the percent increase in mean square error scaled by standard error of the change in accuracy.

The partial dependence plots for the regression RF show that lacustrine sands, till blanket, and glaciofluvial complex cover are associated with more rapid greening (Figure 2.6a). Areas underlain by fine colluvium and till veneer had rates of EVI change lower than the average value (3.07×10^{-3} per year) for significantly trended pixels (Figure 2.6a). Areas covered by till blanket comprised roughly 46% of the entire study area, of which, over 51% are significantly greening (Table 2.3). The partial dependence plot for elevation shows that greening was most rapid at lower elevations (Figure 2.6b). At elevations above 50 metres, the calculated mean EVI trend was below the average EVI trend of significantly greening pixels (red dashed line; Figure 2.6b). Tussock tundra, low shrub, and sparsely vegetated land cover classes exhibited the greatest

predicted EVI trends (Figure 2.6c). The mean EVI trends across low shrub and tussock tundra classes were greater than the average EVI trend of significantly greening pixels (Table 2.4). The predicted EVI trend as a function of TWI decreased with higher index values, dropping below the average mean EVI trend of significantly greening pixels at approximately TWI of 8 (Figure 2.6d).

Table 2.3. Summary of Enhanced Vegetation Index (EVI) trends (per year) by surficial geology class in order of proportional cover of study area (Fulton 1989). The last column shows the proportion within each class that exhibited significant greening.

Class	**Mean EVI Trend of Significantly Greening Pixels**	**Standard Deviation of EVI Trend in Significantly Greening Pixels**	**Proportion of Study Area (%)**	**Proportion of Class that is Significantly Greening (%)**
Till Blanket	3.24×10^{-3}	1.13×10^{-3}	46.54	51.58
Glaciofluvial Plain	2.80×10^{-3}	1.13×10^{-3}	16.66	16.71
Fine Colluvial	2.58×10^{-3}	1.29×10^{-3}	11.75	7.74
Till Veneer	2.55×10^{-3}	9.79×10^{-4}	8.49	7.39
Lacustrine Sand	3.46×10^{-3}	1.15×10^{-3}	5.84	6.15
Glaciofluvial Complex	3.18×10^{-3}	1.05×10^{-3}	5.54	6.31
Alluvial	3.00×10^{-3}	1.62×10^{-3}	3.66	3.21
All Classes	$\boldsymbol{3.07 \times 10^{-3}}$	$\boldsymbol{1.19 \times 10^{-3}}$	**-**	**-**

Table 2.4. Summary of Enhanced Vegetation Index (EVI) trends (per year) by land cover class in order of proportional cover of study area (Wang and others 2019). The last column shows the proportion within each class that exhibited significant greening.

Class	Mean EVI Trend of Significantly Greening Pixels	Standard Deviation of EVI Trend in Significantly Greening Pixels	Proportion of Study Area (%)	Proportion of Class that is Significantly Greening (%)
Herbaceous	3.00×10^{-3}	1.14×10^{-3}	29.08	27.66
Low Shrub	3.24×10^{-3}	1.06×10^{-3}	26.33	28.92
Sparsely Vegetated	2.94×10^{-3}	1.24×10^{-3}	13.89	14.34
Tall Shrub	2.95×10^{-3}	1.26×10^{-3}	13.13	11.80
Tussock Tundra	3.21×10^{-3}	1.02×10^{-3}	11.68	13.30
Barren	2.27×10^{-3}	2.44×10^{-3}	2.20	1.13
Woodland	2.91×10^{-3}	1.53×10^{-3}	1.49	1.27
Fen	2.75×10^{-3}	1.29×10^{-3}	1.48	1.37
All Classes	$\boldsymbol{3.07 \times 10^{-3}}$	$\boldsymbol{1.19 \times 10^{-3}}$	-	-

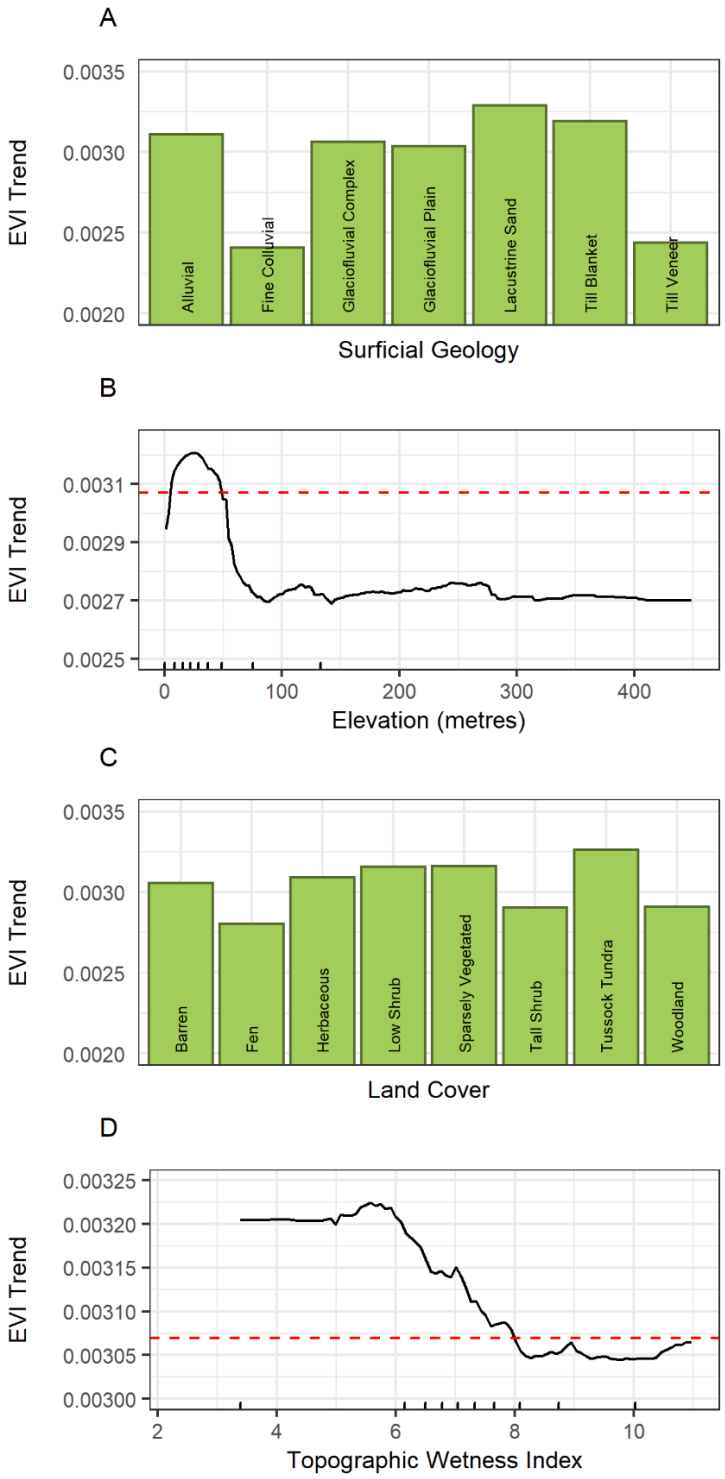

Figure 2.6. Partial dependence plots for the top four variables used in the regression random forest predicting EVI trend (per year): (A) Quaternary surficial geology (Fulton 1989), (B) elevation in metres (Porter and others 2018), (C) land cover in 1984 (Wang and others 2019) and (D) topographic wetness index. Note differing y-axis ranges among plots A-D. The dashed line on the y-axis in plots B and D highlights the mean EVI trend value for significantly greening pixels (3.07×10^{-3} per year). Plots B and D are presented with decile rug marks of training data.

2.4.4 Vegetation Community Analysis

The NMDS ordination shows that heterogeneity in plant community composition was higher in the Tuktoyaktuk Coastlands compared to the Yukon North Slope. Moderate and high greening sites sampled in the Yukon had community composition that was largely indistinguishable from stable sites ($R_{ANOSIM} = 0.039$, $P_{ANOSIM} < 0.05$), whereas the Tuktoyaktuk Coastlands exhibited greater differentiation between sites with moderate and high greening ($R_{ANOSIM} = 0.27$, $P_{ANOSIM} = 0.001$; Figure 2.7).

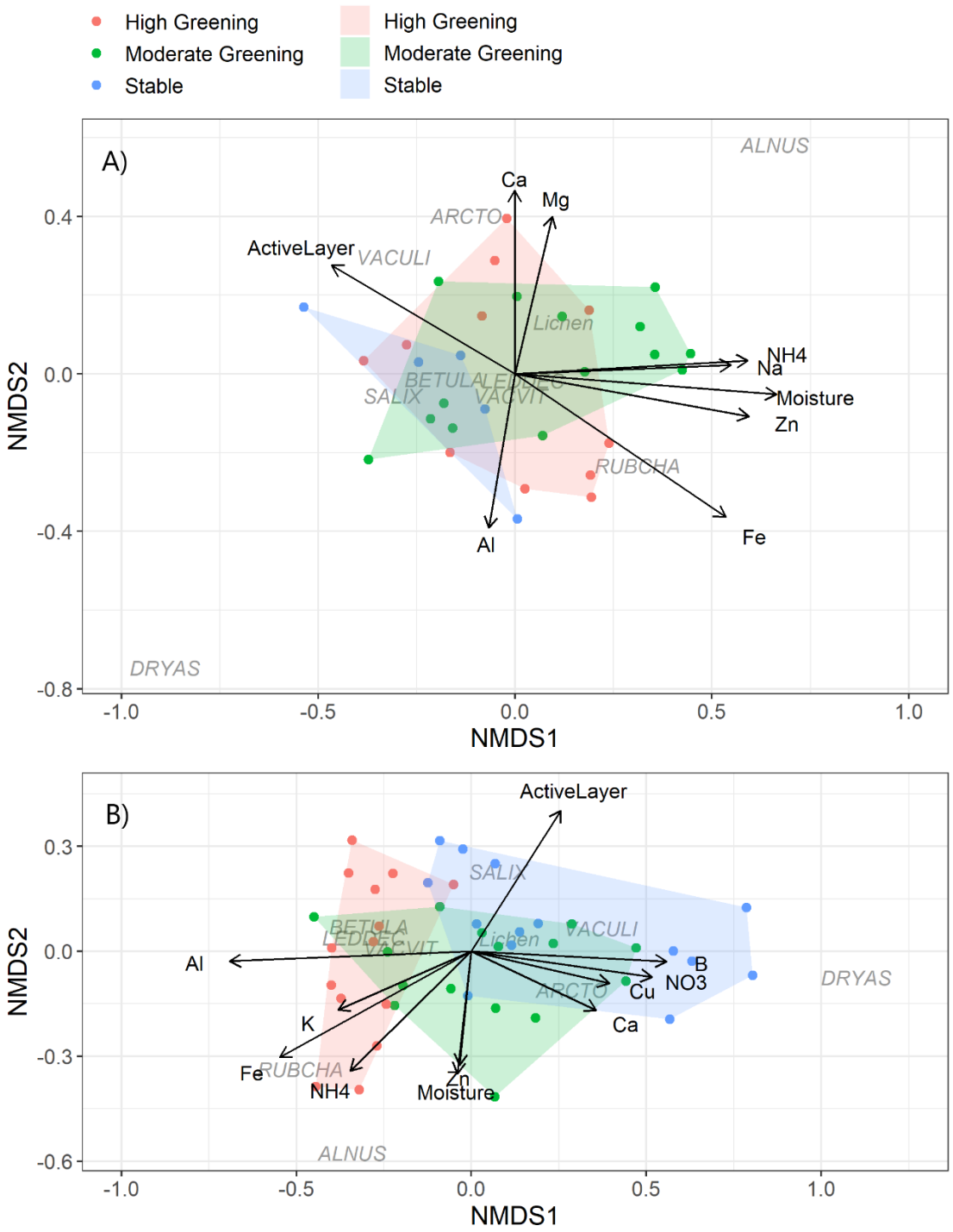

Figure 2.7. Non-metric multidimensional scaling (NMDS) ordination of vegetation community composition across the (A) Yukon North Slope (stress = 0.15) and (B) Tuktoyaktuk Coastlands (stress = 0.13). Sites split by classification with stable, moderate greening, and high greening shown as blue, green, and red points and polygons, respectively with abiotic vectors ($p < 0.1$) overlaid. The ordinations also plot associations between species and functional type (lichen) to cumulative contribution of 65% and NMDS score. Species abbreviations are defined in Table 2.5.

In the Tuktoyaktuk Coastlands, stable and high greening sites exhibited significant differences in community composition (R_{ANOSIM} = 0.27). This difference was driven largely by greater abundance of *Ledum decumbens, Betula spp.* and *Vaccinium vitis-idaea* at high greening sites (Table 2.5). Conversely, we observed greater cover of lichens, *V. uliginosum, Arctostaphylus spp.,* and *Salix spp.* at stable sites (Table 2.5).

Table 2.5. Results of the SIMPER analysis showing the contribution of species and species groups to dissimilarly among site types across the Tuktoyaktuk Coastlands. The table shows the species and species groups accounting for 80% of the total dissimilarity and is ranked by the contribution to dissimilarity. The site type showing higher cover for a given species is shown in bold. The NMDS Code column lists the abbreviations used in Figure 2.7. This analysis was not completed for the Yukon North Slope because there were no differences in community composition among sites.

		Percent Cover		**Contribution to Dissimilarity (%)**	**Cumulative Contribution (%)**
Species	***NMDS Code***	***High Greening***	***Stable***		
Vaccinium uliginosum	VACULI	0.31	**9.80**	8.99	8.99
Ledum decumbens	LEDDEC	**23.53**	3.71	7.12	16.11
Rubus chamaemorus	RUBCHA	**4.81**	0.16	7.06	23.17
Betula spp.	BETULA	**18.49**	3.18	6.93	30.09
Salix spp.	SALIX	2.74	**5.42**	5.9	35.99
Arctostaphylus spp.	ARCTO	1.61	**6.61**	5.79	41.79
Vaccinium vitis-idaea	VACVIT	**23.05**	6.17	5.4	47.19
Alnus crispa	ALNUS	**2.19**	0.39	5.1	52.29
Lichens	-	6.46	**15.44**	4.98	57.27
Dryas spp.	DRYAS	0.00	**2.16**	4.76	62.03
Equisetum spp.	-	0.02	**2.13**	4.62	66.65
Petasites frigidus	-	**3.14**	0.92	4.5	71.15
Graminoids	-	10.47	**13.30**	3.64	74.79
Empetrum nigrum	-	**11.55**	7.67	3.3	78.09
Bryophytes	-	**16.12**	13.44	3.26	81.36

Analysis of data from Wang and others (2019) indicate that sparse and herbaceous cover decreased by 7.5 and 6.2% across the entire study area between 1985 and 2014. These data also

show that low shrub and tall shrub cover increased by 4.8 and 6.0% over this period (Figure 2.8). The pattern of vegetation change was similar in both regions, but the magnitude of increases in shrub-dominant terrain were higher in the Tuktoyaktuk than the Yukon North Slope. The decline in herbaceous cover was also greater in the Tuktoyaktuk Coastlands compared to the Yukon North Slope (Figure 2.8).

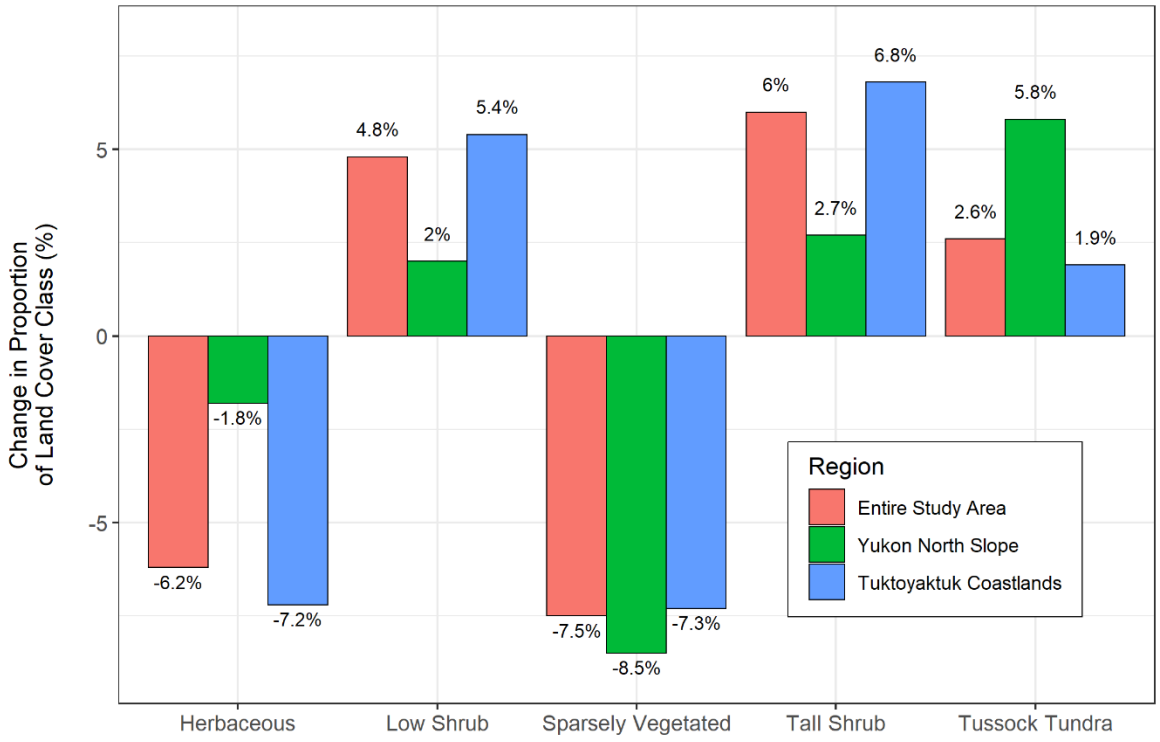

Figure 2.8. Changes in the area of selected land cover classes between 1984 and 2014 across the Yukon North Slope (green), Tuktoyaktuk Coastlands (blue), and both regions combined (red) measured using supervised classifications from Wang and others (2019).

2.5 DISCUSSION

Landscape-scale variation in surficial materials, topography, and vegetation structure were good predictors of changing tundra productivity because these factors influence access to both moisture and soil nutrients. Surficial materials govern the development of tundra soils and control nutrient and moisture availability. Parent materials impact soil formation through differential weathering and the mineral and chemical composition of the substrate (Brady and

Weil 1996; Walker 2000). Poorly sorted materials such as till veneer are often associated with exposed bedrock and are found at higher elevations in the foothills of the Richardson Mountains and on the Anderson Plain (Fulton 1989). These thin tills contain larger gravel and boulders and result in shallow, poorly developed soils that are unable to retain moisture and nutrients (Brady and Weil 1996). Till veneer was associated with stable vegetation in our study area, while the deeper soils that typically develop in areas of till blanket or glaciofluvial complexes were associated with greening (Figure 2.4a) and had higher EVI trend values than the average across the study area (Table 2.3). Finer-grained soils at lower elevation have a larger surface area, are less susceptible to leaching, and are able retain more nutrients for plant uptake (Walker and Everett 1991; Brady and Weil 1996).

The importance of elevation in our RF models indicates that microclimatic variation associated with landscape position also impacts tundra vegetation productivity. Our observation that lower rates of greening and a reduced probability greening were associated with higher elevations suggests that cold temperatures, dry soils, and reduced snowpack on hilltops limit the effects of increasing regional temperatures on tundra productivity. Soils at higher elevation also tend to have more unconsolidated sediments and exposed bedrock, which likely limit productivity because of reduced moisture and nutrients.

Differences in relative elevation drive variation in soil moisture that influence vegetation community development and productivity. Previous research shows that landscape scale variation in temperature, soil moisture and snow accumulation can impact the establishment and growth of tundra plants (Sturm and others 2001; Myers-Smith and others 2011; Niittynen and others 2020a; Niittynen and others 2020b). Our NMDS analysis also showed an association between elevated soil moisture and plant community composition at moderate and high greening

sites (Figure 2.7). A number of recent studies have demonstrated that soil moisture influences tundra vegetation growth (Myers-Smith and others 2015; Cameron and Lantz 2016; Ackerman and others 2017; Bjorkman and others 2018a) and indices of vegetation productivity (Campbell and others 2021; Chen and others 2021). Topographic variation in microclimate and soil moisture have also been shown to be better predictors of tundra greening at fine scales than broader-scale climate-related factors such as the total length of growing season (Gamon and others 2013). Soil moisture levels influenced by microclimate can drive increased nutrient mineralization and are likely an important mechanism of increased productivity (Chapin and others 1988; Deslippe and Simard 2011; Deslippe and others 2012; Mekonnen and others 2021b). More rapid greening associated with moderate levels of topographic wetness indicate that tundra vegetation on mesic to moist soils is most sensitive to regional warming. This is likely because moderate soil moisture limits the negative effects of temperature-induced moisture stress on tundra growth and productivity (Johnson and Caldwell 1975; Dagg and Lafleur 2011; Myers-Smith and others 2015; Ackerman and others 2017). Snowmelt associated with the onset of spring can also increase soil moisture in areas of large drifts, contributing to an influx of moisture to tundra soils. Gamon and others (2013) found that earlier snowmelt was associated with drier soils and lower mid-season NDVI which highlights the complex interaction between moisture availability and growing season. Winter conditions (notably snow cover) are also important to consider since winter is a crucial period in the development of vegetation communities and their functional diversity (Niittynen and others 2020a; Niittynen and others 2020b).

Vegetation type was a good predictor of EVI trends because some functional groups, such as shrubs and graminoids, are more responsive to changes in temperature and soil conditions.

Specifically, many species of deciduous shrub are adapted to respond to changes in nutrients availability, the length of the growing season, and moisture availability at the onset of spring (Chapin and others 1995; Hobbie and Chapin 1998; Bret-Harte and others 2001; Myers-Smith and others 2011; Kelsey and others 2020). Increased productivity in shrub tundra communities was likely also driven by the ability of deciduous shrubs to rapidly allocate resources to secondary growth and asexual reproduction (Bret-Harte and others 2001; Wiedmer and Senn-Irlet 2006; Ropars and Boudreau 2012). Taller, shrub dominated vegetation may also increase soil moisture and nutrient availability via increased snow capture (Sturm and others 2001; Wipf and Rixen 2010; Leffler and others 2016; Niittynen and others 2020a). Observed increases in the productivity of tussock tundra may be related to variability of substrate properties including grain size and soil chemistry that are predicted to favour development of moist-acidic tundra with climate warming (Walker and others 1998; Epstein and others 2004a; Epstein and others 2012). The tussock growth form of species such as *Eriophorum vaginatum* is also highly conducive to growth in nutrient poor environments through nutrient cycling within tussocks (Cholewa and Griffith 2004) and growth of deeper roots (Chapin and others 1988). Our results are also consistent with a number of studies linking tundra greening with productive cover types (Jia and others 2006; McManus and others 2012; Frost and others 2014; Campbell and others 2021; Chen and others 2021) and shrub proliferation in the low Arctic in particular (Tape and others 2006; Ropars and Boudreau 2012; Lantz and others 2013; Frost and others 2014; Moffat and others 2016). Our comparisons of land cover over time also show that the proportion of shrub and tussock tundra have increased since 1984 in our study regions. Higher cover of shrubby vegetation types in the Tuktoyaktuk Coastlands likely drove differences in the extent and distribution of greening between regions. Past research in this region has also shown an

association between gains in shrub and herbaceous cover and increases in NDVI (Wang and Friedl 2019). The Yukon North Slope has experienced less of a transition to shrub tundra than the Tuktoyaktuk Coastlands (Figure 2.8) with greater overall similarity in community composition across the region (Figure 2.7) and we attribute the difference in the extent of observed greening between these two regions (Table 2.2) to differences in the intensity of shrub proliferation.

Average annual and summer temperatures across the Beaufort Delta region have increased by 3.5 ℃ and 1.9 ℃, respectively, between 1926 and 2019 (Travers-Smith and Lantz 2020) with largely homogenous warming across the region (Vincent and others 2015). Widespread increases in tundra productivity are likely a response to the direct and indirect effects of this warming. Productivity responses to warming are well documented, but environmental limitations also drive differences in the response of vegetation across the Arctic (Walker and others 2006; Hudson and Henry 2009; Elmendorf and others 2012; Myers-Smith and others 2015). NDVI trends across the Arctic Coastal Plain of Alaska also show complex responses to changes in temperature and precipitation across terrain types, suggesting that climatic drivers are mediated by regional environmental factors (Lara and others 2018). Underlying climate drivers, landscape and regional variability in soils and topography are key determinants of spatial heterogeneity in vegetation responses (Raynolds and others 2008; McManus and others 2012; Lara and others 2018). This conclusion is consistent with recent studies on spatial patterns of productivity trends across northwestern North America (Chen and others 2021) and on Banks Island (Campbell and others 2021), and complements previous research highlighting terrain variability driving these regional patterns (Jia and others 2006; Tape and others 2006; Walker and others 2009; McManus and others 2012; Tape and others 2012; Berner and others 2020; Niittynen and others 2020a).

Our results using EVI trends to map tundra greening are comparable to those of studies using NDVI responses suggesting similar spatial patterns of greening (Myers-Smith and others 2020) and mechanisms driving vegetation change (Jia and others 2006; Raynolds and others 2008; McManus and others 2012). Further, EVI uses additional spectral and angular information not used by NDVI, implemented to address known issues with NDVI related to solar incidence and atmospheric conditions present (Liu and Huete 1995).

While some researchers recommend accounting for temporal autocorrelation in time series through pre-whitening methods (Guay and others 2014; Berner and others 2020), we do not believe that this is an issue in our analyses given the temporal revisit rate of the data used and the rates of phenological development present in tundra ecosystems. Weak evidence of temporal autocorrelation of NDVI have also been documented in areas dominated by deciduous vegetation compared to evergreen vegetation due to seasonal foliage replacement and other differences in reliance on previous-year nutrient storage (Berner and others 2011). Additionally, our methods are consistent with other studies using vegetation index time series that do not implement pre-whitening procedures (Fraser and others 2014b; Nitze and Grosse 2016; Raynolds and Walker 2016; Lara and others 2018).

The Tuktoyaktuk Coastlands and Yukon North Slope provide habitat to a diversity of mammals including caribou, muskox, bears, wolves, Dall's sheep, red fox, and wolverine (Russell and others 1993; YEWG 2004; Rickbeil and others 2018). Our observation that tussock and dwarf shrub tundra at lower elevations are most prone to increased vegetation productivity suggest that caribou who utilize this habitat type while avoiding upright shrub tundra (Russell and others 1993; Johnstone and others 2002; Rickbeil and others 2018) will be significantly impacted by ongoing vegetation change. The impacts of vegetation change on habitat use in this region

should be assessed by combining landscape-scale data on vegetation change with satellite telemetry data for caribou and other important species (see: Rickbeil and others 2018). Range expansion of moose (Tape and others 2016) and beavers (Jung and others 2016) may also be related to vegetation change and should be explored using systematic surveys and satellite telemetry.

Several recent analyses suggest that coarse resolution imagery can mute the complexities of finer-scale ecological patterns resulting in disagreement among coarse-scale remote sensing platforms (Guay and others 2014; Berner and others 2020; Myers-Smith and others 2020). Our findings show that landscape scale variation in biophysical characteristics strongly influence vegetation dynamics evident in moderate-resolution (30 m) Landsat imagery. Since tundra ecosystems exhibit heterogeneity at scales of 1-2 metres (Epstein and others 2004b; Lantz and others 2010b; Assmann and others 2020; Myers-Smith and others 2020), it is possible that change detection using higher-resolution sensors (such as 0.5 – 3 m resolution imagery from WorldView, QuickBird, and PlanetScope) could account for some of the unexplained variation in our models. We suggest that future research utilize high-resolution sensors calibrated to temporally contemporaneous Landsat (Markham and Helder 2012; Belward and Skøien 2015) or Sentinel-2 (Drusch and others 2012) imagery. This integration of measurements from a greater variety of sensing platforms and the use of Sentinel-2 imagery cross-calibrated with Landsat offers a compelling advance in remote sensing capabilities (Wulder and others 2015; Claverie and others 2018) and to avail upon samples of fine scale earth observations to improve models or offer insights on the nature of local vegetation heterogeneity.

Recent work using remotely piloted aircraft systems (RPAS; or drones) also emphasizes the influence of fine-scale variability in topography on the composition and productivity of tundra

plant communities (Assmann and others 2020; Cunliffe and others 2020; Myers-Smith and others 2020). Increased affordability of RPAS systems has facilitated the collection of higher spatial resolution data representing increasingly large areas and future research can take advantage of these tools to monitor changes at fine scales (Fraser and others 2016; Assmann and others 2020; Cunliffe and others 2020). We encourage the use of RPAS surveying under standardized flight and recording protocols, such as through the High Latitude Drone Ecology Network (HiLDEN; *arcticdrones.org*), to address this gap in spatial data. These data can help further explain the complex interactions between vegetation and environmental and climatic influences across spatial scales while covering greater area than is possible with ground surveys. Vegetation indices derived from satellite imagery (such as EVI or NDVI) may be influenced by factors altering surface reflectance like standing water or vegetative stress (Roy 1989; Ollinger 2011). Higher resolution imagery will make it possible to assess the influence of soil moisture, physiological stress, and disease on vegetation indices.

2.6 CONCLUSIONS

Global climate change is driving rapid increases in vegetation productivity across northern latitudes. The spatial heterogeneity in productivity trends highlighted in this study are the result of finer-scale, landscape processes that mediate the effects of regional climate warming. Surficial geology and topography are among the best predictors of spatial pattern in tundra greening because they influence soil conditions and moisture. Vegetation type also strongly influence changes in productivity because deciduous shrubs can respond rapidly to changes in moisture, nutrients, and temperature. Tundra vegetation change will impact wildlife habitat (Rickbeil and others 2018), surface energy balance, and carbon storage (McGuire and others 2006; Schaefer and others 2014) and understanding the drivers of landscape scale variation in vegetation shifts is

critical to accurately characterize these relationships. We encourage continued research using random forests modelling to identify the role of regional processes as they relate to broader environmental change across spatial and temporal scales.

3 Investigating the effects of data type on species distribution models of tundra shrubs in the western Canadian Arctic and projections under future climate warming

Jordan H. Seider[1], Trevor C. Lantz[1], Christopher Bone[2]

1. School of Environmental Studies, University of Victoria
2. Department of Geography, University of Victoria

3.1 INTRODUCTION

Species distribution modelling is a common technique used to quantify the influence of climate and terrain factors on species' ranges and to assess the impacts of climate warming on their future distributions (Guisan and Zimmermann 2000). Several correlative modelling techniques including linear modelling, machine learning, and ensemble models combining multiple methods are used to relate ecological predictors to species occurrence data. Many species distribution models (SDMs) utilize presence-only data, which are widely available in open-access repositories such as the Global Biodiversity Information System (*gbif.org*). With the exception of profile techniques (e.g. BIOCLIM, DOMAIN, ecological niche factor analysis), models built using presence-only data rely on randomly selected pseudo-absence (or background) data to represent absence locations, which are used to provide information on the total variability in environmental predictors across a selected area (Phillips and others 2009). Previous studies have shown that the use of pseudo-absence data can negatively impact model performance and interpretation through sampling bias and poor data quality and spatial accuracy (Pearce and Boyce 2006). When pseudo-absence locations do not complement spatial coverage and sampling effort of presence observations, model predictions lose the ability to accurately portray distributions across the entire study domain (Phillips and others 2009). However, standard performance metrics indicate that many studies using pseudo-absence data have also performed favourably (Barbet-Massin and others 2018; Zhang and others 2019; Kaky and others 2020).

In their review of 250 SDM studies, Santini and others (2021) found over 84% of SDMs used pseudo-absences or background data. In many such cases, pseudo-absences are used to represent locations where species are not present in logistic regression or other binary response methods that require absence data (Wisz and Guisan 2009). However, a lack of best practices to determine

pseudo-absence locations adds to the confusion and reduced interpretability of SDM studies using this approach (Barbet-Massin and others 2012; Santini and others 2021). To the best of our knowledge, few studies have addressed differences in model predictions and accuracy as a result of differences in data type. In this study, we investigate how data type (true absence or pseudo-absence) influences: 1) SDM performance, 2) estimates of habitat suitability, and 3) projections of change in habitat suitability for three common tundra shrub species. By exploring the use of different data types, we seek to understand how differences in the data type may influence the application of SDMs.

This study focusses on the Beaufort Delta region in the western Canadian Arctic, an area experiencing the most rapid temperature increases in Canada (Vincent and others 2015). This warming is increasing the productivity of tundra landscapes (Tape and others 2006; Lantz and others 2013; Fraser and others 2014a; Campbell and others 2021; Seider and others In Review) and facilitating widespread shrub proliferation (Lantz and others 2013; Moffat and others 2016; Travers-Smith and Lantz 2020). In our analysis, we explore differences in the sensitivity of three shrub species to climate change by comparing projected changes in habitat suitability with climate warming. Specifically, we developed SDMs for *Alnus viridis* (green alder, a deciduous tall shrub), *Betula glandulosa* and *B. nana* (dwarf birch, a deciduous dwarf shrub), and *Vaccinium vitis-idaea* (lingonberry, an evergreen dwarf shrub) and applied a future high-emissions climate scenario projecting habitat suitability to the period between 2061 and 2080.

Documenting variation in the responses of different shrub species to climate change is important as vegetation structure has a significant impact on the climate system (Bonan and others 2003; Port and others 2012). Since shrubs influence carbon cycling and permafrost dynamics, understanding change is important for existing global climate models (McGuire and others

2006). Accurate projections of changes in shrub abundance are also important because shrubs are expected to significantly impact wildlife (Joly and others 2007) and Inuvialuit and Gwich'in communities (Wildlife Management Advisory Council and Aklavik Hunters and Trappers Committee 2018). Our investigation into SDM parameterization can provide insights on the use of these modern techniques as they apply to climate modelling and ecosystem conservation.

3.2 METHODS

3.2.1 Study Area

This study focuses on the Beaufort Delta region of the northern Yukon and Northwest Territories, covering an area of approximately 161,000 km^2 (Figure 3.1). The southern portion of this area includes the Yukon and Tuktoyaktuk Coastal Plains and the Bathurst Peninsula ecoregions, which are characterized by rolling hills dominated by shrub and tussock tundra as well as low lying wetland habitats (Yukon Ecoregions Working Group [YEWG], 2004; Ecosystem Classification Group [ECG], 2012). The Yukon and Tuktoyaktuk Coastal Plain ecoregions are separated by the Mackenzie Delta ecoregion, which consists of low-lying alluvial terrain where a mosaic of forest, woodland, shrubland, and sedge wetland is strongly influenced by the hydrology of the delta (Gill 1972, 1973; Pearce 1986; Burn and Kokelj 2009). The northern part of the study area includes the Banks Island Coastal Plain and Banks Island Lowland ecoregions, a mid-Arctic landscape characterized by hummocky tills and glaciofluvial plains with some exposed bedrock throughout (ECG, 2012). Vegetation communities on Banks Island are controlled primarily by soil moisture (Campbell and others 2021) with well-drained upland terrain occupied by a mix of barrens and dwarf-shrub tundra and wetter lowland terrain dominated by more productive sedge tundra (ECG, 2012). All regions within the study area are underlain by continuous permafrost and exhibit common permafrost features such as polygonal

terrain, hummocks, and thaw slumps (Rampton 1982, 1988; YEWG, 2004; ECG, 2012). With the exception of the Yukon Coastal Plain and of the northern tip of Tuktoyaktuk Peninsula, the study area was covered by the Laurentide Ice Sheet during the Wisconsinan Glaciation (Jessop 1971; Rampton 1988; ECG, 2012).

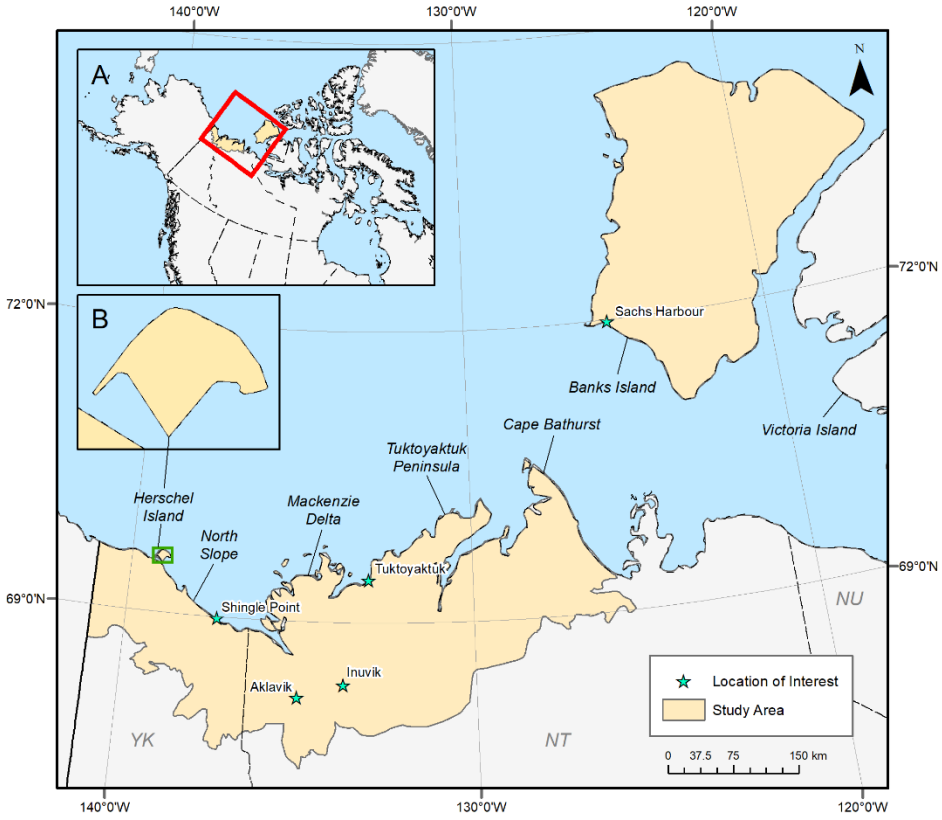

Figure 3.1. Map of the study area in the Beaufort Delta region. Inset A shows the extent of main map (red) in North America and inset B is an enlargement of Herschel Island (the green rectangle on the main map).

3.2.2 Study Design Overview

To investigate the influence of data type on ensemble SDM performance and predictions of habitat suitability of three common tundra shrubs (alder, birch, and lingonberry), we created two models for each species: one using true absence data and one using pseudo-absence data. Since all other model parameters and environmental variables remained constant, we attribute differences in model performance and predictions of suitability to data type. Additionally, we

projected habitat suitability for each species into the future using a high-emissions climate scenario for 2061-2080 to relate our current understanding of tundra shrub to potential shifts in their future distributions.

3.2.3 Species

We selected species for this analysis representing three shrub functional types. Green alder (*Alnus viridis*, also known as *A. crispa*, or more recently, *A. alnobetula*) was selected to represent deciduous tall shrubs. This tall shrub has a broad distribution across the northern hemisphere and is known to establish on newly formed mineral soils after disturbance (Furlow 1979). Green alder is primarily a subarctic species (Furlow 2020), but several recent studies have documented increases in alder stand density and abundance across the low Arctic tundra of Alaska (Tape and others 2006), Northwest Territories (Travers-Smith and Lantz 2020), Labrador (Larking and others 2021), and Siberia (Frost and Epstein 2014). As an exemplar of deciduous dwarf shrubs, we used a species complex including *Betula glandulosa* and *B. nana*. These dwarf birches are both found on nutrient-poor, well-drained, moist-acidic soils across the circumpolar (De Groot and others 1997). They are taxonomically confused, particularly where their ranges overlap and hybridization makes species identification difficult (De Groot and others 1997). For this reason, we consider observations of both these species to represent the deciduous shrub functional type. Finally, lingonberry (*Vaccinium vitis-idaea*) is an evergreen dwarf shrub common across the low Arctic and southern boreal on dry to moist soils (Taulavuori and others 2013). Throughout this paper, we refer to each species by its common name (alder, birch, and lingonberry).

Plot-level presence/absence data used to parameterize regional models were obtained from a number of sources. Vegetation data from the NWT were collected from surveys conducted between 2005 and 2019 (see: Lantz and others 2009; Lantz and others 2010a; Gill and others

2014; Steedman 2014; Cameron and Lantz 2016; Chen 2020; Travers-Smith and Lantz 2020; Shipman 2021; Seider and others In Review). Vegetation cover data from across northern Yukon were obtained, with permission, from the Yukon Biophysical Inventory System (Yukon Territorial Government 2021). These data were collected from field surveys conducted between 2000 and 2015. Data from southern Banks Island were obtained, with permission, from the Canadian Wildlife Service (see: Campbell and others 2021). To use these percent cover data in our SDMs, we converted them to presence/absence for each species at each site. The spatial accuracy of the plot locations all of these data sources is much greater that the 30 arcseconds resolution of the environmental predictors. To minimize the possibility of pseudo-replication and to ensure that models were not trained using multiple observations within the same cell, we implemented a spatial thinning procedure to ensure no two observations were closer than 5 km using the *ensemble.spatialThin* function from the *BiodiversityR* package (version 2.12-3; Kindt and Coe 2005). We chose the thinning distance of 5 km as a conservative buffer since the spatial resolution of 30 arcseconds of predictor variables at the northern-most point of our study area is approximately 1 km. Maps of the presence and absence locations post-thinning for each species are presented in Supplementary Figures 4-6.

To use these data in presence-only models, we converted presence/absence data to presence-only data by removing any observations of true absences from the data. We then used a random pseudo-absence strategy selecting points with a minimum distance of 5 km from presence locations to generate pseudo-absence points using the *BIOMOD_FormatingData* function. This strategy implements a random selection of points from all possible cells of predictor data outside the pre-determined buffer (see: Fournier and others 2017; Kaky and others 2020) providing a sample of predictor variability that can be contrasted to the variability within presence locations

(Phillips and others 2009). We used three repeats of pseudo-absence selection with the total number of pseudo-absence points in each selection equal to the number of observed presence locations. We used the average model predictions from all pseudo-absence selections to generate ensemble predictions of habitat suitability.

3.2.4 Climate Predictor Variables

Historic (1970-2000) climate data (30 arcsecond resolution) used to parameterize our models were obtained from the WorldClim v2.1 dataset (Fick and Hijmans 2017). Climate parameters in this dataset consist of 19 ecologically relevant variables derived from average monthly temperature and precipitation values (Fick and Hijmans 2017). We performed a hierarchical cluster analysis on these data and grouped the 19 variables using the resulting correlation matrix. Variables were grouped if they had a Pearson's r greater than 0.7, following the method used by Fournier and others (2017). We then selected one variable from each group to best represent a diversity of climate factors relating to temperature and precipitation. Based on this clustering (Supplementary Figure 7), we chose the following seven variables to represent climate across the study area: annual mean temperature, mean diurnal range, isothermality, temperature seasonality, mean temperature of the coldest quarter, precipitation seasonality, and precipitation of the warmest quarter (Table 3.1).

Table 3.1. Bioclimatic variables from WorldClim (Fick and Hijmans 2017) used in this analysis. Variable descriptions are from on O'Donnell and Ignizio (2012).

Identifier	Bioclimatic Variable	Variable Description
BIO_01	Annual Mean Temperature	Average of monthly mean temperature (°C)
BIO_02	Mean Diurnal Range	Average of monthly temperature ranges (°C)
BIO_03	Isothermality	Mean diurnal temperature range divided by annual temperature range
BIO_04	Temperature Seasonality	Temperature variability over the year measured as a ratio of the standard deviation of the monthly mean temperatures to the mean monthly temperature (%)
BIO_11	Mean Temperature of the Coldest Quarter	Mean temperature of the coldest consecutive three months (°C)
BIO_15	Precipitation Seasonality	Variation in monthly precipitation over the year measured as a ratio of the standard deviation of the monthly total precipitation to the mean monthly total precipitation (%)
BIO_18	Precipitation of the Warmest Quarter	Sum of monthly precipitation values for the three warmest consecutive months

Species range projections utilized downscaled global climate model (GCM) data from the Coupled Model Intercomparison Project Phase 5 (CMIP5; Taylor and others 2012). To obtain these data, we followed methods described in Lee et al. (2019) and used a multi-model ensemble of four GCMs (CCSM4 from the National Center for Atmospheric Research, GFDL-CM3 from the Geophysical Fluid Dynamics Laboratory, HadGEM2-ES from the Met Office Hadley Centre, and MPI-ESM-LR from the Max Planck Institute for Meteorology). We chose the RCP8.5 scenario developed for CMIP5 to base our models on the most severe estimates of future warming. This "worst-case" scenario presents a future defined by high carbon emissions with radiative forcing of 8.5 W/m^2 by 2100 (Moss and others 2010). These GCMs are available as downscaled data using WorldClim (version 1.4) as the climate baseline and averaged from 2061 to 2080 to 30 arcseconds resolution (Hijmans and others 2005). To create the ensemble climate projection, we took a simple average of each individual bioclimatic variable from each GCM, as obtained from WorldClim, using the *terra* package. Maps of each variable under current and future climate conditions are presented in Supplementary Figures 8 and 9.

3.2.5 Environmental Predictor Variables

We used elevation data from the ArcticDEM available from the Polar Geospatial Center (Porter and others 2018) to create a 2-metre resolution digital elevation model (DEM) across the study area. We aggregated the DEM to 30-metre resolution by taking the mean of the sub-pixels before applying any further transformations to improve data processing efficiency. Cells of missing data in this DEM were filled using the Multi-Error-Removed Improved Terrain (MERIT) DEM (Yamazaki and others 2017) that we resampled to match the resolution and extent of the ArcticDEM area using the bilinear method in the *resample* function of the *terra* package. We calculated slope using the *terrain* function from the *terra* package and the vector ruggedness measure (VRM) using the tool developed by Sappington et al. (2007) implemented in ESRI ArcMap (version 10.6.1). VRM provides a measure of ruggedness that is independent of slope and is represented as an index value between 0 and 1, where 0 is considered flat and 1 is most rugged (Sappington and others 2007). Throughout this paper, we refer to VRM as "ruggedness". We resampled all environmental data from 30 metres to match the 30 arcseconds resolution used in this analysis using the bilinear method of the *resample* function in the *terra* package. Maps of elevation, slope, and ruggedness are presented in Supplementary Figure 10. We also used the NASA ABoVE annual land cover classification (Wang and others 2019) to remove any cells from the analysis that were classified as "water" in 2014 (the last available year of data).

3.2.6 Species Distribution Modelling

We evaluated the influence of data type: 1) presence/absence data and 2) presence/pseudo-absence data on species distribution models (SDMs) for three tundra shrub species representing different functional types (deciduous tall shrub, deciduous dwarf shrub, and evergreen dwarf

shrub). We also used these models to investigate the relative response of each species to climate change under projected climate warming scenarios.

Ensemble SDMs were generated using the *biomod2* package (version 3.4.13; Thuiller and others 2020) in the R statistical software (R Core Team 2019). Ensemble models included generalized linear models (GLM), generalized boosted models (GBM), multiple adaptive regression splines (MARS), artificial neural networks (ANN), and random forests (RF) algorithms, which were set to use default modelling options in the *biomod2* package. These models represent a mix of traditional linear techniques (GLM and MARS), decision trees (GBM, and RF), and machine learning (ANN, GBM, and RF) algorithms. Ensemble SDM analyses commonly use a wide variety of such algorithms with successful results (Fournier and others 2017; Lee and others 2019; Kaky and others 2020). We chose to use an ensemble method because recent work has shown that no single SDM algorithm has superior prediction power (Segurado and Araújo 2004; Hao and others 2020). The ensemble method has also been shown to out-perform individual models in SDM studies (Marmion and others 2009). We generated ensemble models to create projections of species habitat suitability by taking the mean of individual models as described in Table 3.2. We also used ensemble models to project future habitat suitability using CMIP5 RCP8.5 climate data.

Table 3.2. Model descriptions.

Algorithm	R Package	Description
Generalized Linear Model (GLM)	*glm*	Extension of ordinary linear regression allowing for error distributions other than Gaussian.
Generalized Boosted Model (GBM)	*gbm*	Non-parametric method using a combination of decision tree models implemented with boosting methods for weighted randomization of data in each successive tree.
Multiple Adaptive Regression Splines (MARS)	*earth*	Non-parametric method creating multiple linear regression models (with different slopes) across the range of data and finding the optimal connection points between each segment to create one model.
Artificial Neural Networks (ANN)	*nnet*	Single hidden layer neural network using back-propagation to adjust weights and biases to increase model performance.
Random Forests (RF)	*randomForest*	Ensemble decision tree algorithm incorporating randomized bagging method to subset available data used in each individual tree. Data are run through all trees and the final classification is based on the majority vote.

To independently evaluate the performance of ensemble SDMs, we used independent validation data to calculate the true skill statistic (TSS). For each ensemble model, we set aside a random subset of 20% of the data for this purpose. TSS values between 0.41 and 0.6 are interpreted as exhibiting "moderate" agreement while values greater than 0.6 are interpreted as exhibiting "substantial" agreement or predictive performance (Landis and Koch 1977). TSS is preferred over the area under the receiver operating characteristic curve (commonly, AUC) because it is independent of species prevalence (Allouche and others 2006).

To understand the potential drivers of shrub species' distributions in the Beaufort Delta region and assess the influence of environmental predictors on habitat suitability under projected climate warming we used the variable importance function in *biomod2*. This function calculates variable importance by randomizing a single variable in each of five randomized permutations to

calculate the correlation between the predictions of the complete and randomized-variable ensemble models (Thuiller and others 2020). Variables that have a lower correlation value when removed from the model are assumed have greater influence on model predictions.

3.3 RESULTS

All the SDMs constructed in this analysis had TSS scores indicating reasonable model performance with scores ranging from 0.600 (for the birch pseudo-absence model) to 0.762 (for the alder true absence model; Table 3.3). TSS scores were similar among all models but there were large differences in habitat suitability projections between true absence and pseudo-absence models (Figures 3.2-3.4). The SDMs for current climate conditions showed clear differences in habitat suitability predictions between data types. For alder, the pseudo-absence model projected greater suitability along the coastal margin of the Yukon North Slope and near the community of Tuktoyaktuk compared to the true absence model, in which the highest habitat suitability was located in the southern part of the study area (Figure 3.2). Birch and lingonberry had similar habitat suitability, but the spatial pattern varied between models using true absence and pseudo-absence data (Figures 3.3 and 3.4). The true absence models for these species showed high suitability over a large area including the Tuktoyaktuk Coastlands and Bathurst Peninsula and extending eastward to the area south of Cape Bathurst (locations referenced in Figure 3.1). In contrast to this, the pseudo-absence models for birch and lingonberry had the highest suitability across the Yukon North Slope, Herschel Island, and a more restricted portion of the Tuktoyaktuk Coastlands. The pseudo-absence models for birch and lingonberry also had lower overall suitability across the entire study area compared to the true absence models for these species (Table 3.4).

Differences in projected future habitat suitability also varied between true absence and pseudo-absence models. The spatial pattern of future suitability for alder was similar between data types with the notable difference that the pseudo-absence model predicted a weaker response to warming (Figure 3.2). The projected responses of birch habitat suitability to future climate using the true absence model showed a moderate increase in suitability across the southern regions, while the pseudo-absence model showed a reduction in habitat suitability in the southern part of the study area accompanied by a relatively small increase on Banks Island (Figure 3.3). This same pattern was evident in the models for lingonberry (Figure 3.4).

True absence and pseudo-absence models also showed considerable variation in the variables driving model projections (Table 3.5). For all species, elevation was a more important variable the pseudo-absence models compared to their true absence counterparts. Differences in variable importance between data types were otherwise species-dependent. Precipitation of the warmest quarter was the second most important variable in the pseudo-absence model for alder whereas this variable ranked sixth in the true absence model (Table 3.5). Precipitation and temperature seasonality ranked top in the true absence alder model with these same variables ranking lower at third and seventh in the pseudo-absence model, respectively (Table 3.5). Mean temperature of the coldest quarter was important in pseudo-absence models for birch and lingonberry, whereas mean diurnal range was important in true absence models for these species (Table 3.5).

Projected shifts in habitat suitability in response to climate warming showed similar patterns, but large differences in the magnitude of change among species. SDMs projected that climate warming will enhance habitat suitability beyond the current range limits of alder, birch and lingonberry (Table 3.4). However, contrary to our expectations, climate warming reduced habitat suitability for all three species in the centre of the study area (Figure 3.2-3.4). Projections of

alder habitat suitability under RCP8.5 in the true absence model showed reduced suitability in the centre of the study area and moderate increases in suitability beyond its current range on Banks Island. A similar response was evident for birch and lingonberry, but the overall increases in suitability were greater than that of alder. Lingonberry modelled using true absence data exhibited the greatest increase in suitability across the entire study area (increase of 0.267; Table 3.4). The response for birch and alder were slightly lower at 0.162 and 0.173, respectively (Table 3.4). Histograms of the distribution of habitat suitability for each SDM are presented in Supplementary Figures 11-13. Average current and future habitat suitability for alder was the lowest among the three shrubs; however, increases in suitability were of a similar magnitude as birch. Important variables in the true absence alder model were different than in both birch and lingonberry models. In the alder model, precipitation and temperature seasonality were the most important, while mean annual temperature and mean diurnal range were most important in birch and lingonberry models (Figure 3.5). Across both data types and all species, slope, ruggedness, and isothermality were the variables with the lowest importance.

Table 3.3. Ensemble model performance measured using the True Skill Statistic (TSS) calculated using independent data. Bolded values indicate the highest performing model for each species.

	True Absence Model	**Pseudo-absence Model**
Alder (*Alnus viridis*) Deciduous Tall Shrub	**0.762**	0.726
Birch (*Betula nana* and *B. glandulosa*) Deciduous Dwarf Shrub	**0.733**	0.600
Lingonberry (*Vaccinium vitis-idaea*) Evergreen Dwarf Shrub	0.603	**0.746**

Table 3.4. Mean and standard deviation of habitat suitability across the entire study area for each model under current (1970 to 2000) and future (2061 to 2080) climate.

		True Absence		**Pseudo-absence**	
		Mean	*Standard Deviation*	*Mean*	*Standard Deviation*
Alder (*Alnus viridis*) Deciduous Tall Shrub	*Current*	0.122	0.171	0.122	0.210
	Future	0.295	0.079	0.212	0.082
	Change	*0.173*	-	*0.090*	-
Birch (*Betula nana* and *B. glandulosa*) Deciduous Dwarf Shrub	*Current*	0.345	0.316	0.247	0.280
	Future	0.507	0.097	0.312	0.063
	Change	*0.162*	-	*0.065*	-
Lingonberry (*Vaccinium vitis-idaea*) Evergreen Dwarf Shrub	*Current*	0.341	0.311	0.228	0.274
	Future	0.608	0.088	0.315	0.083
	Change	*0.267*	-	*0.087*	-

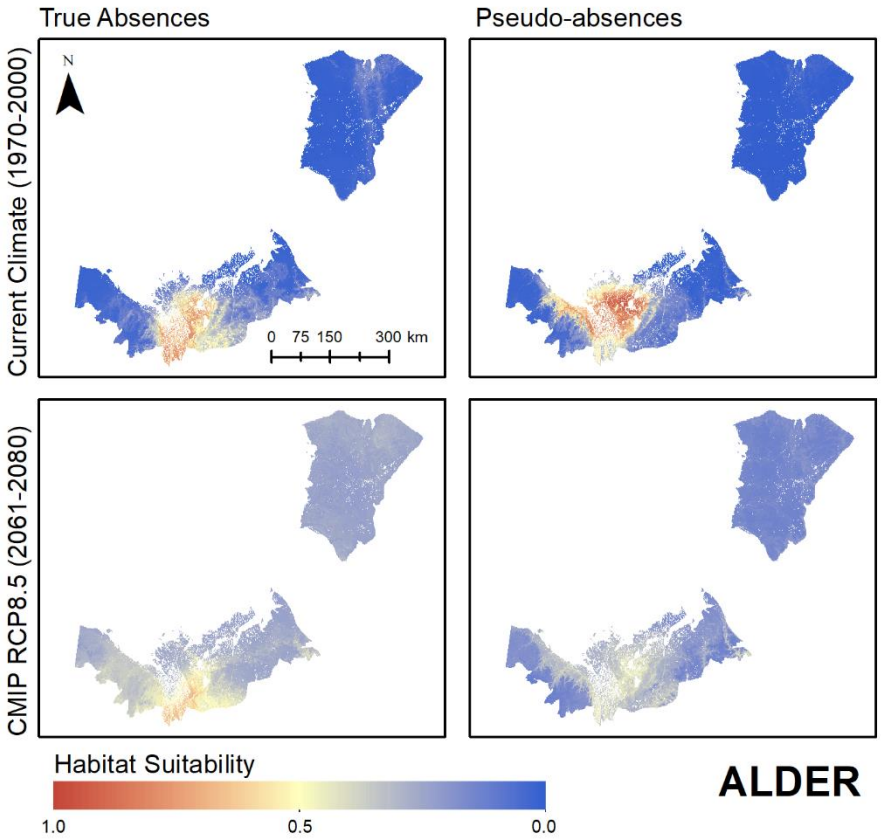

Figure 3.2. Ensemble habitat suitability maps for alder (*Alnus viridis*) projected under current and future climate conditions using true absence and pseudo-absence models.

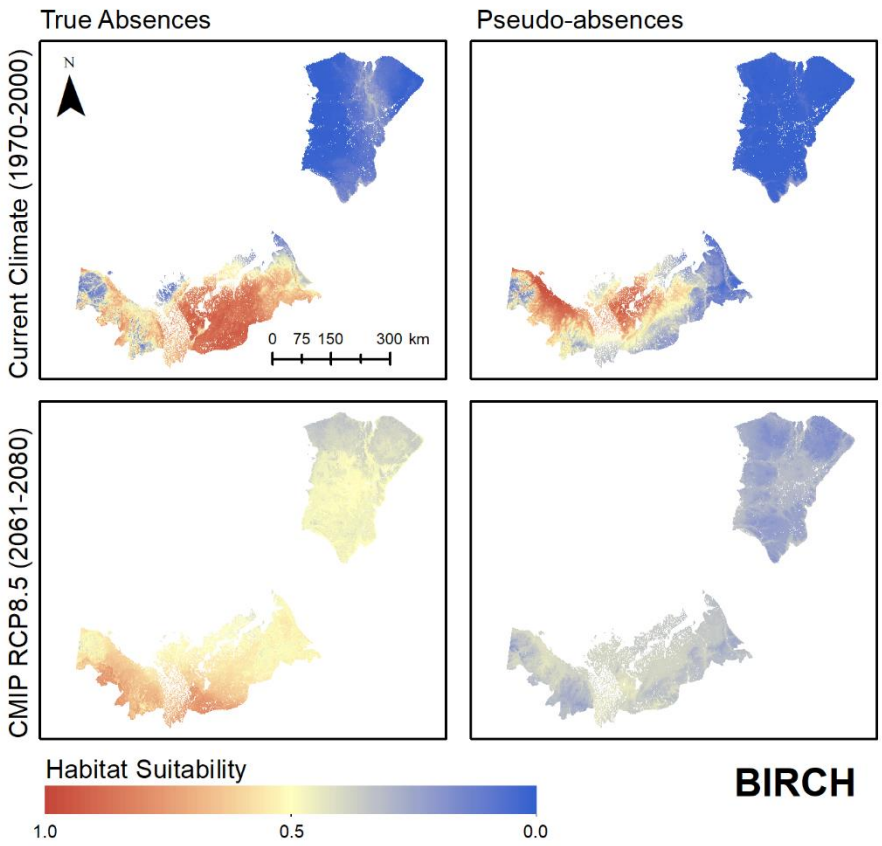

Figure 3.3. Ensemble habitat suitability maps for birch (*Betula nana* and *B. glandulosa*) projected under current and future climate conditions using true absence and pseudo-absence models.

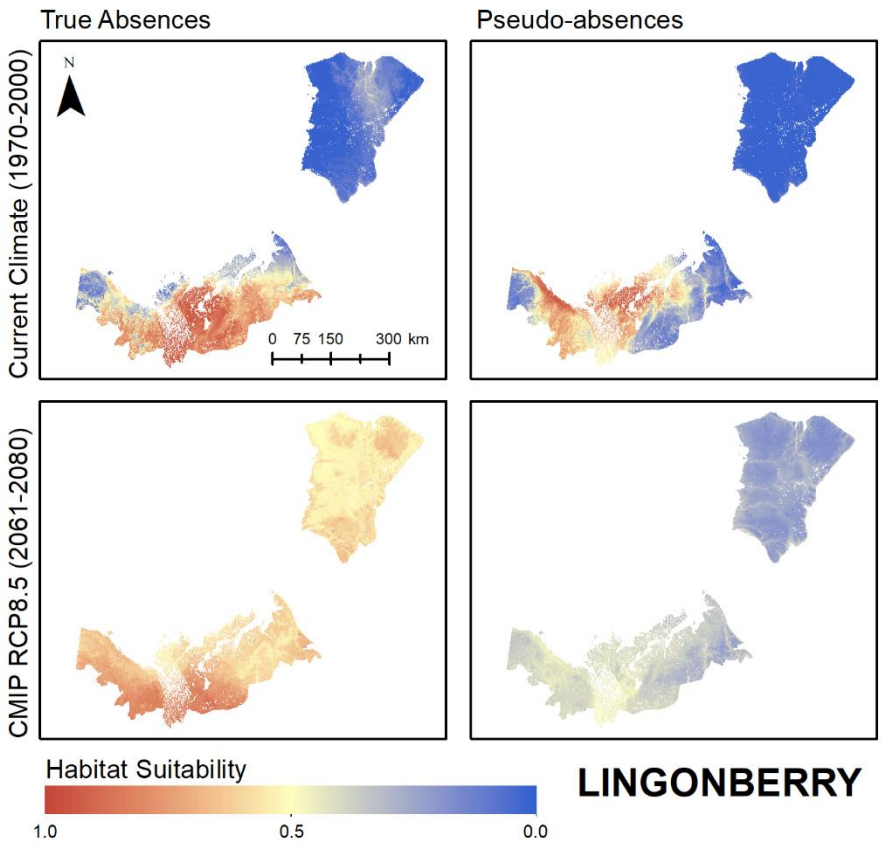

Figure 3.4. Ensemble habitat suitability maps for lingonberry *(Vaccinium vitis-idaea)* projected under current and future climate conditions using true absences and pseudo-absences models.

Table 3.5. Ranking of variables in order of importance (1 is most important and 10 is least important) for each species for both true absence (TA) and pseudo-absence (PA) models. The top three variables in each model are shown in bold.

	Alder		**Birch**		**Lingonberry**	
Variable	*TA*	*PA*	*TA*	*PA*	*TA*	*PA*
Annual Mean Temperature	4	4	**1**	**3**	**1**	**2**
Mean Diurnal Range	10	9	**2**	5	**2**	5
Isothermality	8	10	8	8	8	10
Temperature Seasonality	**2**	7	9	6	10	6
Mean Temperature of the Coldest Quarter	9	5	4	**1**	6	**3**
Precipitation Seasonality	**1**	**3**	6	7	**3**	7
Precipitation of the Warmest Quarter	6	**2**	**3**	4	4	4
Elevation	**3**	**1**	7	**2**	7	**1**
Slope	5	8	10	9	9	8
Ruggedness	7	6	5	10	5	9

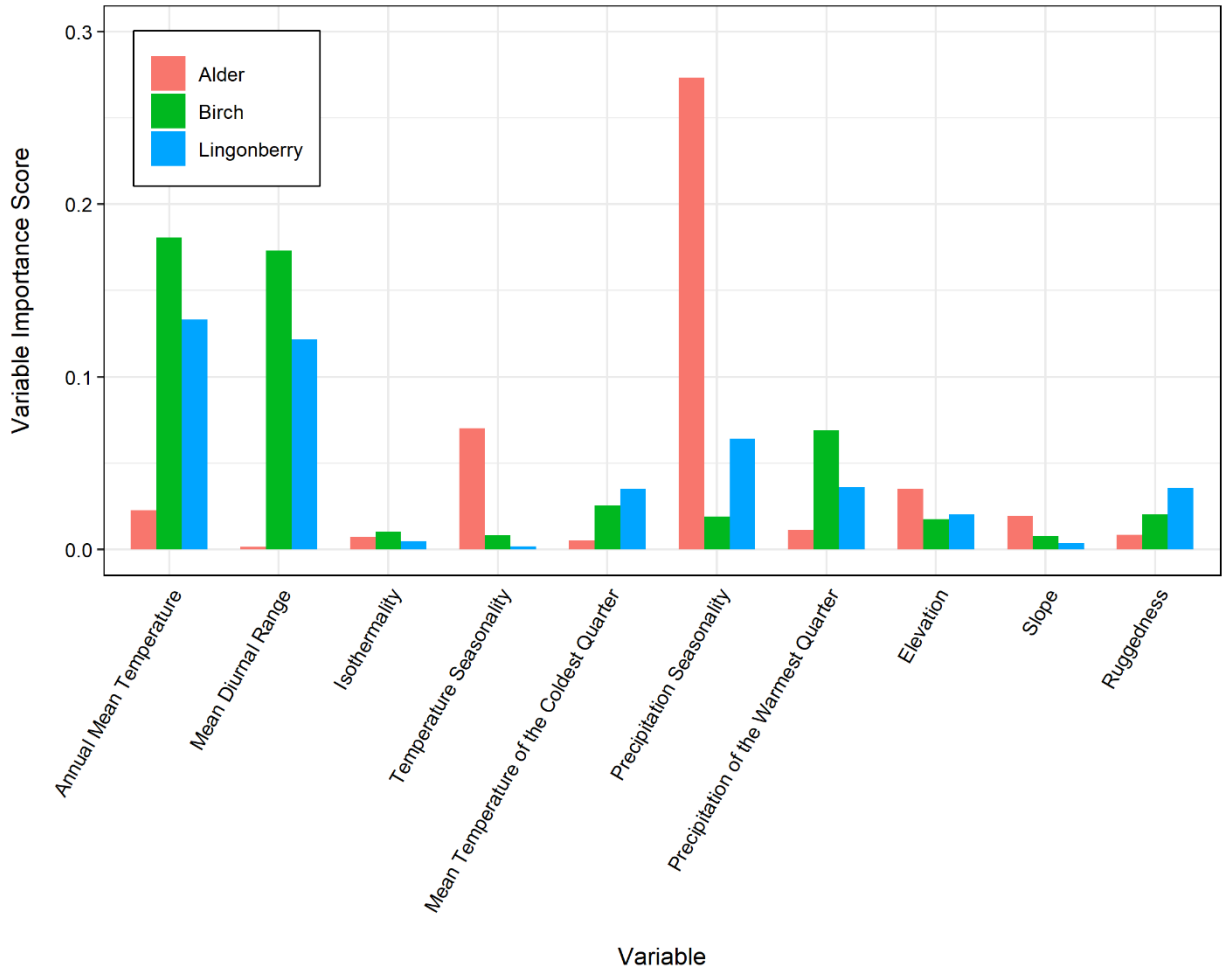

Figure 3.5. Importance scores for the predictor variables used in true absence ensemble SDM for each species.

3.4 DISCUSSION

3.4.1 Influence of Data Type

Our results highlight the importance of using true absence data to construct SDMs for terrestrial vegetation. Projected species distributions, model performance, and ranked variable importance from models built using pseudo-absence data deviated considerably from models that used true-absence data. Pseudo-absence models also showed reduced TSS scores for two of the three species compared to models that used true absence data (see Table 3.3). Differences between true absence and pseudo-absence models suggest that true absence data are needed to reliably define

low suitability habitats that are not adequately sampled through the pseudo-absence selection process (Brotons and others 2004; Soberón and Nakamura 2009).

Differences in projected habitat suitability in our pseudo-absence models were likely caused by the random allocation of pseudo-absence locations across a wider range of climate and terrain conditions compared to true absences. Since pseudo-absences are not definitive locations of absence, they do not accurately represent limiting environmental conditions, but provide a random sample of representative background data (Soberón and Nakamura 2009). Further, the possible allocation of pseudo-absence locations within the known distribution of a species could be reflected in model predictions as having lower suitability since the model will interpret truly suitable habitats as unsuitable. Another common SDM algorithm that uses pseudo-absence data (referred to as background data) called MAXENT (Phillips and others 2006) has also been shown to be highly sensitive to sampling bias caused in both presence and background data (Elith and others 2006; Elith and others 2011). Although true absence models are preferred as they provide information on low habitat suitability (Brotons and others 2004), the accessibility of presence-only data makes the use of pseudo-absences in SDMs very popular (Santini and others 2021). The widespread use of pseudo-absence models (Santini and others 2021) is concerning because our results indicate that models built using pseudo-absence data yield different results that models built using true absence data. There is also no clear evidence to support best practices for pseudo-absence selection (Santini and others 2021), and as such the optimal number of pseudo-absence points has been found to vary considerably between modelling algorithms (Barbet-Massin and others 2012). The spatial extent from which pseudo-absences are selected also poses potential problems, as too large or small an area can create models that are not biologically relevant (VanDerWal and others 2009). To facilitate the development of accurate,

reliable, and better performing models, we encourage the use of open data repositories to make true absence data more widely accessible. In addition, we suggest the use of comprehensive, systematic presence/absence data collection as part of botanical inventories (Saarela and others 2017; Saarela and others 2020).

Our results have important implications for predicting vegetation changes across northern ecotones, and conservation and land management decision-making (Guisan and others 2013). Recent work has stressed the importance of including SDM research in IUCN Red List developments (Breiner and others 2017), conservation of endemic and rare species (Marcer and others 2013; Wang and others 2015), and monitoring species invasion in protected areas (Pěknicová and Berchová-Bímová 2016; Barbet-Massin and others 2018). In all these cases, models built with pseudo-absence data that may not adequately describe species' distributions and responses to change may contribute to ineffective or potentially harmful decisions (VanDerWal and others 2009).

3.4.2 Tundra Shrub Response Dynamics

Our finding that future habitat suitability differed among species suggests that shrubs will respond individualistically to climate warming based on resource requirements and physiological adaptations (Chapin III and others 1996). This is also evidenced by our observations of differences in variable importance between alder and dwarf shrubs (birch and lingonberry). The importance of precipitation seasonality in the SDM for alder shows that climate-driven expansion in this species will likely be mediated by soil moisture. Precipitation seasonality is linked to the temporal availability of water across the landscape, which, in conjunction with the physical properties of soil, influences a plant's ability to retain moisture (O'Donnell and Ignizio 2012; Renne and others 2019). This explanation is consistent with recent findings showing that

growth and productivity of alder in upslope areas is moisture-limited (Black and others 2021). Higher soil moisture has been associated with green alder proliferation (Tape and others 2006; Frost and Epstein 2014; Cameron and Lantz 2016) and increased vegetation growth (Elmendorf and others 2012; Ackerman and others 2017; Bjorkman and others 2018a). Reduced alder habitat suitability in parts of our study area exhibiting lower spring and summer precipitation compared to winter precipitation (Vincent and others 2015) is also consistent with these observations.

Our analysis also suggests that physiological tolerances in birch and lingonberry will mediate how their ranges will respond to ongoing warming. The reduced importance of precipitation variables (precipitation seasonality and precipitation of the warmest quarter) in models for these species suggests that they will be less moisture-limited under a warmer climate (Figure 3.5). This finding is consistent with previous research showing the greater tolerance of birch and lingonberry to a range of environmental conditions (De Groot and others 1997; Taulavuori and others 2013). Several studies also show that these species can respond rapidly to increased temperature. Lingonberry exhibits increased shoot growth in response to rising temperature (Shevtsova and others 1997) and dwarf birch responds to experimental warming with earlier germination and higher recruitment (Milbau and others 2009). Dwarf birch is also capable of rapid secondary growth and reproduction under warming-induced increases in soil nutrient mineralization (Bret-Harte and others 2002).

Our results highlight the potential for high Arctic landscapes not currently dominated by alder, birch, lingonberry, and other woody vegetation to become climatically suitable for these species in the near future. This finding is consistent with recent remote sensing and field-based studies that have documented the proliferation of shrubs in tundra landscapes across the circumpolar (Tape and others 2006; Myers-Smith and others 2011; Jørgensen and others 2013; Lantz and

others 2013; Fraser and others 2014a; Frost and Epstein 2014; Martin and others 2017). Of particular note, greater increases in temperature across Banks Island compared to the Yukon North Slope, Tuktoyaktuk Coastlands, and Bathurst Peninsula (Supplementary Figure 8a) resulted in predictions of higher future suitability in this region. It is important to note that the shifts in habitat suitability predicted by our SDMs do not consider all ecological factors that can limit dispersal and recruitment. For example, small populations of birch and lingonberry on Banks Island (Aiken and others 2007) provide seed sources that could facilitate range expansion consistent with our SDMs. However, the absence of alder on Banks Island suggests that seed limitation will cause range expansion in this species to lag behind the presence of a suitable climate. Increased density of birch (Ropars and Boudreau 2012) and alder (Travers-Smith and Lantz 2020) across the low and sub Arctic without significant range expansion also indicates that dispersal limitation can cause temporal lags between warming and range expansion (Svenning and Sandel 2013). The statistical outputs of SDMs based on observations of presences and absences also do not account for factors including microsite availability and predation that frequently limit recruitment (Soberón and Nakamura 2009).

Differences in the projected response of alder, birch and lingonberry also highlight the importance of using species-based assessments of change to parameterize larger scale dynamic vegetation models. Dynamic vegetation models are commonplace in coupled earth system models and GCMs, and advances in the implementation and accuracy of species-based modelling will benefit climate projections (Bonan and others 2003; Quillet and others 2010). Parametrizing these models appropriately is important because terrestrial vegetation also impacts the climate system by influencing energy fluxes (ie. surface reflectance, carbon exchange) and surface conditions (ie. moisture, nutrients, temperature; Bonan and others 2003). Coupled earth

system models typically ignore dynamic trait-based vegetation response to climate in favour of static functional tolerances (Van Bodegom and others 2012; Wullschleger and others 2014). While simplification is necessary in global models, the use of broad vegetation functional types (grass, tree, cropland, etc.) may not accurately characterize vegetation change at high latitudes. Individual-based models (see: Kruse and others 2016) can be used to incorporate ecophysiological responses and species traits to determine responses to climate change. There are also promising advances in joint species distribution modelling, using a combination of traditional single-species SDM methods and ordination techniques to understand the interactions of multiple species from a community ecology perspective (Ovaskainen and Abrego 2020). These models can more directly account for interactions among species and can handle rare species better than traditional SDMs (Ovaskainen and Abrego 2020). With these advances in mind, it is still important to consider the data type used in modelling efforts. Our results show that data type can have a strong influence on models and as such, decisions regarding which parameterization data to use must be made carefully.

3.5 CONCLUSIONS

We used vegetation survey data across the Beaufort Delta region to model habitat suitability of three tundra shrubs to determine the effect that data type (true absences vs. pseudo-absences) has on model predictions and projected shifts in habitat suitability. Our analysis highlights the challenges of using pseudo-absence data to assess changes in habitat suitability or to identify environmental or climatic determinants of species' distributions. We also observed distinct responses among shrub species to climate warming, indicating that physiological and ecological differences among species will mediate their responses. Additional modelling using best practices in SDM research to identify differences among species will enhance our ability to

predict feedbacks between climate warming and tundra vegetation change. We stress the importance of using true absence data whenever possible, particularly when making conservation or management decisions. To improve the accuracy and utility of SDMs in global change research, we suggest that presence/absence data be made more widely available using open data repositories.

4 Conclusion

4.1 RESEARCH SUMMARY

Global climate warming is driving rapid increases in vegetation productivity and changes to community structure and composition across northern latitudes (Jia and others 2003; Berner and others 2020; Chen and others 2021). Large changes to the geographic distributions of many plant species have also been associated with climate change (Pearson and Dawson 2003; Pearson and others 2013). These changes are concerning because the trend of increasing greening, driven largely by increasing dominance of shrubs (Mekonnen and others 2021a), influences positive feedbacks to climate warming (Sturm and others 2001), alters soil temperature (Frost and others 2018), and negatively impacts wildlife such as caribou (Rickbeil and others 2018) while facilitating the range expansion of others such as moose (Tape and others 2016) and beaver (Jung and others 2016). The objective of my MSc thesis was to understand and quantify the response of tundra vegetation to recent climate warming in Beaufort Delta region of the western Canadian Arctic, and to assess how data type influences model performance and interpretation. To accomplish this I used machine learning analyses and species distribution modelling.

In Chapter 2, I used field sampling of soils and vegetation and random forests modelling of trends in vegetation productivity measured using Landsat to investigate the response of tundra vegetation to climate warming. My analysis documented spatial heterogeneity in productivity trends (signalling variable intensities of tundra greening), which were the result of landscape-scale terrain variables that mediate the effects of regional climate warming. Surficial geology and topography are among the best predictors of spatial patterns in tundra greening because they strongly influence soil conditions and moisture. My analysis also showed that the dominant vegetation is an important determinant of tundra productivity dynamics. Rapid greening was

associated with higher productivity in low shrub-dominated areas and stable productivity was more common in areas of barren ground or those already dominated by tall shrubs. Regional increases in low and tall shrub cover between 1984 and 2016, and the loss of less productive cover types (herbaceous, sparse) were also evident in land cover classifications created by Wang and others (2019). My analysis is significant because it identifies regional drivers of shifting vegetation productivity and provides insight into areas that may be particularly sensitive to climate warming.

In Chapter 3, I ran a series of species distribution models (SDMs) to investigate the influence of data type (the use of true absences or pseudo-absences) on habitat suitability projections of three tundra shrubs: (1) green alder (*Alnus viridis*), (2) dwarf birch (*Betula nana* and *B. glandulosa*), and (3) lingonberry (*Vaccinium vitis-idaea*) under current and future climates. This analysis revealed notable differences in projected habitat suitability and driving variables between data types. While all models indicated overall increases in habitat suitability across the entire study area under the RCP8.5 climate scenario, differences in habitat suitability predictions and variable importance between data types indicated pseudo-absences had a notable impact on model outputs. These results lead me to recommend the use of true absence data when possible and demonstrates the significance of understanding the effects of model parameterization in terms of conservation and management decisions. My analysis also highlights the individualistic responses of different shrubs to climate warming driven by differences in physiological adaptations and environmental tolerances. This suggests that the use of broader plant functional type groupings are inherently missing essential information. My results are relevant to the global change and climate modelling research communities because changes in Arctic and subarctic

vegetation will drive large changes in energy fluxes and carbon storage (McGuire and others 2006; Schaefer and others 2014).

4.2 LIMITATIONS AND FUTURE RESEARCH

My MSc research offers significant insight into changes in Low Arctic tundra vegetation, but there are several areas that would benefit from more data and additional investigation. In Chapter 2, I used Landsat imagery to map trends in EVI across the Tuktoyaktuk Coastlands and Yukon North Slope. The 30-metre resolution of the Landsat archive constrained the grain at which I could map landscape heterogeneity. At this resolution, I found variability in topography to be important in driving EVI trends, but past research has highlighted that tundra vegetation exhibits heterogeneity at the sub-metre scale and suggests that processes at this scale may be critical to understanding the response of vegetation to microclimate variability (Assmann and others 2020; Myers-Smith and others 2020; Mekonnen and others 2021b). I recommend future research make use of finer resolution imagery, including remotely piloted aircraft systems (RPAS) that are capable of describing landscape patterns at the resolution of a few centimetres (Fraser and others 2016). The greater affordability and accessibility of consumer-grade RPAS with multispectral capabilities (such as the DJI P4 Multispectral Drone) makes it possible to collect repeatable EVI (or other vegetation indices) data at the users discretion, an alternative to more expensive, coarser resolution, satellite imagery (Quickbird or WorldView). Random forests modelling using higher resolution data would also complement recent broad-scale analysis (Wang and Friedl 2019; Berner and others 2020; Chen and others 2021).

To strengthen higher resolution analyses, I suggest that future studies be paired with field data collection across a greater variety of habitat types. My research shows that vegetation type strongly influence changes in productivity because deciduous shrubs can respond rapidly to

changes in moisture, nutrients, and temperature. The field sampling that I conducted for this research focused on upland tundra terrain and did not adequately capture variability in lowland areas. To better understand the influence of soil moisture on vegetation productivity, additional sampling should be conducted in low-lying terrain (wetland complexes, water tracks, and lake margins). Additional sampling in the subarctic transition zone and at higher elevations in the Richardson Mountains would also provide more information on the role of elevation and heterogeneous topography, two factors we know to be important, but were not fully characterized during field sampling.

Tundra vegetation change impacts wildlife habitat (Rickbeil and others 2018), surface energy balance, and carbon storage (McGuire and others 2006; Schaefer and others 2014), and so understanding the drivers of landscape scale variation in vegetation shifts is critical to accurately describe these relationships (Mekonnen and others 2021a). As such, I also recommend that my research be expanded to study the impacts of changing vegetation dynamics on the movement and habitat selection of mammals (caribou, moose, and muskox). Harvesting of local plants species is also of cultural importance to Inuvialuit and Gwich'in peoples (Alunik and Morrison 2003; Parlee and others 2005) and an interdisciplinary study exploring the impacts of increasing shrub dominance on berry production would provide insight relevant to local communities.

Species distribution models, habitat suitability models, and ecological niche models are a popular topic of current scientific research. New and innovative modelling techniques are in development that seek to improve upon current inadequacies inherent in common SDMs such as poor performance on rare species, integration of complex biological interactions, and scale-dependent ecological drivers (Guisan and Thuiller 2005; Zimmermann and others 2010; Keil and others 2013). In Chapter 3, I showed how data used in model training has an influence on habitat

suitability predictions. Given the widespread use of pseudo-absences in research, I recommend that future work consider the impact of pseudo-absences in newer techniques such as joint species distribution modelling (Ovaskainen and Abrego 2020). Additionally, due to the differences I observed in projected species responses to warming, I suggest further development of individual-based models (see: Kruse and others 2016) to understand vegetation response to environmental and climatic change. These mechanistic models may provide more realistic interpretation of potential species' distributions that account for individual variation in detail (DeAngelis and Mooij 2005), but require greater amounts of data to describe fundamental physiological and ecological responses to environmental gradients. Databases such as that of the Tundra Trait Team (Bjorkman and others 2018b) are leading the way on providing open access data on functional traits that may be implemented in these models.

Repositories such as the Global Biodiversity Information System (GBIF) that provide free and open data are an essential resource for ecologists. GBIF, in particular, aggregates data from sources including herbariums, university collections, and citizen science projects (like *iNaturalist* or *eBird*) making such data easily accessible through browser-based tools (*gbif.org*) or packages for use in coding languages such as R, Python, or Ruby (Chamberlain and Boettiger 2017). The wide variety of survey methods and data formats makes aggregating data such as true absences, percent cover, or abundances difficult to implement at such a large scale. Current efforts such as the Group on Earth Observations Biodiversity Observation Network (Scholes and others 2012) are already seeking ways to coordinate large-scale biodiversity monitoring. Understanding the importance of high quality, descriptive data leads me to suggest and encourage further research into developing widely accessible data reporting standards. Having access to these data will drive

researchers to develop higher quality and more reliable models that will provide a better understanding of the impacts of climate change on vegetation dynamics across the globe.

Long-term environmental monitoring is a crucial part of understanding the response of sensitive ecosystems to climate change and are important for implementation in global climate modelling and policy decision (Lovett and others 2007). Such monitoring provides unique insight into trends not visible over short periods of time or even developments not thought possible. Examples of such breakthroughs include early mentions of increasing atmospheric carbon dioxide (Keeling and others 1976) or the development of the Antarctic ozone hole (Farman and others 1985). I believe the increasing accessibility of high quality remote sensing data, open source data processing languages and GIS tools, and large datasets will continue to promote exploration and research into our changing environment.

Supplementary Information

Supplementary Table 1. Description of surficial geology classes (from Fulton 1989) that cover more than 1% of the study area.

Classification	Description (quoted from Fulton 1989)
Alluvial	Stratified silt, sand, clay, and gravel; floodplain, delta and fan deposits; in places overlies and includes glaciofluvial deposits
Fine colluvial	Silt, clay, and fine sand; derived from weakly consolidated shale and siltstone substrate
Glaciofluvial complex	Sand and gravel and diamicton; undifferentiated ice contact stratified drift, and outwash; locally includes till and rock
Glaciofluvial plain	Sand and gravel; deposited as outwash sheets, valley trains, and terrace deposits
Lacustrine sand	Sand and gravel; deposited as sheet sands, lags, and beaches
Till blanket	Thick and continuous till
Till veneer	Thin and discontinuous till; may include extensive areas of rock outcrop

Supplementary Table 2. Description of land cover classes (from Wang and others 2019) that cover more than 1% of the study area.

Classification	Description (quoted from Wang and others 2019)
Barren	Less than 10% vegetation, mostly rock.
Fen	Hydrologically connected, sedge/grass dominated wetland.
Herbaceous	Area dominated by herbaceous land cover greater than 60% cover and tree/shrub cover less than 10%.
Low shrub	Area dominated by dense hemi-prostrate to low-erect shrubs (5-30 cm in height) with greater than 60% area coverage. Analogous to "prostrate dwarf-shrub" and primarily occurring in tundra areas.
Sparsely vegetated	10-30% canopy coverage, any vegetation but typically herbaceous/bryophyte, with rock underneath.
Tall shrub	Area dominated by woody vegetation between 50 cm and 3 m tall and shrub canopy coverage greater than 60% coverage. Typically deciduous.
Tussock tundra	Herbaceous tundra dominated by *Eriophorum vaginatum* and other tussock-forming herbaceous species with over 60% coverage.
Woodland	Area dominated by trees taller than 3 m with between 30-60% canopy coverage. Frequently co-exists with peatlands and typically evergreen.

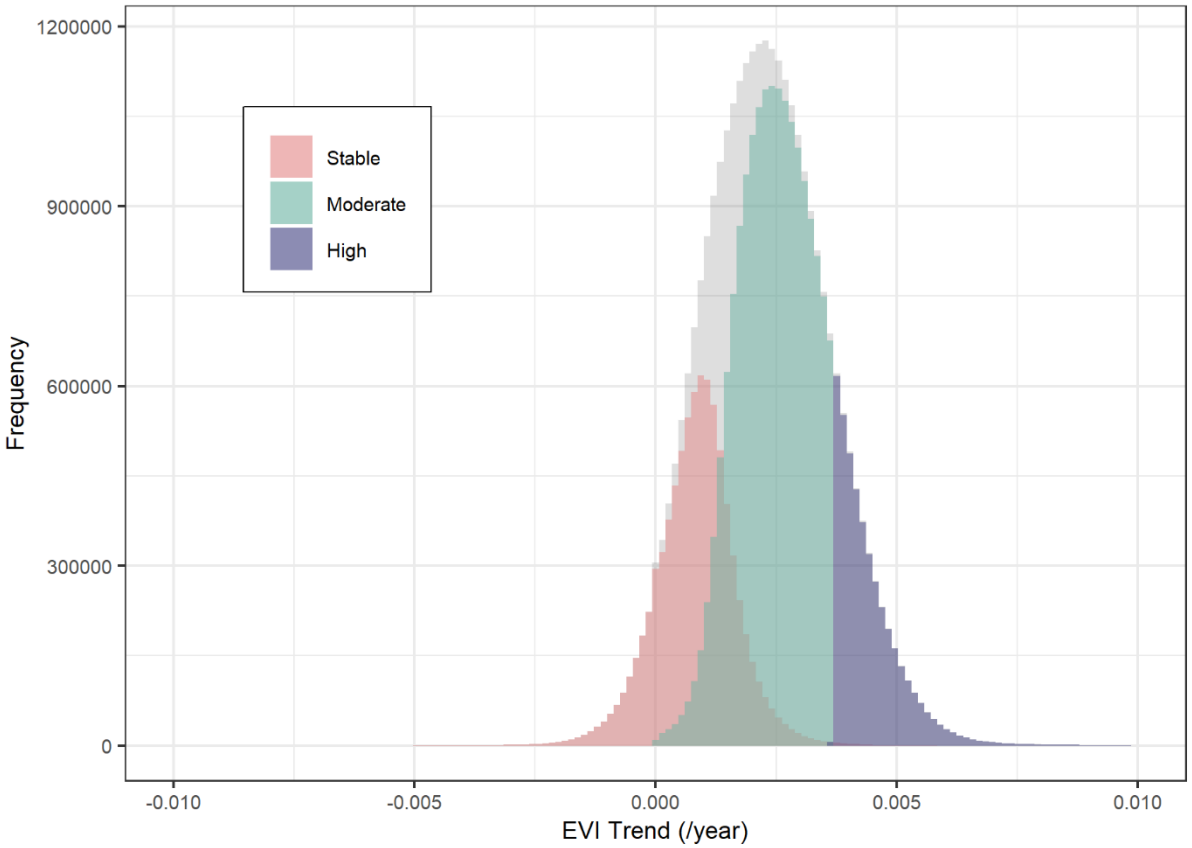

Supplementary Figure 1. Histogram of Enhanced Vegetation Index (EVI) trend values (grey) from Chen and others (2021) in the study area. Coloured portions represent the subset of data within each greening classification and show overlap between stable and moderate greening classes. The mean EVI trend is 2.24 x 10^{-3} EVI units/year and separation between moderate and high greening classifications is at one standard deviation above the mean (3.69 x 10^{-3} EVI units/year).

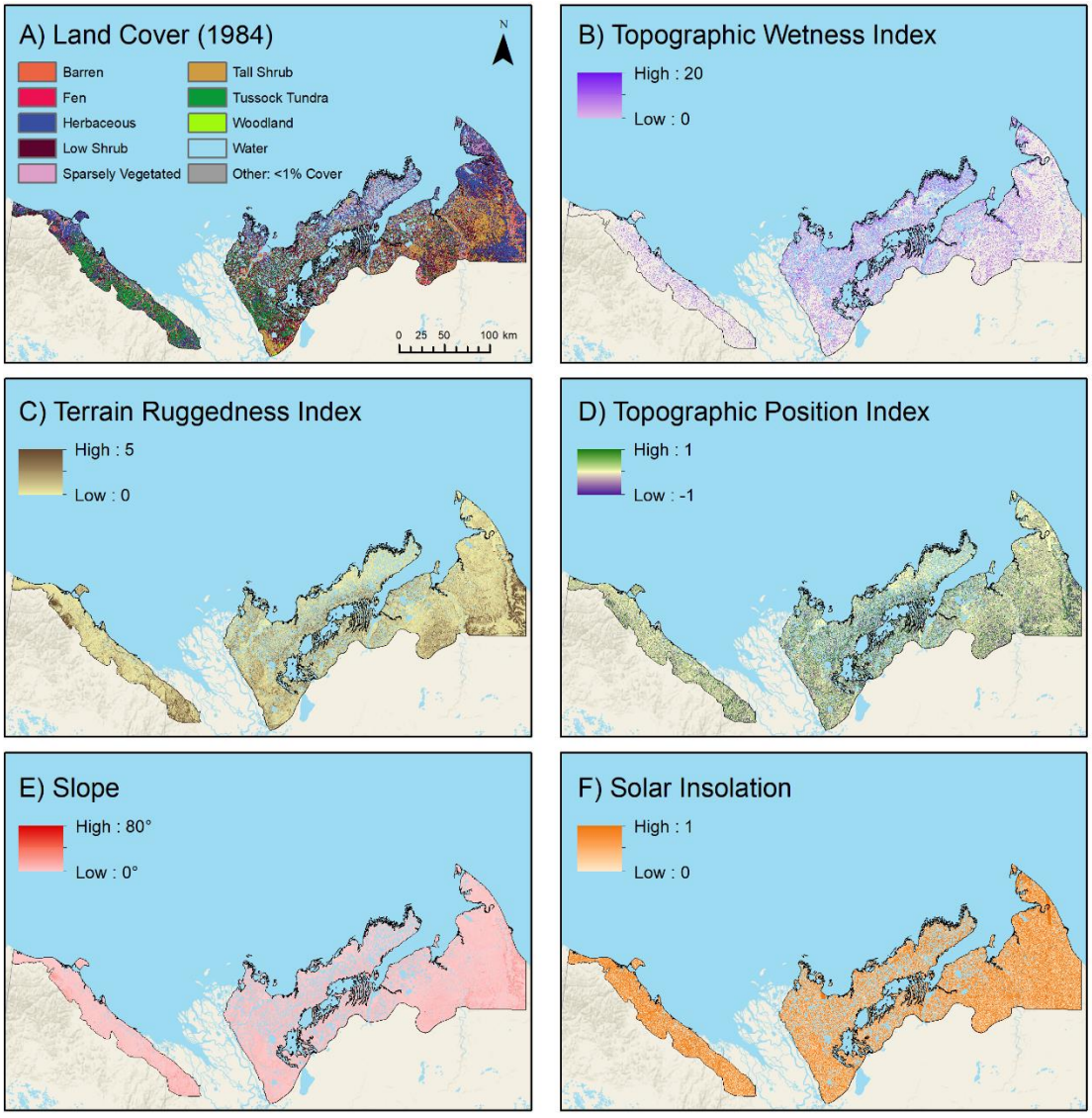

Supplementary Figure 2. Explanatory variables used in random forests modelling. A) Land cover data from Wang and others (2019); B-F) Derivatives of elevation data from Porter and others (2018).

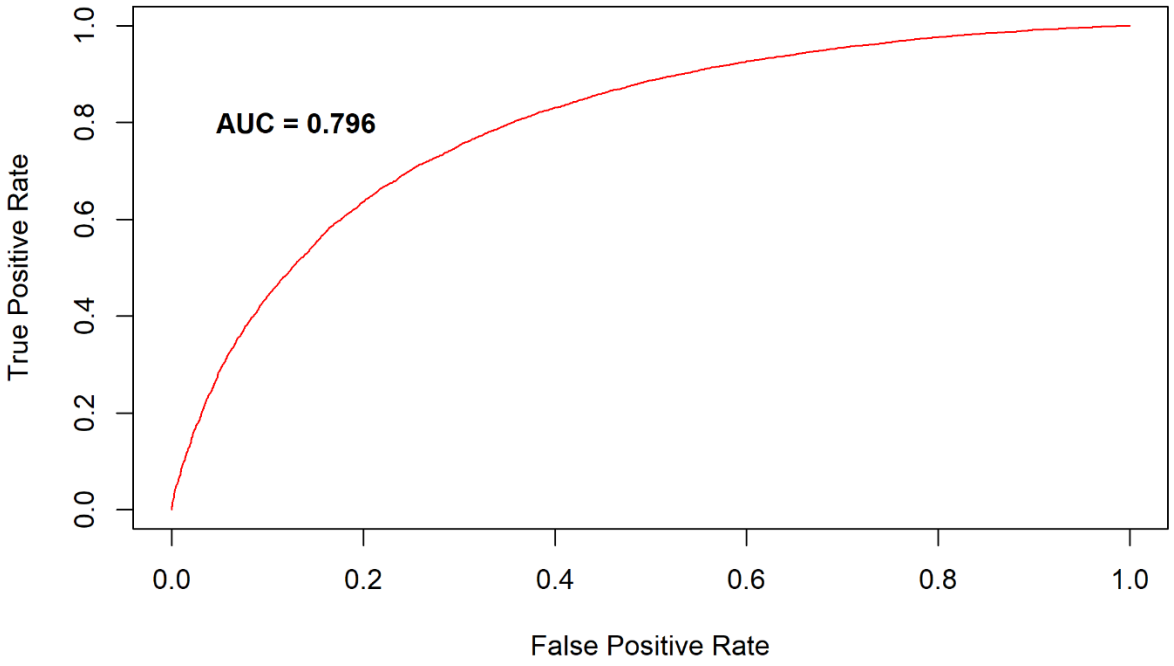

Supplementary Figure 3. Receiver operating characteristic (ROC) curve with area under the curve (AUC) of 0.796 for the classification random forests model.

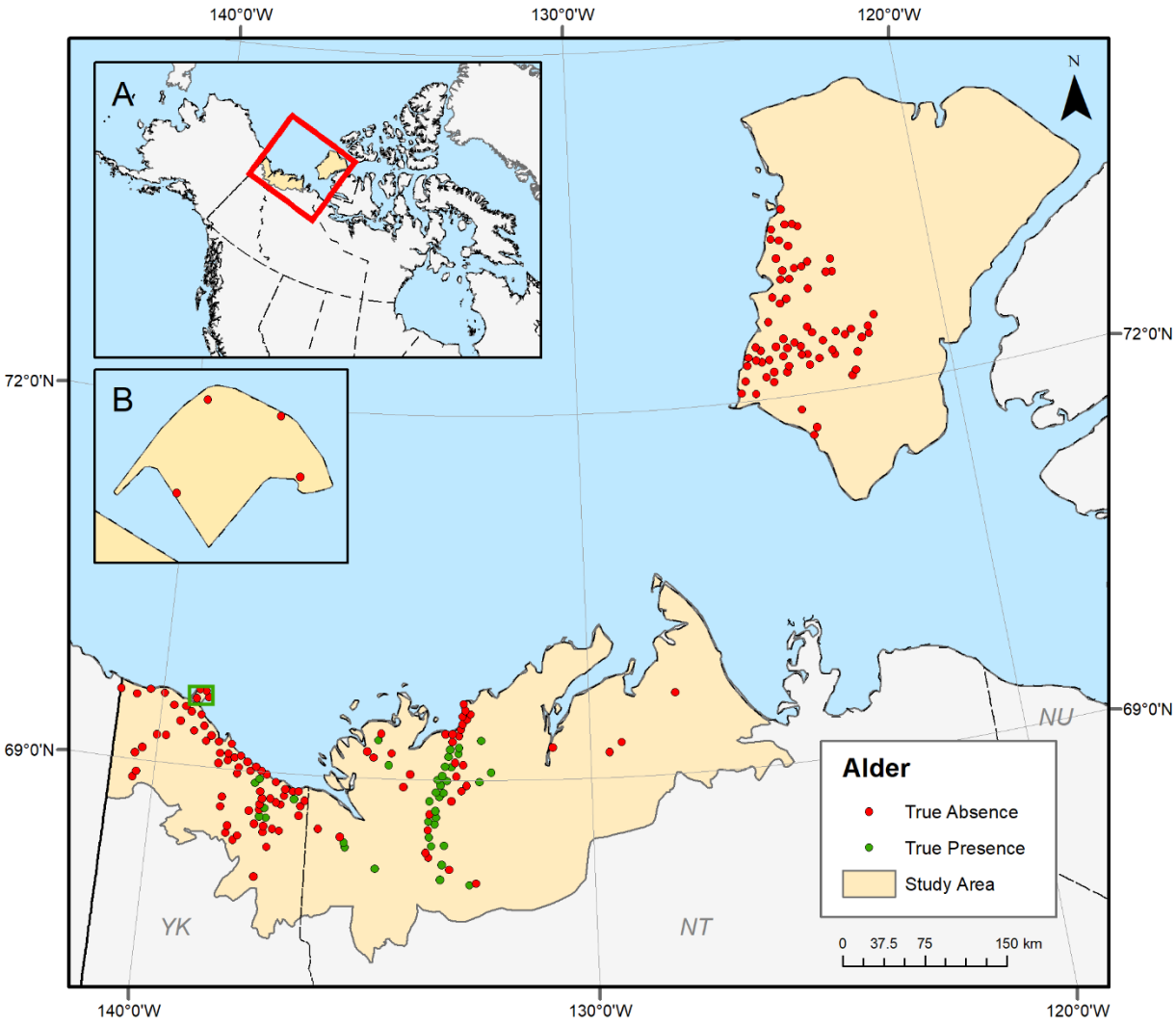

Supplementary Figure 4. True presence and absence locations for alder (*Alnus viridis*) from field sampling locations. These data represent the 5 km thinned data used to train the species distribution models.

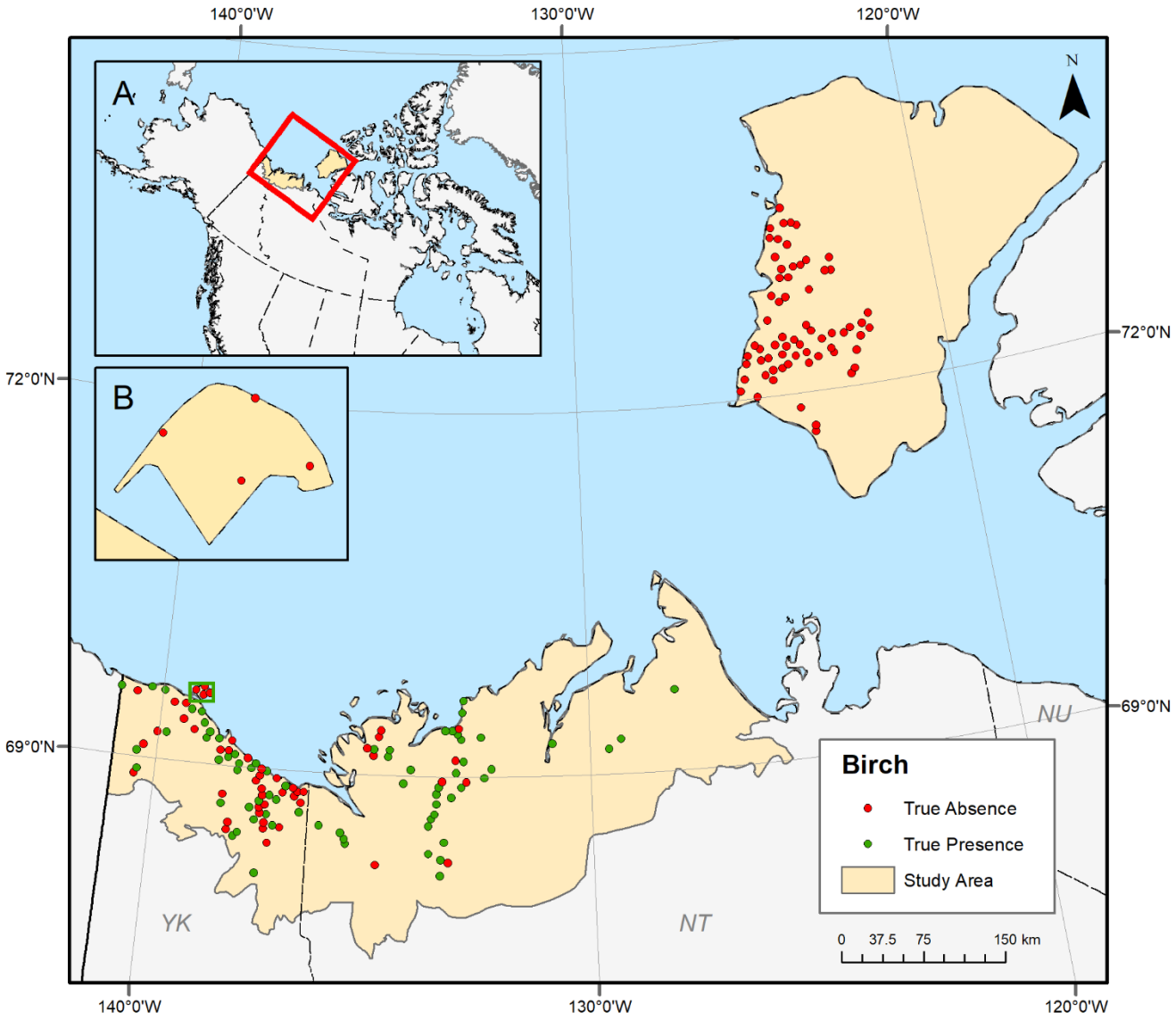

Supplementary Figure 5. True presence and absence locations for birch (*Betula nana* and *B. glandulosa*) from field sampling locations. These data represent the 5 km thinned data used to train the species distribution models.

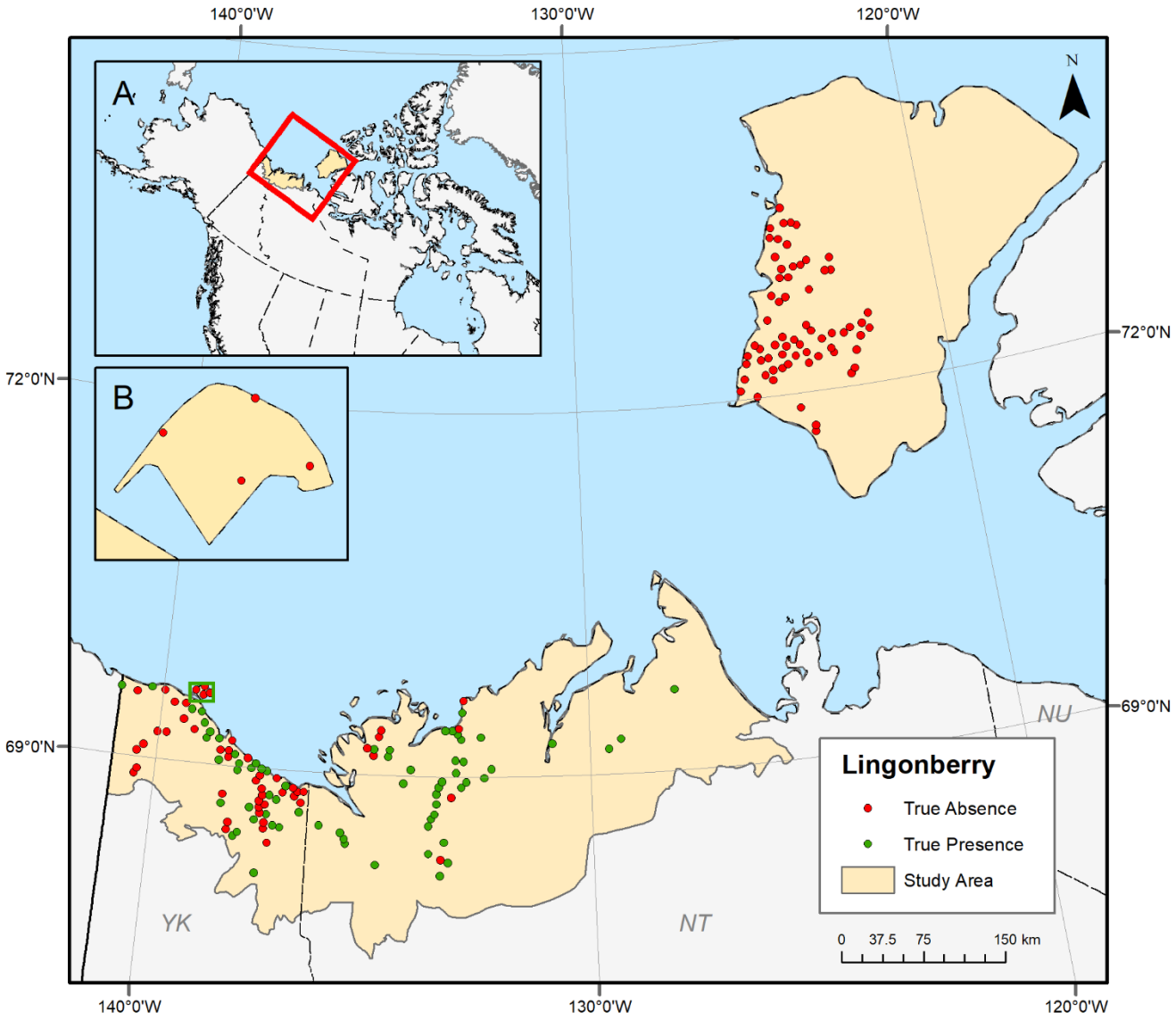

Supplementary Figure 6. True presence and absence locations for lingonberry (*Vaccinium vitis-idaea*) from field sampling locations. These data represent the 5 km thinned data used to train the species distribution models.

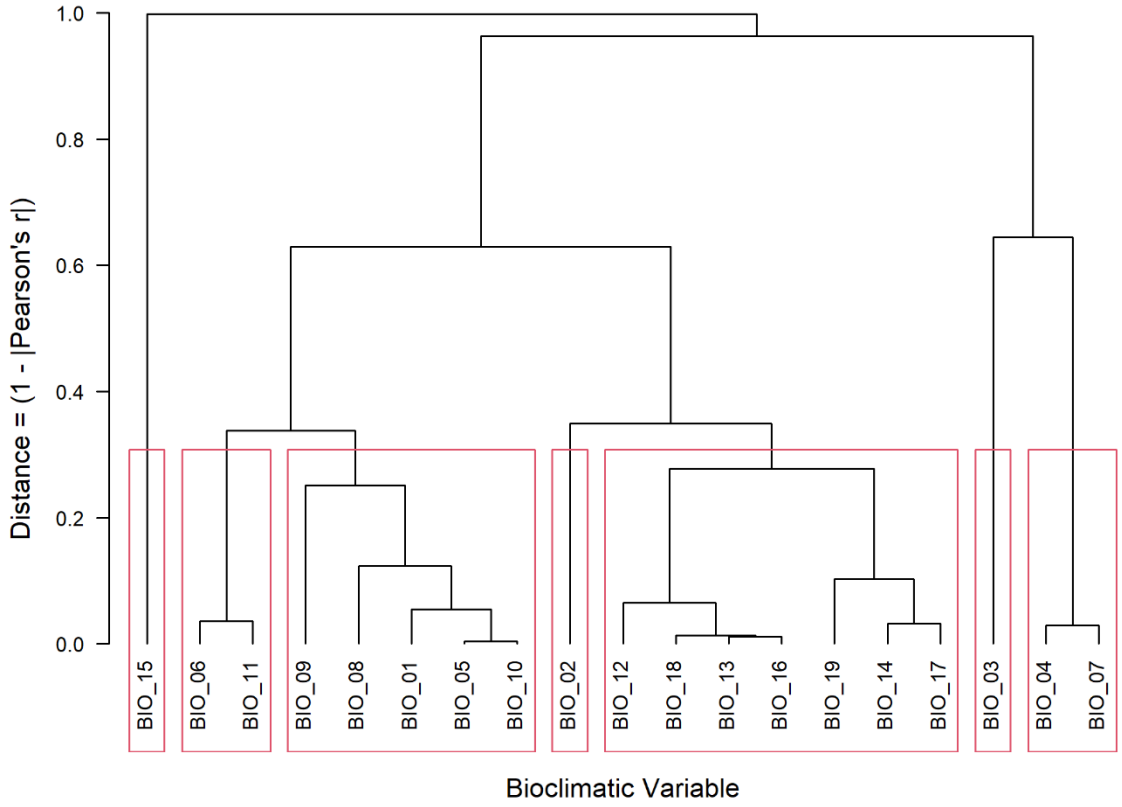

Supplementary Figure 7. Hierarchical clustering of WorldClim bioclimatic variables at 30 arcseconds resolution across study area. Red boxes show groups of variables with Pearson's r greater than 0.7 (distance less than 0.3). Refer to Table 3.1 for complete variable names.

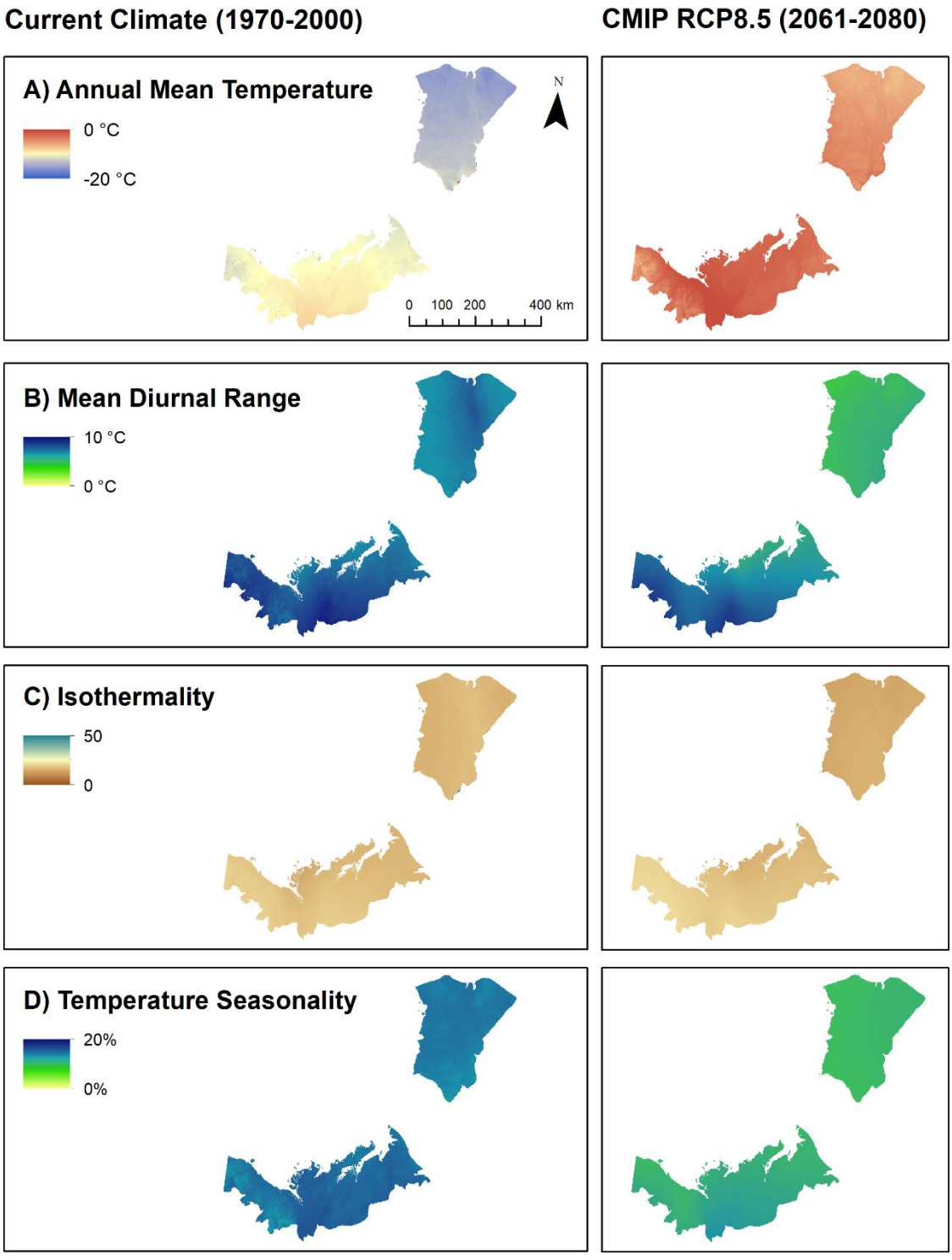

Supplementary Figure 8. Maps of bioclimatic variables used in ensemble species distribution models under current (left column) and future (right column) climate projections.

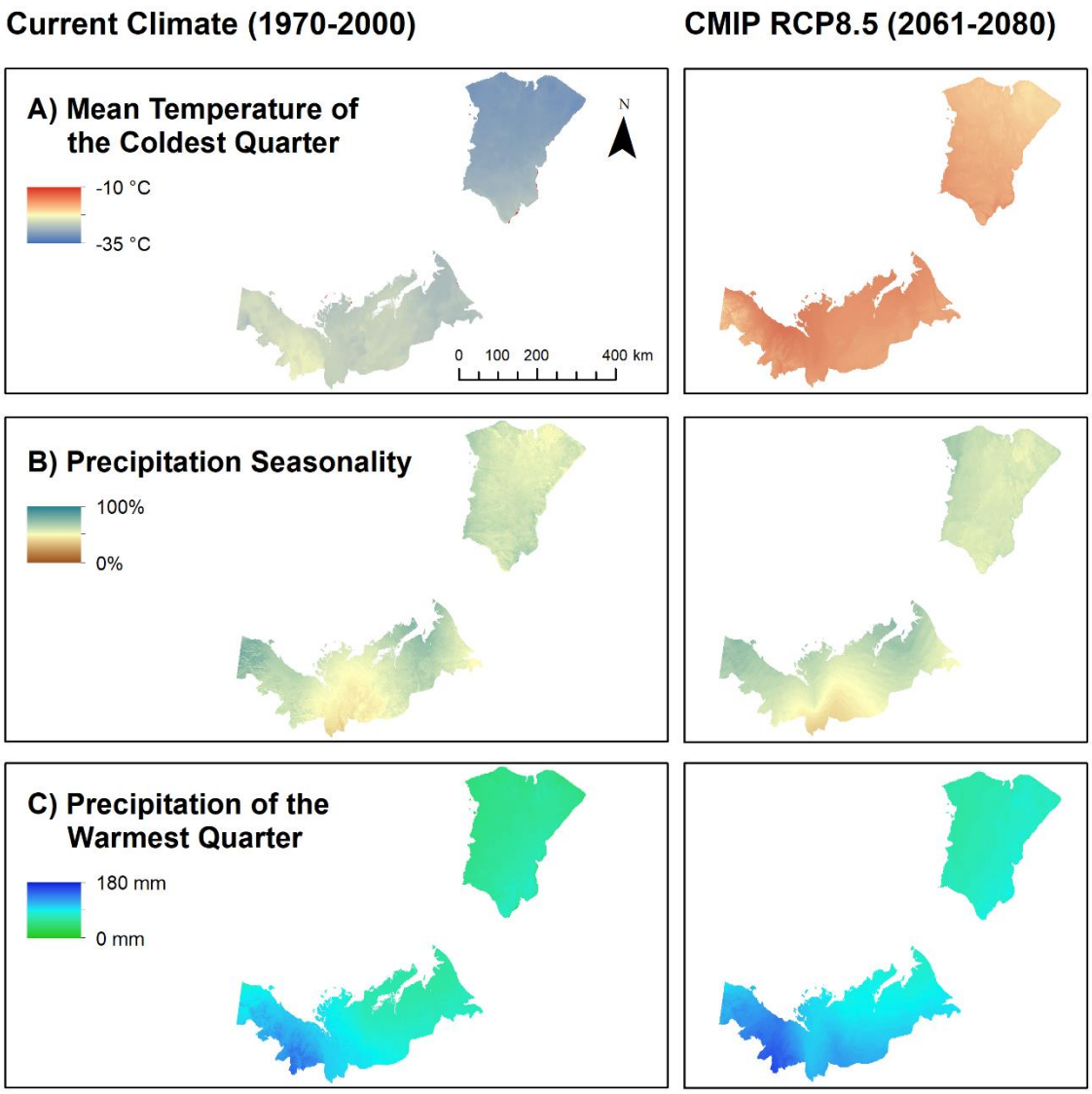

Supplementary Figure 9. Maps of bioclimatic variables used in ensemble species distribution models under current (left column) and future (right column) climate projections.

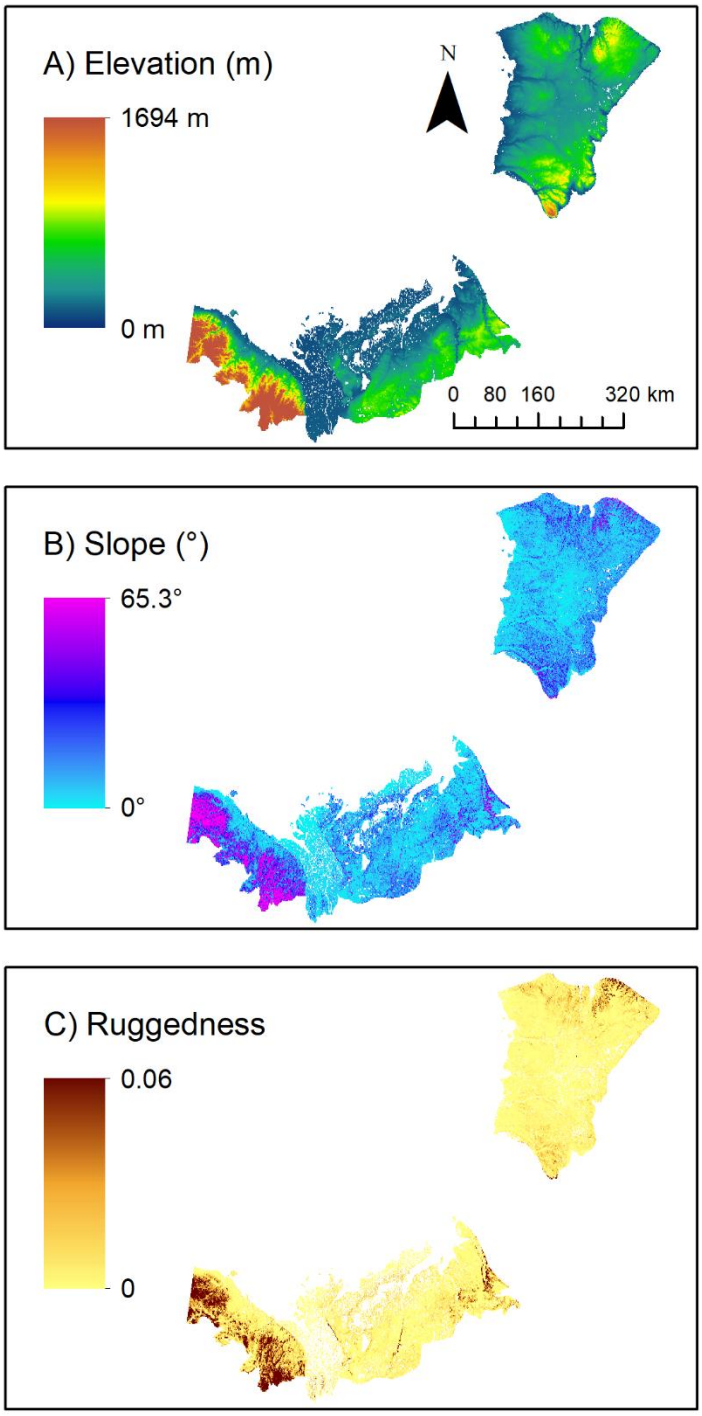

Supplementary Figure 10. Maps of A) elevation, B) slope, and C) ruggedness (as vector ruggedness index) as used in the ensemble species distribution models.

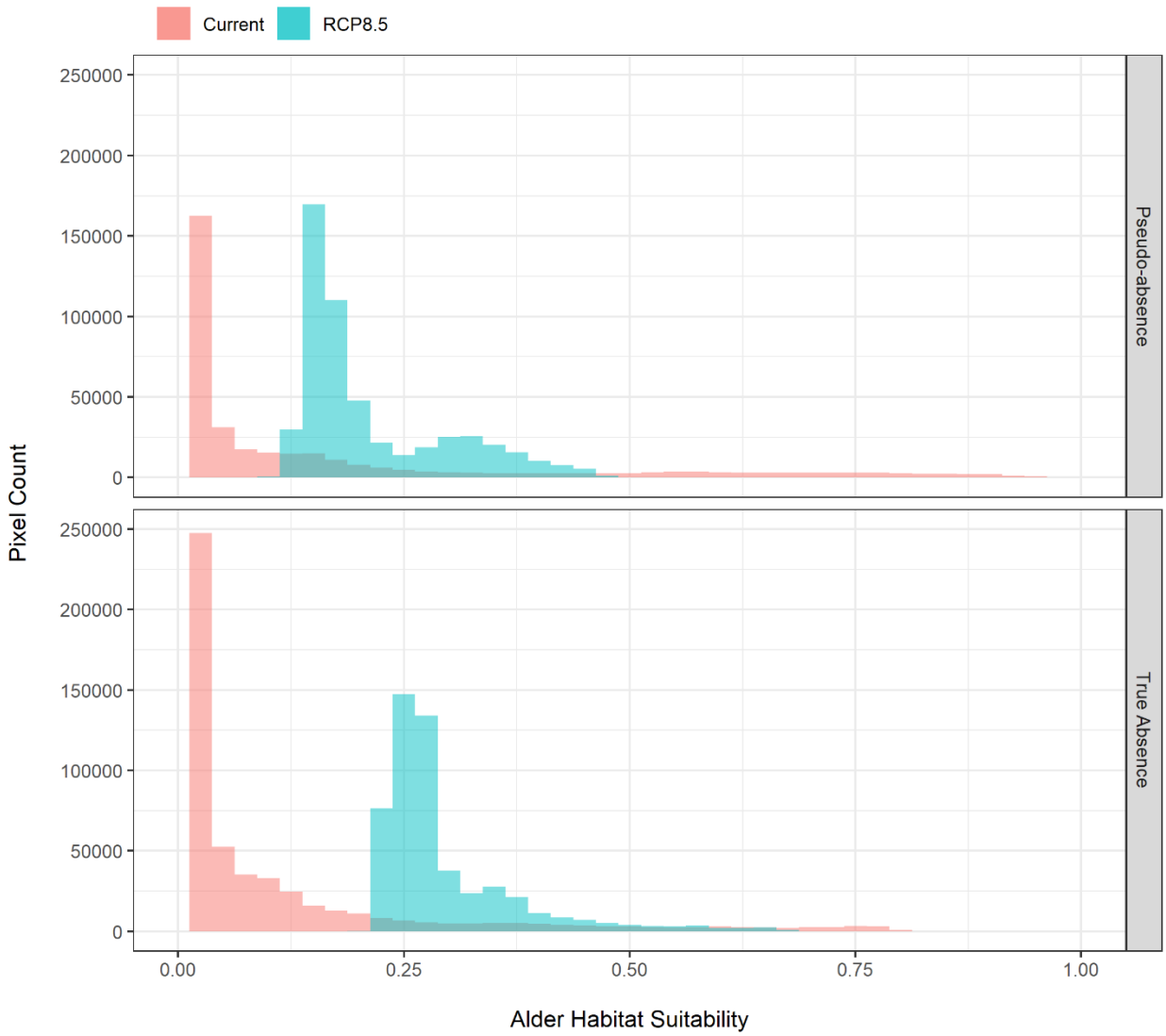

Supplementary Figure 11. Histogram of habitat suitability predictions from true absence and pseudo-absence models across the entire study area for alder (*Alnus viridis*).

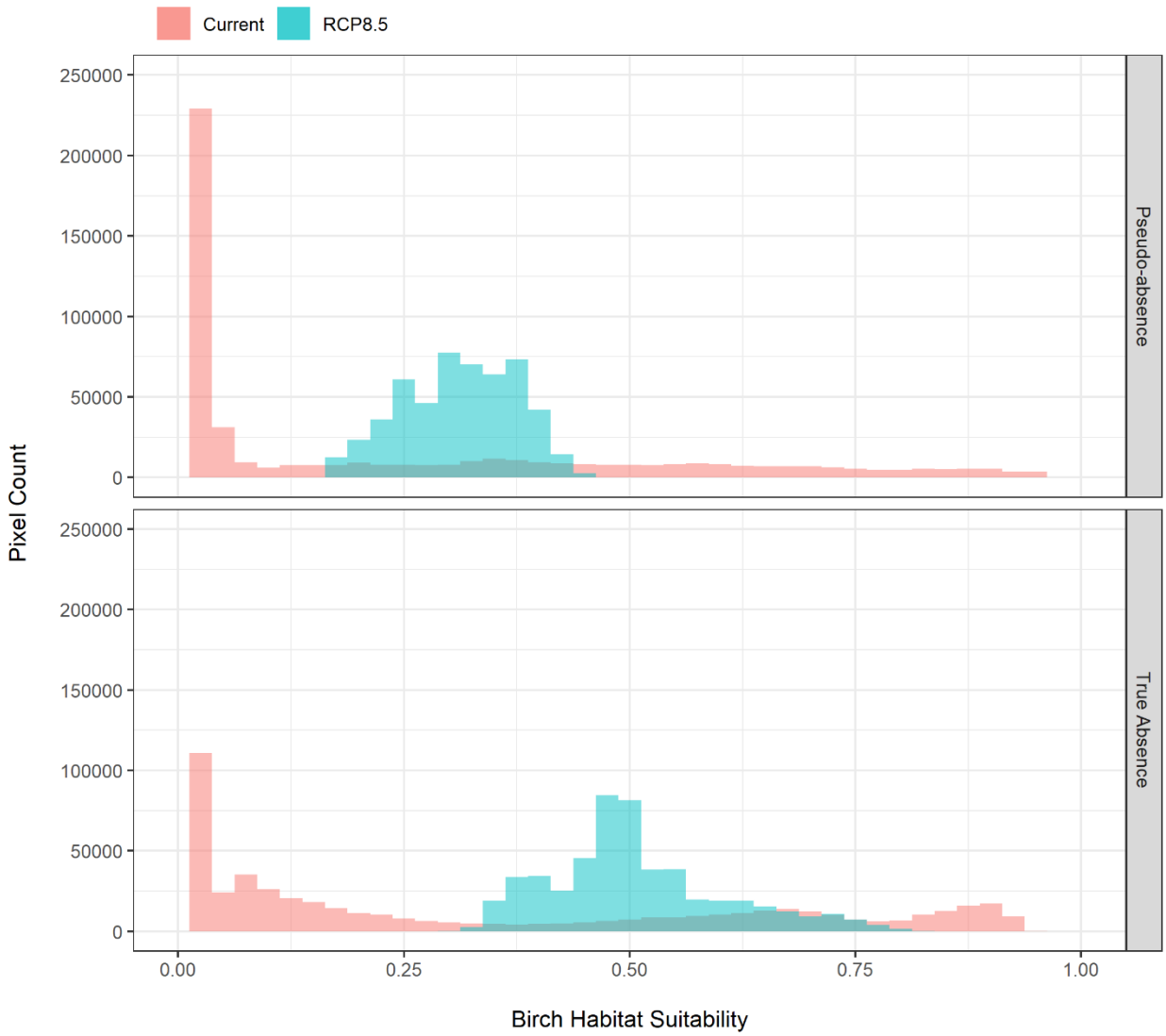

Supplementary Figure 12. Histogram of habitat suitability predictions from true absence and pseudo-absence models across the entire study area for birch (*Betula nana* and *B. glandulosa*).

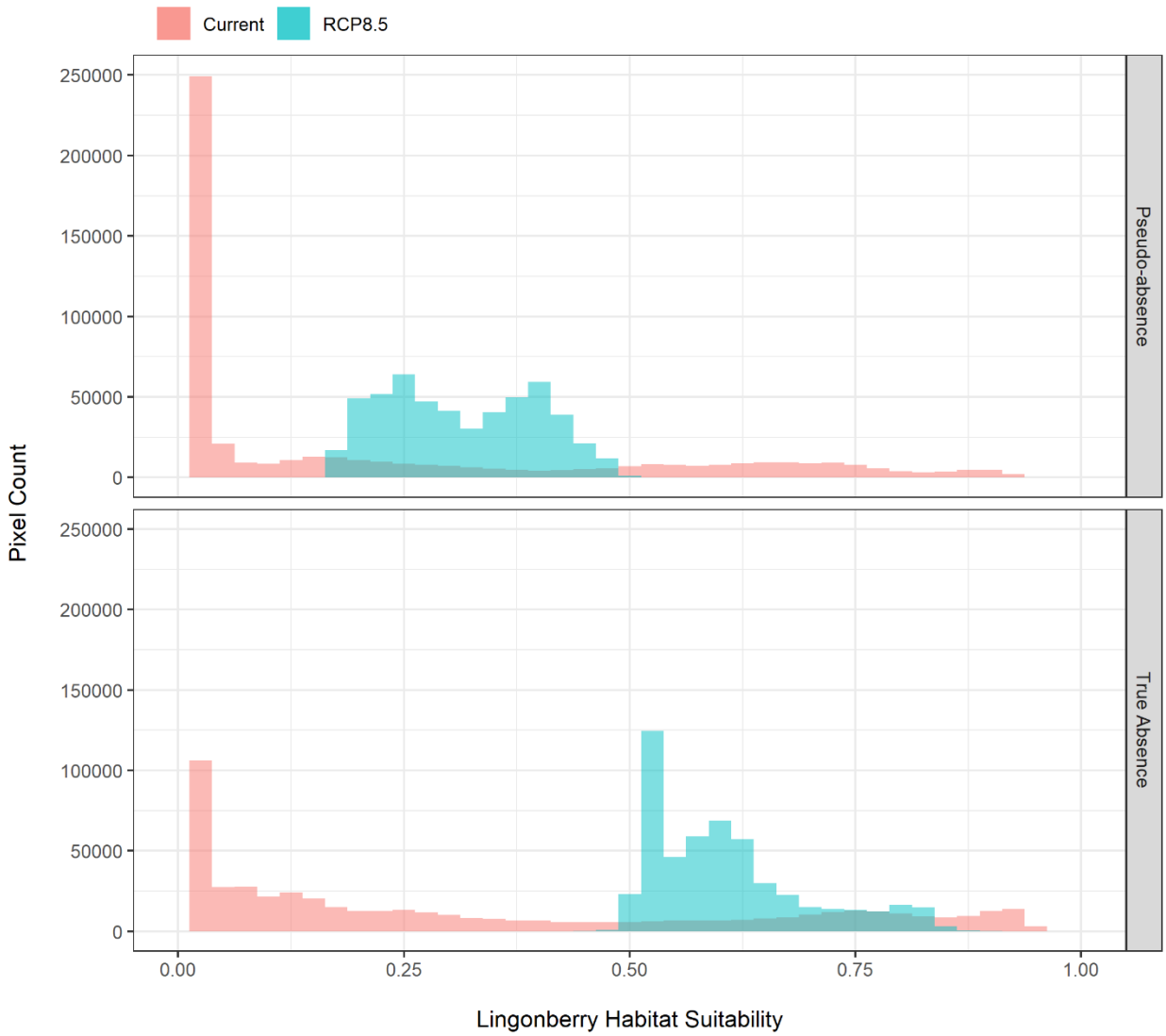

Supplementary Figure 13. Histogram of habitat suitability predictions from true absence and pseudo-absence models across the entire study area for lingonberry (*Vaccinium vitis-idaea*).

Bibliography

Ackerman D, Griffin D, Hobbie SE, Finlay JC. 2017. Arctic shrub growth trajectories differ across soil moisture levels. Global Change Biology 23: 4294-4302.

Aiken S, Dallwitz M, Consaul L, McJannet C, Boles G, Argus G, Gillett J, Scott P, Elven R, LeBlanc M, Gillespie L, Brysting A, Solstad H, Harris J. 2007. Flora of the Canadian arctic archipelago: NRC Research Press.

Allouche O, Tsoar A, Kadmon R. 2006. Assessing the accuracy of species distribution models: prevalence, kappa and the true skill statistic (TSS). Journal of Applied Ecology 43: 1223-1232.

Alunik I, Morrison DA. 2003. Across time and tundra: The Inuvialuit of the Western Arctic: Raincoast Books.

Araújo MB, Guisan A. 2006. Five (or so) challenges for species distribution modelling. Journal of Biogeography 33: 1677-1688.

Arctic Monitoring and Assessment Programme. 2004. Impacts of a Warming Arctic: Arctic Climate Impact Assessment. Cambridge, UK: Cambridge University Press.

Assmann JJ, Myers-Smith IH, Kerby JT, Cunliffe AM, Daskalova GN. 2020. Drone data reveal heterogeneity in tundra greenness and phenology not captured by satellites. Environmental Research Letters 15.

Austin M, Nicholls A, Margules CR. 1990. Measurement of the realized qualitative niche: environmental niches of five Eucalyptus species. Ecological Monographs 60: 161-177.

Austin MP, Van Niel KP. 2011. Improving species distribution models for climate change studies: variable selection and scale. Journal of Biogeography 38: 1-8.

Baldwin S. 2012. Compute Canada: advancing computational research. Journal of Physics: Conference Series: IOP Publishing, p012001.

Barbet-Massin M, Rome Q, Villemant C, Courchamp F. 2018. Can species distribution models really predict the expansion of invasive species? PLoS ONE 13: e0193085.

Barbet-Massin M, Jiguet F, Albert CH, Thuiller W. 2012. Selecting pseudo-absences for species distribution models: how, where and how many? Methods in Ecology and Evolution 3: 327-338.

Belward AS, Skøien JO. 2015. Who launched what, when and why; trends in global land-cover observation capacity from civilian earth observation satellites. Journal of Photogrammetry and Remote Sensing 103: 115-128.

Berner LT, Beck PSA, Bunn AG, Lloyd AH, Goetz SJ. 2011. High-latitude tree growth and satellite vegetation indices: Correlations and trends in Russia and Canada (1982–2008). Journal of Geophysical Research: Biogeosciences 116.

Berner LT, Massey R, Jantz P, Forbes BC, Macias-Fauria M, Myers-Smith I, Kumpula T, Gauthier G, Andreu-Hayles L, Gaglioti BV. 2020. Summer warming explains widespread but not uniform greening in the Arctic tundra biome. Nature Communications 11: 1-12.

Bhatt US, Walker DA, Raynolds MK, Comiso JC, Epstein HE, Jia G, Gens R, Pinzon JE, Tucker CJ, Tweedie CE. 2010. Circumpolar Arctic tundra vegetation change is linked to sea ice decline. Earth Interactions 14: 1-20.

Bjorkman AD, Criado MG, Myers-Smith IH, Ravolainen V, Jónsdóttir IS, Westergaard KB, Lawler JP, Aronsson M, Bennett B, Gardfjell H. 2020. Status and trends in Arctic vegetation: Evidence from experimental warming and long-term monitoring. Ambio 49: 678-692.

Bjorkman AD, Myers-Smith IH, Elmendorf SC, Normand S, Rüger N, Beck PS, Blach-Overgaard A, Blok D, Cornelissen JHC, Forbes BC. 2018a. Plant functional trait change across a warming tundra biome. Nature 562: 57-62.

Bjorkman AD, Myers-Smith IH, Elmendorf SC, Normand S, Thomas HJD, Alatalo JM, Alexander H, Anadon-Rosell A, Angers-Blondin S, Bai Y, Baruah G, te Beest M, Berner L, Björk RG, Blok D, Bruelheide H, Buchwal A, Buras A, Carbognani M, Christie K, Collier LS, Cooper EJ, Cornelissen JHC, Dickinson KJM, Dullinger S, Elberling B, Eskelinen A, Forbes BC, Frei ER, Iturrate-Garcia M, Good MK, Grau O, Green P, Greve M, Grogan P, Haider S, Hájek T, Hallinger M, Happonen K, Harper KA, Heijmans MMPD, Henry GHR, Hermanutz L, Hewitt RE, Hollister RD, Hudson J, Hülber K, Iversen CM, Jaroszynska F, Jiménez-Alfaro B, Johnstone J, Jorgensen RH, Kaarlejärvi E, Klady R, Klimešová J, Korsten A, Kuleza S, Kulonen A, Lamarque LJ, Lantz T, Lavalle A, Lembrechts JJ, Lévesque E, Little CJ, Luoto M, Macek P, Mack MC, Mathakutha R, Michelsen A, Milbau A, Molau U, Morgan JW, Mörsdorf MA, Nabe-Nielsen J, Nielsen SS, Ninot JM, Oberbauer SF, Olofsson J, Onipchenko VG, Petraglia A, Pickering C, Prevéy JS, Rixen C, Rumpf SB, Schaepman-Strub G, Semenchuk P, Shetti R, Soudzilovskaia NA, Spasojevic MJ, Speed JDM, Street LE, Suding K, Tape KD, Tomaselli M, Trant A, Treier UA, Tremblay J-P, Tremblay M, Venn S, Virkkala A-M, Vowles T, Weijers S, Wilmking M, Wipf S, Zamin T. 2018b. Tundra Trait Team: A database of plant traits spanning the tundra biome. Global Ecology and Biogeography 27: 1402-1411.

Black KL, Wallace CA, Baltzer JL. 2021. Seasonal thaw and landscape position determine foliar functional traits and whole-plant water use in tall shrubs on the low arctic tundra. New Phytologist 231: 94-107.

Bonan GB, Levis S, Sitch S, Vertenstein M, Oleson KW. 2003. A dynamic global vegetation model for use with climate models: concepts and description of simulated vegetation dynamics. Global Change Biology 9: 1543-1566.

Bonney MT, Danby RK, Treitz PM. 2018. Landscape variability of vegetation change across the forest to tundra transition of central Canada. Remote Sensing of Environment 217: 18-29.

Brady NC, Weil RR. 1996. The Nature and Properties of Soils: Prentice Hall.

Breiman L. 2001. Random forests. Machine Learning 45: 5-32.

Breiner FT, Guisan A, Nobis MP, Bergamini A. 2017. Including environmental niche information to improve IUCN Red List assessments. Diversity and Distributions 23: 484-495.

Bret-Harte MS, Shaver GR, Zoerner JP, Johnstone JF, Wagner JL, Chavez AS, Gunkelman IV RF, Lippert SC, Laundre JA. 2001. Developmental plasticity allows Betula nana to dominate tundra subjected to an altered environment. Ecology 82: 18-32.

Bret-Harte MS, Shaver GR, Chapin III FS. 2002. Primary and secondary stem growth in arctic shrubs: implications for community response to environmental change. Journal of Ecology 90: 251-267.

Brotons L, Thuiller W, Araújo MB, Hirzel AH. 2004. Presence-absence versus presence-only modelling methods for predicting bird habitat suitability. Ecography 27: 437-448.

Burn CR, Kokelj S. 2009. The environment and permafrost of the Mackenzie Delta area. Permafrost and Periglacial Processes 20: 83-105.

Burn CR, Zhang Y. 2009. Permafrost and climate change at Herschel Island (Qikiqtaruq), Yukon Territory, Canada. Journal of Geophysical Research: Earth Surface 114.

Callaghan TV, Tweedie CE, Åkerman J, Andrews C, Bergstedt J, Butler MG, Christensen TR, Cooley D, Dahlberg U, Danby RK. 2011. Multi-decadal changes in tundra environments and ecosystems: synthesis of the International Polar Year-Back to the Future Project (IPY-BTF). Ambio 40: 705.

Cameron EA, Lantz TC. 2016. Drivers of tall shrub proliferation adjacent to the Dempster Highway, Northwest Territories, Canada. Environmental Research Letters 11: 045006.

Campbell TKF, Lantz TC, Fraser RH, Hogan D. 2021. High arctic vegetation change mediated by hydrological conditions. Ecosystems 24: 106-121.

Chamberlain SA, Boettiger C. 2017. R Python, and Ruby clients for GBIF species occurrence data. PeerJ Preprints.

Chapin III FS, Bret-Harte MS, Hobbie SE, Zhong H. 1996. Plant functional types as predictors of transient responses of arctic vegetation to global change. Journal of Vegetation Science 7: 347-358.

Chapin III FS, Fetcher N, Kielland K, Everett KR, Linkins AE. 1988. Productivity and nutrient cycling of Alaskan tundra: enhancement by flowing soil water. Ecology 69: 693-702.

Chapin III FS, Shaver GR, Giblin AE, Nadelhoffer KJ, Laundre JA. 1995. Responses of arctic tundra to experimental and observed changes in climate. Ecology 76: 694-711.

Chase JM, Leibold MA. 2003. Ecological niches: University of Chicago Press.

Chen A. 2020. The effects of climate change and fire on tundra vegetation change in the western Canadian Arctic. School of Environmental Studies: University of Victoria.

Chen A, Lantz TC, Hermosilla T, Wulder MA. 2021. Biophysical controls of increased tundra productivity in the western Canadian Arctic. Remote Sensing of Environment 258: 112358.

Cholewa E, Griffith M. 2004. The unusual vascular structure of the corm of Eriophorum vaginatum: implications for efficient retranslocation of nutrients. Journal of Experimental Botany 55: 731-741.

Clarke KR. 1993. Non-parametric multivariate analyses of changes in community structure. Australian Journal of Ecology 18: 117-143.

Claverie M, Ju J, Masek JG, Dungan JL, Vermote EF, Roger J-C, Skakun SV, Justice C. 2018. The Harmonized Landsat and Sentinel-2 surface reflectance data set. Remote Sensing of Environment 219: 145-161.

Cunliffe AM, Assmann JJ, Daskalova GN, Kerby JT, Myers-Smith IH. 2020. Aboveground biomass corresponds strongly with drone-derived canopy height but weakly with greenness (NDVI) in a shrub tundra landscape. Environmental Research Letters 15: 125004.

Cutler DR, Edwards Jr TC, Beard KH, Cutler A, Hess KT, Gibson J, Lawler JJ. 2007. Random forests for classification in ecology. Ecology 88: 2783-2792.

Dagg J, Lafleur P. 2011. Vegetation community, foliar nitrogen, and temperature effects on tundra CO2 exchange across a soil moisture gradient. Arctic, Antarctic, and Alpine Research 43: 189-197.

Davy R, Chen L, Hanna E. 2018. Arctic amplification metrics. International Journal of Climatology 38: 4384-4394.

De'ath G. 2007. Boosted trees for ecological modeling and prediction. Ecology 88: 243-251.

De'ath G, Fabricius KE. 2000. Classification and regression trees: a powerful yet simple technique for ecological data analysis. Ecology 81: 3178-3192.

De Groot W, Thomas P, Wein RW. 1997. Betula nana L. and Betula glandulosa Michx. Journal of Ecology 85: 241-264.

De Reu J, Bourgeois J, Bats M, Zwertvaegher A, Gelorini V, De Smedt P, Chu W, Antrop M, De Maeyer P, Finke P. 2013. Application of the topographic position index to heterogeneous landscapes. Geomorphology 186: 39-49.

DeAngelis DL, Mooij WM. 2005. Individual-based modeling of ecological and evolutionary processes. Annual Review of Ecology, Evolution, and Systematics 36: 147-168.

Deslippe JR, Hartmann M, Simard SW, Mohn WW. 2012. Long-term warming alters the composition of Arctic soil microbial communities. FEMS Microbiology Ecology 82: 303-315.

Deslippe JR, Simard SW. 2011. Below-ground carbon transfer among Betula nana may increase with warming in Arctic tundra. New Phytologist 192: 689-698.

Drusch M, Del Bello U, Carlier S, Colin O, Fernandez V, Gascon F, Hoersch B, Isola C, Laberinti P, Martimort P. 2012. Sentinel-2: ESA's optical high-resolution mission for GMES operational services. Remote Sensing of Environment 120: 25-36.

Duk-Rodkin A, Hughes OL. 1995. Quaternary geology of the northeastern part of the central Mackenzie Valley corridor, District of Mackenzie, Northwest Territories: Geological Survey of Canada.

Ecosystem Classification Group. 2012. Ecological Regions of the Northwest Territories, Southern Arctic. Yellowknife, NT, p170.

Elith J, H. Graham C, P. Anderson R, Dudík M, Ferrier S, Guisan A, J. Hijmans R, Huettmann F, R. Leathwick J, Lehmann A, Li J, G. Lohmann L, A. Loiselle B, Manion G, Moritz C, Nakamura M, Nakazawa Y, McC. M. Overton J, Townsend Peterson A, J. Phillips S, Richardson K, Scachetti-Pereira R, E. Schapire R, Soberón J, Williams S, S. Wisz M, E. Zimmermann N. 2006. Novel methods improve prediction of species' distributions from occurrence data. Ecography 29: 129-151.

Elith J, Leathwick JR. 2009. Species distribution models: ecological explanation and prediction across space and time. Annual Review of Ecology, Evolution, and Systematics 40: 677-697.

Elith J, Phillips SJ, Hastie T, Dudík M, Chee YE, Yates CJ. 2011. A statistical explanation of MaxEnt for ecologists. Diversity and Distributions 17: 43-57.

Elmendorf SC, Henry GH, Hollister RD, Björk RG, Boulanger-Lapointe N, Cooper EJ, Cornelissen JH, Day TA, Dorrepaal E, Elumeeva TG. 2012. Plot-scale evidence of tundra vegetation change and links to recent summer warming. Nature Climate Change 2: 453-457.

Environment and Climate Change Canada. 2018a. Canadian climate normals 1981-2010 station data, Tuktoyaktuk A. Ottawa, Ontario.

Environment and Climate Change Canada. 2018b. Canadian climate normals 1981–2010 station data, Shingle Point A. Ottawa, Ontario.

Environment and Climate Change Canada. 2021. Canadian climate normals.

Epstein HE, Beringer J, Gould WA, Lloyd AH, Thompson C, Chapin III FS, Michaelson GJ, Ping CL, Rupp T, Walker DA. 2004a. The nature of spatial transitions in the Arctic. Journal of Biogeography 31: 1917-1933.

Epstein HE, Calef MP, Walker MD, Chapin III FS, Starfield AM. 2004b. Detecting changes in arctic tundra plant communities in response to warming over decadal time scales. Global Change Biology 10: 1325-1334.

Epstein HE, Raynolds MK, Walker DA, Bhatt US, Tucker CJ, Pinzon JE. 2012. Dynamics of aboveground phytomass of the circumpolar Arctic tundra during the past three decades. Environmental Research Letters 7: 015506.

Euskirchen ES, McGuire AD, Chapin III FS, Yi S, Thompson CC. 2009. Changes in vegetation in northern Alaska under scenarios of climate change, 2003–2100: implications for climate feedbacks. Ecological Applications 19: 1022-1043.

Evans J. 2020. spatialEco: R package version 1.3-0.

Evans JS, Cushman SA. 2009. Gradient modeling of conifer species using random forests. Landscape Ecology 24: 673-683.

Farman JC, Gardiner BG, Shanklin JD. 1985. Large losses of total ozone in Antarctica reveal seasonal ClO x/NO x interaction. Nature 315: 207-210.

Fick SE, Hijmans RJ. 2017. WorldClim 2: new 1-km spatial resolution climate surfaces for global land areas. International Journal of Climatology 37: 4302-4315.

Fournier A, Barbet-Massin M, Rome Q, Courchamp F. 2017. Predicting species distribution combining multi-scale drivers. Global Ecology and Conservation 12: 215-226.

Fraser RH, Lantz TC, Olthof I, Kokelj SV, Sims RA. 2014a. Warming-induced shrub expansion and lichen decline in the Western Canadian Arctic. Ecosystems 17: 1151-1168.

Fraser RH, Olthof I, Kokelj SV, Lantz TC, Lacelle D, Brooker A, Wolfe S, Schwarz S. 2014b. Detecting Landscape Changes in High Latitude Environments Using Landsat Trend Analysis: 1. Visualization. 6: 11533-11557.

Fraser RH, Olthof I, Lantz TC, Schmitt C. 2016. UAV photogrammetry for mapping vegetation in the low-Arctic. Arctic Science 2: 79-102.

Friedman JH. 2001. Greedy function approximation: a gradient boosting machine. Annals of Statistics: 1189-1232.

Frost GV, Epstein HE. 2014. Tall shrub and tree expansion in Siberian tundra ecotones since the 1960s. Global Change Biology 20: 1264-1277.

Frost GV, Epstein HE, Walker DA. 2014. Regional and landscape-scale variability of Landsat-observed vegetation dynamics in northwest Siberian tundra. Environmental Research Letters 9: 025004.

Frost GV, Epstein HE, Walker DA, Matyshak G, Ermokhina K. 2018. Seasonal and Long-Term Changes to Active-Layer Temperatures after Tall Shrubland Expansion and Succession in Arctic Tundra. Ecosystems 21: 507-520.

Fulton RJ. 1989. Quaternary geology of Canada and Greenland. Ottawa, Ontario: Geological Survey of Canada.

Furlow JJ. 1979. The systematics of the American species of Alnus (Betulaceae). Rhodora 81: 1-121.

Furlow JJ. 2020. Alnus viridis. Flora of North America Editorial Committee editor. Flora of North America North of Mexico. New York and Oxford.

Gamon JA, Huemmrich KF, Stone RS, Tweedie CE. 2013. Spatial and temporal variation in primary productivity (NDVI) of coastal Alaskan tundra: Decreased vegetation growth following earlier snowmelt. Remote Sensing of Environment 129: 144-153.

Gao X, Huete AR, Ni W, Miura T. 2000. Optical–biophysical relationships of vegetation spectra without background contamination. Remote Sensing of Environment 74: 609-620.

Gill D. 1972. The point bar environment in the Mackenzie River Delta. Canadian Journal of Earth Sciences 9: 1382-1393.

Gill D. 1973. Floristics of a plant succession sequence in the Mackenzie Delta, Northwest Territories. Polarforschung 43: 55-65.

Gill HK, Lantz TC, O'Neill B, Kokelj SV. 2014. Cumulative impacts and feedbacks of a gravel road on shrub tundra ecosystems in the Peel Plateau, Northwest Territories, Canada. Arctic, Antarctic, and Alpine Research 46: 947-961.

Greaves HE, Vierling LA, Eitel JUH, Boelman NT, Magney TS, Prager CM, Griffin KL. 2015. Estimating aboveground biomass and leaf area of low-stature Arctic shrubs with terrestrial LiDAR. Remote Sensing of Environment 164: 26-35.

Guay KC, Beck PS, Berner LT, Goetz SJ, Baccini A, Buermann W. 2014. Vegetation productivity patterns at high northern latitudes: A multi-sensor satellite data assessment. Global Change Biology 20: 3147-3158.

Guisan A, Thuiller W. 2005. Predicting species distribution: offering more than simple habitat models. Ecology Letters 8: 993-1009.

Guisan A, Tingley R, Baumgartner JB, Naujokaitis-Lewis I, Sutcliffe PR, Tulloch AIT, Regan TJ, Brotons L, McDonald-Madden E, Mantyka-Pringle C, Martin TG, Rhodes JR, Maggini R, Setterfield SA, Elith J, Schwartz MW, Wintle BA, Broennimann O, Austin M, Ferrier S, Kearney MR, Possingham HP, Buckley YM. 2013. Predicting species distributions for conservation decisions. Ecology Letters 16: 1424-1435.

Guisan A, Zimmermann NE. 2000. Predictive habitat distribution models in ecology. Ecological Modelling 135: 147-186.

Gutman G, Huang C, Chander G, Noojipady P, Masek JG. 2013. Assessment of the NASA–USGS global land survey (GLS) datasets. Remote Sensing of Environment 134: 249-265.

Hao T, Elith J, Lahoz-Monfort JJ, Guillera-Arroita G. 2020. Testing whether ensemble modelling is advantageous for maximising predictive performance of species distribution models. Ecography 43: 549-558.

Hastie T, Tibshirani R, Friedman J. 2009. The elements of statistical learning: data mining, inference, and prediction: Springer Science & Business Media.

Hermosilla T, Wulder MA, White JC, Coops NC, Hobart GW. 2017. Updating Landsat time series of surface-reflectance composites and forest change products with new observations. International Journal of Applied Earth Observation Geoinformation 63: 104-111.

Hermosilla T, Wulder MA, White JC, Coops NC, Hobart GW, Campbell LB. 2016. Mass data processing of time series Landsat imagery: pixels to data products for forest monitoring. International Journal of Digital Earth 9: 1035-1054.

Hijmans RJ. 2020. raster: geographic data analysis and modeling: R package version 3.0-12.

Hijmans RJ, Cameron SE, Parra JL, Jones PG, Jarvis A. 2005. Very high resolution interpolated climate surfaces for global land areas. International Journal of Climatology 25: 1965-1978.

Hirzel AH, Le Lay G. 2008. Habitat suitability modelling and niche theory. Journal of Applied Ecology 45: 1372-1381.

Hobbie SE, Chapin III FS. 1998. The response of tundra plant biomass, aboveground production, nitrogen, and CO2 flux to experimental warming. Ecology 79: 1526-1544.

Hudson JM, Henry GH. 2009. Increased plant biomass in a High Arctic heath community from 1981 to 2008. Ecology 90: 2657-2663.

Hughes O, Harington CR, Janssens J, Matthews Jr J, Morlan RE, Rutter N, Schweger CE. 1981. Upper Pleistocene stratigraphy, paleoecology, and archaeology of the northern Yukon interior, eastern Beringia 1. Bonnet Plume Basin. Arctic: 329-365.

Hutchinson GE. 1957. Concluding remarks Cold spring harbor symposium on quantitative biology 22: 415-427.

Indian and Northern Affairs Canada. 1984. Western Arctic Claim: The Inuvialuit Final Agreement. Ottawa, ON.

Indian and Northern Affairs Canada. 1992. Comprehensive Land Claim Agreement Between Her Majesty The Queen In Right Of Canada And The Gwich'in As Represented By The Gwich'in Tribal Council. Ottawa, ON.

James G, Witten D, Hastie T, Tibshirani R. 2013. An Introduction to Statistical Learning: Springer.

Jessop AM. 1971. The distribution of glacial perturbation of heat flow in Canada. Canadian Journal of Earth Sciences 8: 162-166.

Jia GJ, Epstein HE, Walker DA. 2003. Greening of arctic Alaska, 1981–2001. Geophysical Research Letters 30.

Jia GJ, Epstein HE, Walker DA. 2006. Spatial heterogeneity of tundra vegetation response to recent temperature changes. Global Change Biology 12: 42-55.

Johannessen OM, Kuzmina SI, Bobylev LP, Miles MW. 2016. Surface air temperature variability and trends in the Arctic: new amplification assessment and regionalisation. Tellus A: Dynamic Meteorology and Oceanography 68: 28234.

Johnson DA, Caldwell MM. 1975. Gas exchange of four arctic and alpine tundra plant species in relation to atmospheric and soil moisture stress. Oecologia 21: 93-108.

Johnstone J, Russell DE, Griffith B. 2002. Variations in plant forage quality in the range of the Porcupine caribou herd. Rangifer 22: 83-91.

Joly K, Jandt RR, Meyers CR, Cole MJ. 2007. Changes in vegetative cover on Western Arctic Herd winter range from 1981 to 2005: potential effects of grazing and climate change. Rangifer: 199-207.

Jørgensen RH, Meilby H, Kollmann J. 2013. Shrub Expansion in SW Greenland Under Modest Regional Warming: Disentangling Effects of Human Disturbance and Grazing. Arctic, Antarctic, and Alpine Research 45: 515-525.

Ju J, Masek JG. 2016. The vegetation greenness trend in Canada and US Alaska from 1984–2012 Landsat data. Remote Sensing of Environment 176: 1-16.

Jung TS, Frandsen J, Gordon DC, Mossop DH. 2016. Colonization of the Beaufort coastal plain by beaver (Castor canadensis): A response to shrubification of the tundra? The Canadian Field-Naturalist 130: 332-335.

Kaky E, Nolan V, Alatawi A, Gilbert F. 2020. A comparison between Ensemble and MaxEnt species distribution modelling approaches for conservation: A case study with Egyptian medicinal plants. Ecological Informatics 60: 101150.

Keeling CD, Bacastow RB, Bainbridge AE, Ekdahl Jr CA, Guenther PR, Waterman LS, Chin JF. 1976. Atmospheric carbon dioxide variations at Mauna Loa observatory, Hawaii. Tellus 28: 538-551.

Keil P, Belmaker J, Wilson AM, Unitt P, Jetz W. 2013. Downscaling of species distribution models: a hierarchical approach. Methods in Ecology and Evolution 4: 82-94.

Kelsey KC, Pedersen SH, Leffler AJ, Sexton JO, Feng M, Welker JM. 2020. Winter snow and spring temperature have differential effects on vegetation phenology and productivity across plant communities. Global Change Biology.

Kendall MG. 1948. Rank correlation methods. London: Griffin.

Kindt R, Coe R. 2005. Tree diversity analysis. A manual and software for common statistical methods for ecological and biodiversity studies. (ICRAF) WAC editor. Nairobi, Kenya.

Kopecký M, Čížková Š. 2010. Using topographic wetness index in vegetation ecology: does the algorithm matter? Journal of Applied Vegetation Science 13: 450-459.

Kruse S, Gerdes A, Kath NJ, Herzschuh U. 2018. Implementing spatially explicit wind-driven seed and pollen dispersal in the individual-based larch simulation model: LAVESI-WIND 1.0. Geoscientific Model Development 11: 4451-4467.

Kruse S, Wieczorek M, Jeltsch F, Herzschuh U. 2016. Treeline dynamics in Siberia under changing climates as inferred from an individual-based model for Larix. Ecological Modelling 338: 101-121.

Kuhn C, Butman D. 2021. Declining greenness in Arctic-boreal lakes. Proceedings of the National Academy of Sciences 118.

Kushida K, Hobara S, Tsuyuzaki S, Kim Y, Watanabe M, Setiawan Y, Harada K, Shaver GR, Fukuda M. 2015. Spectral indices for remote sensing of phytomass, deciduous shrubs, and productivity in Alaskan Arctic tundra. International Journal of Remote Sensing 36: 4344-4362.

Laidler GJ, Treitz P. 2003. Biophysical remote sensing of arctic environments. Progress in Physical Geography 27: 44-68.

Landis JR, Koch GG. 1977. The measurement of observer agreement for categorical data. Biometrics: 159-174.

Lantz TC, Gergel SE, Henry GHR. 2010a. Response of green alder (Alnus viridis subsp. fruticosa) patch dynamics and plant community composition to fire and regional temperature in north-western Canada. Journal of Biogeography 37: 1597-1610.

Lantz TC, Gergel SE, Kokelj SV. 2010b. Spatial heterogeneity in the shrub tundra ecotone in the Mackenzie Delta region, Northwest Territories: implications for Arctic environmental change. Ecosystems 13: 194-204.

Lantz TC, Kokelj SV, Gergel SE, Henry GHR. 2009. Relative impacts of disturbance and temperature: persistent changes in microenvironment and vegetation in retrogressive thaw slumps. Global Change Biology 15: 1664-1675.

Lantz TC, Marsh P, Kokelj SV. 2013. Recent shrub proliferation in the Mackenzie Delta uplands and microclimatic implications. Ecosystems 16: 47-59.

Lantz TC, Moffat ND, Fraser RH, Walker X. 2019. Reproductive limitation mediates the response of white spruce (Picea glauca) to climate warming across the forest–tundra ecotone. Arctic Science 5: 167-184.

Lara MJ, Nitze I, Grosse G, Martin P, McGuire AD. 2018. Reduced arctic tundra productivity linked with landform and climate change interactions. Scientific Reports 8: 2345.

Larking T, Davis E, Way R, Hermanutz L, Trant A. 2021. Recent greening driven by species-specific shrub growth characteristics in Nunatsiavut, Labrador, Canada. Arctic Science: 1-17.

Lee CK, Williams PH, Pearson RG. 2019. Climate change vulnerability higher in arctic than alpine bumblebees. Frontiers of Biogeography 11.

Leffler AJ, Klein ES, Oberbauer SF, Welker JM. 2016. Coupled long-term summer warming and deeper snow alters species composition and stimulates gross primary productivity in tussock tundra. Oecologia 181: 287-297.

Levin SA. 1992. The problem of pattern and scale in ecology: the Robert H. MacArthur award lecture. Ecology 73: 1943-1967.

Liaw A, Wiener M. 2002. Classification and regression by randomForest. R News 2: 18-22.

Liu HQ, Huete A. 1995. A feedback based modification of the NDVI to minimize canopy background and atmospheric noise. IEEE Transactions on Geoscience and Remote Sensing 33: 457-465.

Lovett GM, Burns DA, Driscoll CT, Jenkins JC, Mitchell MJ, Rustad L, Shanley JB, Likens GE, Haeuber R. 2007. Who needs environmental monitoring? Frontiers in Ecology and the Environment 5: 253-260.

Macander MJ, Swingley CS, Joly K, Raynolds MK. 2015. Landsat-based snow persistence map for northwest Alaska. Remote Sensing of Environment 163: 23-31.

Mann HB. 1945. Nonparametric tests against trend. Econometrica: Journal of the Econometric Society 13: 245-259.

Marcer A, Sáez L, Molowny-Horas R, Pons X, Pino J. 2013. Using species distribution modelling to disentangle realised versus potential distributions for rare species conservation. Biological Conservation 166: 221-230.

Markham BL, Helder DL. 2012. Forty-year calibrated record of earth-reflected radiance from Landsat: A review. Remote Sensing of Environment 122: 30-40.

Marmion M, Parviainen M, Luoto M, Heikkinen RK, Thuiller W. 2009. Evaluation of consensus methods in predictive species distribution modelling. Diversity and Distributions 15: 59-69.

Martin AC, Jeffers ES, Petrokofsky G, Myers-Smith I, Macias-Fauria M. 2017. Shrub growth and expansion in the Arctic tundra: an assessment of controlling factors using an evidence-based approach. Environmental Research Letters 12: 085007.

Masek JG, Wulder MA, Markham B, McCorkel J, Crawford CJ, Storey J, Jenstrom DT. 2020. Landsat 9: Empowering open science and applications through continuity. Remote Sensing of Environment 248: 111968.

McGuire AD, Chapin III FS, Walsh JE, Wirth C. 2006. Integrated regional changes in arctic climate feedbacks: implications for the global climate system. Annual Review of Environment and Resources 31: 61-91.

McLeod A. 2011. Kendall: Kendall rank correlation and Mann-Kendall trend test: R package version 2.2.

McManus KM, Morton DC, Masek JG, Wang D, Sexton JO, Nagol JR, Ropars P, Boudreau S. 2012. Satellite-based evidence for shrub and graminoid tundra expansion in northern Quebec from 1986 to 2010. Global Change Biology 18: 2313-2323.

Mekonnen ZA, Riley WJ, Berner LT, Bouskill NJ, Torn MS, Iwahana G, Breen AL, Myers-Smith IH, Criado MG, Liu Y, Euskirchen ES, Goetz SJ, Mack MC, Grant RF. 2021a. Arctic tundra shrubification: a review of mechanisms and impacts on ecosystem carbon balance. Environmental Research Letters 16: 053001.

Mekonnen ZA, Riley WJ, Grant RF, Salmon VG, Iversen CM, Biraud SC, Breen AL, Lara MJ. 2021b. Topographical Controls on Hillslope-Scale Hydrology Drive Shrub Distributions on the Seward Peninsula, Alaska. Journal of Geophysical Research: Biogeosciences 126: e2020JG005823.

Metcalfe P, Beven K, Freer J. 2018. dynatopmodel: implementation of the Dynamic TOPMODEL Hydrological Model: R package version 1.2.1.

Milbau A, Graae BJ, Shevtsova A, Nijs I. 2009. Effects of a warmer climate on seed germination in the subarctic. Annals of Botany 104: 287-296.

Miller PA, Smith B. 2012. Modelling tundra vegetation response to recent arctic warming. Ambio 41: 281-291.

Moffat ND, Lantz TC, Fraser RH, Olthof I. 2016. Recent vegetation change (1980–2013) in the tundra ecosystems of the Tuktoyaktuk Coastlands, NWT, Canada. Arctic, Antarctic, and Alpine Research 48: 581-597.

Moss RH, Edmonds JA, Hibbard KA, Manning MR, Rose SK, Van Vuuren DP, Carter TR, Emori S, Kainuma M, Kram T. 2010. The next generation of scenarios for climate change research and assessment. Nature 463: 747-756.

Murray G, Boxall PC, Wein RW. 2005. Distribution, abundance, and utilization of wild berries by the Gwich'in people in the Mackenzie River Delta Region. Economic Botany 59: 174-184.

Myers-Smith IH, Elmendorf SC, Beck PS, Wilmking M, Hallinger M, Blok D, Tape KD, Rayback SA, Macias-Fauria M, Forbes BC. 2015. Climate sensitivity of shrub growth across the tundra biome. Nature Climate Change 5: 887-891.

Myers-Smith IH, Forbes BC, Wilmking M, Hallinger M, Lantz T, Blok D, Tape KD, Macias-Fauria M, Sass-Klaassen U, Lévesque E. 2011. Shrub expansion in tundra ecosystems: dynamics, impacts and research priorities. Environmental Research Letters 6: 045509.

Myers-Smith IH, Kerby JT, Phoenix GK, Bjerke JW, Epstein HE, Assmann JJ, John C, Andreu-Hayles L, Angers-Blondin S, Beck PS. 2020. Complexity revealed in the greening of the Arctic. Nature Climate Change 10: 106-117.

Myers-Smith IH, Grabowski MM, Thomas HJ, Angers-Blondin S, Daskalova GN, Bjorkman AD, Cunliffe AM, Assmann JJ, Boyle JS, McLeod E. 2019. Eighteen years of ecological monitoring reveals multiple lines of evidence for tundra vegetation change. Ecological Monographs 89: e01351.

Niittynen P, Heikkinen RK, Aalto J, Guisan A, Kemppinen J, Luoto M. 2020a. Fine-scale tundra vegetation patterns are strongly related to winter thermal conditions. Nature Climate Change 10: 1143-1148.

Niittynen P, Heikkinen RK, Luoto M. 2020b. Decreasing snow cover alters functional composition and diversity of Arctic tundra. Proceedings of the National Academy of Sciences 117: 21480-21487.

Nitze I, Grosse G. 2016. Detection of landscape dynamics in the Arctic Lena Delta with temporally dense Landsat time-series stacks. Remote Sensing of Environment 181: 27-41.

O'Donnell MS, Ignizio DA. 2012. Bioclimatic predictors for supporting ecological applications in the conterminous United States. US Geological Survey Data Series 691: 4-9.

Oksanen J, Blanchet G, Friendly M, Kindt R, Legendre P, McGlinn D, Minchin P, O'Hara R, Simpson G, Solymos P, Stevens M, Szoecs E, Wagner H. 2019. vegan: community ecology package: R package version 2.5-6.

Ollinger SV. 2011. Sources of variability in canopy reflectance and the convergent properties of plants. New Phytologist 189: 375-394.

Ovaskainen O, Abrego N. 2020. Joint Species Distribution Modelling: With Applications in R. Cambridge: Cambridge University Press.

Parlee B, Berkes F, Gwich'in Ti. 2005. Health of the Land, Health of the People: A Case Study on Gwich'in Berry Harvesting in Northern Canada. EcoHealth 2: 127-137.

Parlee B, Furgal C. 2012. Well-being and environmental change in the arctic: a synthesis of selected research from Canada's International Polar Year program. Climatic Change 115: 13-34.

Pastick NJ, Jorgenson MT, Wylie BK, Nield SJ, Johnson KD, Finley AO. 2015. Distribution of near-surface permafrost in Alaska: Estimates of present and future conditions. Remote Sensing of Environment 168: 301-315.

Pearce C. 1986. The distribution and ecology of the shoreline vegetation on the Mackenzie Delta, NWT. University of Calgary.

Pearce JL, Boyce MS. 2006. Modelling distribution and abundance with presence-only data. Journal of Applied Ecology 43: 405-412.

Pearson RG, Dawson TP. 2003. Predicting the impacts of climate change on the distribution of species: are bioclimate envelope models useful? Global Ecology and Biogeography 12: 361-371.

Pearson RG, Phillips SJ, Loranty MM, Beck PS, Damoulas T, Knight SJ, Goetz SJ. 2013. Shifts in Arctic vegetation and associated feedbacks under climate change. Nature Climate Change 3: 673-677.

Pěknicová J, Berchová-Bímová K. 2016. Application of species distribution models for protected areas threatened by invasive plants. Journal for Nature Conservation 34: 1-7.

Pettorelli N, Vik JO, Mysterud A, Gaillard J-M, Tucker CJ, Stenseth NC. 2005. Using the satellite-derived NDVI to assess ecological responses to environmental change. Trends in Ecology and Evolution 20: 503-510.

Phillips SJ, Anderson RP, Schapire RE. 2006. Maximum entropy modeling of species geographic distributions. Ecological Modelling 190: 231-259.

Phillips SJ, Dudík M, Elith J, Graham CH, Lehmann A, Leathwick J, Ferrier S. 2009. Sample selection bias and presence-only distribution models: implications for background and pseudo-absence data. Ecological Applications 19: 181-197.

Pironon S, Villellas J, Thuiller W, Eckhart VM, Geber MA, Moeller DA, García MB. 2018. The 'Hutchinsonian niche'as an assemblage of demographic niches: implications for species geographic ranges. Ecography 41: 1103-1113.

Port U, Brovkin V, Claussen M. 2012. The influence of vegetation dynamics on anthropogenic climate change. Earth System Dynamics 3: 233-243.

Porter C, Morin P, Howat I, Noh M, Bates B, Peterman K, Keesey S, Schlenk M, Gardiner J, Tomko K, Willis M, Kelleher C, Cloutier M, Husby E, Foga S, Nakamura H, Platson M, Wethington M, Williamson C, Bauer G, Enos J, Arnold G, Kramer W, Becker P, Doshi A, D'Souza C, Cummens P, Laurier F, Bojesen M. 2018. ArcticDEM. Harvard Dataverse.

Post E, Forchhammer MC, Bret-Harte MS, Callaghan TV, Christensen TR, Elberling B, Fox AD, Gilg O, Hik DS, Høye TT. 2009. Ecological dynamics across the Arctic associated with recent climate change. Science 325: 1355-1358.

Prasad AM, Iverson LR, Liaw A. 2006. Newer classification and regression tree techniques: bagging and random forests for ecological prediction. Ecosystems 9: 181-199.

Proverbs TA, Lantz TC. 2020. Cumulative Environmental Impacts in the Gwich'in Cultural Landscape. Sustainability 12: 4667.

Quillet A, Peng C, Garneau M. 2010. Toward dynamic global vegetation models for simulating vegetation–climate interactions and feedbacks: recent developments, limitations, and future challenges. Environmental Reviews 18: 333-353.

R Core Team. 2019. R: A language and environment for statistical computing. Vienna, Austria: R Foundation for Statistical Computing.

Rampton V. 1982. Quaternary geology of the Yukon Coastal Plain. Ottawa, Ontario: Geological Survey of Canada.

Rampton V. 1988. Quaternary geology of the Tuktoyaktuk Coastlands, Northwest Territories. Ottawa, Ontario: Geological Survey of Canada.

Raynolds MK, Comiso JC, Walker DA, Verbyla D. 2008. Relationship between satellite-derived land surface temperatures, arctic vegetation types, and NDVI. Remote Sensing of Environment 112: 1884-1894.

Raynolds MK, Walker DA. 2016. Increased wetness confounds Landsat-derived NDVI trends in the central Alaska North Slope region, 1985–2011. Environmental Research Letters 11: 085004.

Renne RR, Bradford JB, Burke IC, Lauenroth WK. 2019. Soil texture and precipitation seasonality influence plant community structure in North American temperate shrub steppe. Ecology 100: e02824.

Rickbeil GJ, Hermosilla T, Coops NC, White JC, Wulder MA, Lantz TC. 2018. Changing northern vegetation conditions are influencing barren ground caribou (Rangifer tarandus groenlandicus) post-calving movement rates. Journal of Biogeography 45: 702-712.

Riley SJ, DeGloria SD, Elliot R. 1999. Index that quantifies topographic heterogeneity. Intermountain Journal of Sciences 5: 23-27.

Roberts DW, Cooper SV. 1989. Concepts and techniques of vegetation mapping. Land Classifications Based on Vegetation: Applications for Resource Management. Moscow, ID, p90-96.

Ropars P, Boudreau S. 2012. Shrub expansion at the forest–tundra ecotone: spatial heterogeneity linked to local topography. Environmental Research Letters 7: 015501.

Roser L, Ferreyra L, Saidman B, Vilardi J. 2017. EcoGenetics: an R package fro the management and explortory analysis of spatial data in landscape genetics. Molecular Ecology Resources 17: e241-e250.

Roy PS. 1989. Spectral reflectance characteristics of vegetation and their use in estimating productive potential. Proceedings: Plant Sciences 99: 59-81.

Russell DE, Martell AM, Nixon WA. 1993. Range ecology of the Porcupine caribou herd in Canada. Rangifer: 1-168.

Saarela JM, Sokoloff PC, Bull RD. 2017. Vascular plant biodiversity of the lower Coppermine River valley and vicinity (Nunavut, Canada): an annotated checklist of an Arctic flora. PeerJ 5: e2835.

Saarela JM, Sokoloff PC, Gillespie LJ, Bull RD, Bennett BA, Ponomarenko S. 2020. Vascular plants of Victoria Island (Northwest Territories and Nunavut, Canada): a specimen-based study of an Arctic flora. PhytoKeys 141: 1-330.

Santini L, Benítez-López A, Maiorano L, Čengić M, Huijbregts MAJ. 2021. Assessing the reliability of species distribution projections in climate change research. Diversity and Distributions 27: 1035-1050.

Sappington JM, Longshore KM, Thompson DB. 2007. Quantifying Landscape Ruggedness for Animal Habitat Analysis: A Case Study Using Bighorn Sheep in the Mojave Desert. The Journal of Wildlife Management 71: 1419-1426.

Schaefer K, Lantuit H, Romanovsky VE, Schuur EA, Witt R. 2014. The impact of the permafrost carbon feedback on global climate. Environmental Research Letters 9: 085003.

Scholes RJ, Walters M, Turak E, Saarenmaa H, Heip CHR, Tuama ÉÓ, Faith DP, Mooney HA, Ferrier S, Jongman RHG, Harrison IJ, Yahara T, Pereira HM, Larigauderie A, Geller G. 2012. Building a global observing system for biodiversity. Current Opinion in Environmental Sustainability 4: 139-146.

Segurado P, Araújo MB. 2004. An evaluation of methods for modelling species distributions. Journal of Biogeography 31: 1555-1568.

Seider JH, Lantz TC, Hermosilla T, Wulder MA, Wang JA. In Review. Biophysical determinants of shifting tundra vegetation productivity in the Beaufort Delta region of Canada. Ecosystems.

Sen PK. 1968. Estimates of the regression coefficient based on Kendall's tau. Journal of the American Statistical Association 63: 1379-1389.

Serreze M, Barrett A, Stroeve J, Kindig D, Holland M. 2009. The emergence of surface-based Arctic amplification. The Cryosphere 3: 11-19.

Serreze MC, Barry RG. 2011. Processes and impacts of Arctic amplification: A research synthesis. Global Planetary Change 77: 85-96.

Shevtsova A, Haukioja E, Ojala A. 1997. Growth Response of Subarctic Dwarf Shrubs, Empetrum nigrum and Vaccinium vitis-idaea, to Manipulated Environmental Conditions and Species Removal. Oikos 78: 440-458.

Shipman N. 2021. Summer 2019 vegetation monitoring in the Mackenzie Delta, NWT.

Soberón J, Nakamura M. 2009. Niches and distributional areas: Concepts, methods, and assumptions. Proceedings of the National Academy of Sciences 106: 19644.

Steedman AE. 2014. The ecology and dynamics of ice wedge degradation in high-centre polygonal terrain in the uplands of the Mackenzie Delta region, Northwest Territories. School of Environmental Studies: University of Victoria.

Sturm M, Holmgren J, McFadden JP, Liston GE, Chapin III FS, Racine CH. 2001. Snow–shrub interactions in Arctic tundra: a hypothesis with climatic implications. Journal of Climate 14: 336-344.

Svenning JC, Sandel B. 2013. Disequilibrium vegetation dynamics under future climate change. American Journal of Botany 100: 1266-1286.

Tape KD, Gustine DD, Ruess RW, Adams LG, Clark JA. 2016. Range expansion of moose in Arctic Alaska linked to warming and increased shrub habitat. PLoS ONE 11: e0152636.

Tape KD, Hallinger M, Welker JM, Ruess RW. 2012. Landscape heterogeneity of shrub expansion in Arctic Alaska. Ecosystems 15: 711-724.

Tape KD, Sturm M, Racine C. 2006. The evidence for shrub expansion in Northern Alaska and the Pan-Arctic. Global Change Biology 12: 686-702.

Taulavuori K, Laine K, Taulavuori E. 2013. Experimental studies on Vaccinium myrtillus and Vaccinium vitis-idaea in relation to air pollution and global change at northern high latitudes: a review. Environmental and Experimental Botany 87: 191-196.

Taylor KE, Stouffer RJ, Meehl GA. 2012. An overview of CMIP5 and the experiment design. Bulletin of the American Meteorological Society 93: 485-498.

Theil H. 1950. A rank-invariant method of linear and polynomial regression analysis. Indagationes Mathematicae 12: 173.

Thuiller W, Georges D, Gueguen M, Engler R, Breiner F. 2020. biomod2: Ensemble Platform for Species Distribution Modeling. R package version 3.4.13. Ecography 32: 369-373.

Timoney K, La Roi G, Zoltai S, Robinson AJA. 1992. The high subarctic forest-tundra of northwestern Canada: position, width, and vegetation gradients in relation to climate. 1-9.

Travers-Smith HZ, Lantz TC. 2020. Leading-edge disequilibrium in alder and spruce populations across the forest–tundra ecotone. Ecosphere 11: e03118.

Trivedi MR, Berry PM, Morecroft MD, Dawson TP. 2008. Spatial scale affects bioclimate model projections of climate change impacts on mountain plants. Global Change Biology 14: 1089-1103.

Tucker CJ. 1978. Red and photographic infrared linear combinations for monitoring vegetation. Remote Sensing of Environment.

Tyson W, Lantz TC, Ban NC. 2016. Cumulative effects of environmental change on culturally significant ecosystems in the Inuvialuit Settlement Region. Arctic: 391-405.

Vale CG, Tarroso P, Brito JC. 2014. Predicting species distribution at range margins: testing the effects of study area extent, resolution and threshold selection in the Sahara–Sahel transition zone. Diversity and Distributions 20: 20-33.

Van Bodegom PM, Douma JC, Witte JPM, Ordoñez JC, Bartholomeus RP, Aerts R. 2012. Going beyond limitations of plant functional types when predicting global ecosystem–atmosphere

fluxes: exploring the merits of traits-based approaches. Global Ecology and Biogeography 21: 625-636.

VanDerWal J, Shoo LP, Graham C, Williams SE. 2009. Selecting pseudo-absence data for presence-only distribution modeling: how far should you stray from what you know? Ecological Modelling 220: 589-594.

Verseghy D, McFarlane N, Lazare M. 1993. CLASS—A Canadian land surface scheme for GCMs, II. Vegetation model and coupled runs. International Journal of Climatology 13: 347-370.

Verseghy DL. 1991. CLASS—A Canadian land surface scheme for GCMs. I. Soil model. International Journal of Climatology 11: 111-133.

Verseghy DL. 2000. The Canadian land surface scheme (CLASS): its history and future. Atmosphere-Ocean 38: 1-13.

Vincent L, Zhang X, Brown R, Feng Y, Mekis E, Milewska E, Wan H, Wang X. 2015. Observed trends in Canada's climate and influence of low-frequency variability modes. Journal of Climate 28: 4545-4560.

Vuntut Gwitch'in First Nation, Smith S. 2010. People of the lakes: stories of our Van Tat Gwich'in Elders/Googwandak Nakhwach'anjoo Van Tat Gwich'in: University of Alberta.

Walker D, Auerbach N, Bockheim J, Chapin F, Eugster W, King J, McFadden J, Michaelson G, Nelson F, Oechel W. 1998. Energy and trace-gas fluxes across a soil pH boundary in the Arctic. Nature 394: 469-472.

Walker D, Everett K. 1991. Loess ecosystems of northern Alaska: regional gradient and toposequence at Prudhoe Bay. Ecological Monographs 61: 437-464.

Walker D, Leibman M, Epstein H, Forbes B, Bhatt U, Raynolds M, Comiso J, Gubarkov A, Khomutov A, Jia G. 2009. Spatial and temporal patterns of greenness on the Yamal Peninsula, Russia: interactions of ecological and social factors affecting the Arctic normalized difference vegetation index. Environmental Research Letters 4: 045004.

Walker DA. 2000. Hierarchical subdivision of Arctic tundra based on vegetation response to climate, parent material and topography. Global Change Biology 6: 19-34.

Walker MD, Wahren CH, Hollister RD, Henry GH, Ahlquist LE, Alatalo JM, Bret-Harte MS, Calef MP, Callaghan TV, Carroll AB. 2006. Plant community responses to experimental warming across the tundra biome. Proceedings of the National Academy of Sciences 103: 1342-1346.

Wang H-H, Wonkka CL, Treglia ML, Grant WE, Smeins FE, Rogers WE. 2015. Species distribution modelling for conservation of an endangered endemic orchid. AoB PLANTS 7.

Wang J, Sulla-Menashe D, Woodcock CE, Sonnentag O, Keeling R, Friedl M. 2019. ABoVE: Landsat-derived Annual Dominant Land Cover Across ABoVE Core Domain, 1984-2014. Oak Ridge, Tennessee, USA: ORNL DAAC.

Wang JA, Friedl MA. 2019. The role of land cover change in Arctic-Boreal greening and browning trends. Environmental Research Letters 14: 125007.

White J, Wulder M, Hobart G, Luther J, Hermosilla T, Griffiths P, Coops N, Hall R, Hostert P, Dyk A. 2014. Pixel-based image compositing for large-area dense time series applications and science. Canadian Journal of Remote Sensing 40: 192-212.

Wiedmer E, Senn-Irlet B. 2006. Biomass and primary productivity of an Alnus viridis stand–a case study from the Schächental valley, Switzerland. Botanica Helvetica 116: 55-64.

Wiens JA. 1989. Spatial scaling in ecology. Functional Ecology 3: 385-397.

Wildlife Management Advisory Council, North Slope, Aklavik Hunters and Trappers Committee. 2018. Yukon North Slope Inuvialuit Traditional Use Study. Whitehorse, YK.

Wipf S, Rixen C. 2010. A review of snow manipulation experiments in Arctic and alpine tundra ecosystems. Polar Research 29: 95-109.

Wisz MS, Guisan A. 2009. Do pseudo-absence selection strategies influence species distribution models and their predictions? An information-theoretic approach based on simulated data. BMC Ecology 9: 8.

Wulder MA, Hilker T, White JC, Coops NC, Masek JG, Pflugmacher D, Crevier Y. 2015. Virtual constellations for global terrestrial monitoring. Remote Sensing of Environment 170: 62-76.

Wulder MA, Loveland TR, Roy DP, Crawford CJ, Masek JG, Woodcock CE, Allen RG, Anderson MC, Belward AS, Cohen WB. 2019. Current status of Landsat program, science, and applications. Remote Sensing of Environment 225: 127-147.

Wulder MA, Masek JG, Cohen WB, Loveland TR, Woodcock CE. 2012. Opening the archive: How free data has enabled the science and monitoring promise of Landsat. Remote Sensing of Environment 122: 2-10.

Wullschleger SD, Epstein HE, Box EO, Euskirchen ES, Goswami S, Iversen CM, Kattge J, Norby RJ, van Bodegom PM, Xu X. 2014. Plant functional types in Earth system models: past experiences and future directions for application of dynamic vegetation models in high-latitude ecosystems. Annals of Botany 114: 1-16.

Yamazaki D, Ikeshima D, Tawatari R, Yamaguchi T, O'Loughlin F, Neal JC, Sampson CC, Kanae S, Bates PD. 2017. A high-accuracy map of global terrain elevations. Geophysical Research Letters 44: 5844-5853.

Yukon Ecoregions Working Group. 2004. Ecoregions of the Yukon Territory: Biophysical properties of Yukon landscapes. PARC Technical Bulletin, p63-72.

Yukon Territorial Government. 2021. Yukon Biophysical Inventory System. Government YT editor. Whitehorse, Yukon.

Zhang Z, Xu S, Capinha C, Weterings R, Gao T. 2019. Using species distribution model to predict the impact of climate change on the potential distribution of Japanese whiting Sillago japonica. Ecological Indicators 104: 333-340.

Zimmermann NE, Edwards Jr TC, Graham CH, Pearman PB, Svenning J-C. 2010. New trends in species distribution modelling. Ecography 33: 985-989.